04

E75-10249

CR-141209

(E75-10249) EVALUATION OF ERTS-1 DATA FOR CERTAIN HYDROLOGICAL USES Final Report, Jul. 1972 - Nov. 1974 (National Environmental Satellite Service) 94 p HC $4.75 CSCL 08H

N75-21771

Unclas G3/43 00249

1109A

TECHNICAL REPORT STANDARD TITLE PAGE

1. Report No.	2. Government Accession No.	3. Recipient's Catalog No.
FINAL		

4. Title and Subtitle	5. Report Date
Evaluation of ERTS Data for Certain Hydrological Uses	November 30, 1974
	6. Performing Organization Code
7. Author(s) D.R. Wiesnet, D.F. McGinnis, and M.C. McMillan	8. Performing Organization Report No.
9. Performing Organization Name and Address NOAA/National Environmental Satellite Service F.O.B. 4, Room 3010 Washington, D.C. 20233	10. Work Unit No.
	11. Contract or Grant No. 432-641-14-04-03
	13. Type of Report and Period Covered Final July 1972 - Nov. 1974
12. Sponsoring Agency Name and Address NASA/GSFC Greenbelt, Maryland 20771 TM: Fred Gordon	14. Sponsoring Agency Code

15. Supplementary Notes

GSFC ID No. C0313, Proposal No. 109

16. Abstract

ERTS-1 MSS data have been used in a variety of hydrologic research including snow-extent mapping; studies of snowmelt, snowmelt-runoff, spectral reflectance of snow for assessing snowpack conditions, and snow albedo; lake ice formation, breakup, and migration; lake current measurements; multispectral studies of lake ice; and flood studies. MSS sensing of soil moisture over a well-vegetated test site was unsuccessfully attempted. Although a powerful research tool, ERTS-1 has very limited use as an operational system for the hydrologic community because of its 18-day revisit cycle and its lack of a "quick-look" capability.

17. Key Words Suggested by Author	18. Distribution Statement
snow, snowmelt, satellite, runoff, hydrology, snow-extent mapping, limnology, lake ice, lake currents, flood mapping, soil moisture.	

19. Security Classif. (of this report)	20. Security Classif. (of this page)	21. No. of Pages	22. Price
NONE	NONE		

EVALUATION OF ERTS-1 DATA FOR CERTAIN HYDROLOGICAL USES

Donald R. Wiesnet — Principal Investigator
David F. McGinnis — Co-investigator
Michael C. McMillan — Associate

National Oceanic and Atmospheric Administration
National Environmental Satellite Service
Environmental Sciences Group
Suitland, Maryland 20233

November 1974

Final Report

Prepared for:
GODDARD SPACE FLIGHT CENTER
Greenbelt, Maryland 20771

PREFACE

"Spaceship Earth," as it has been aptly termed, consists of about 70% water at its surface. This all-important resource--water--moves eternally and dynamically through changes of state from gas to liquid to solid and back again, permeating to great depths and rising to stratospheric heights. Everywhere it goes, water sustains and nurtures life. Those of us who study the incredible and complex writhings of the hydrologic cycle are termed "hydrologists". None of us has an expert's knowledge of the entire cycle; each of us tends to concentrate on one or two small aspects of this vast, interdisciplinary subject. The practical difficulties and the high cost of attempting a detailed study of even a small, say 2,000 km^2, river basin are staggering and cannot be appreciated by the layman. Yet efficient management of our water resources becomes more important every day for those of us aboard "Spaceship Earth."

Within the Federal Government, the responsibility for effective monitoring of the Nation's water resources is vested in a host of agencies; NOAA is one of those agencies. As part of NOAA, the National Environmental Satellite Service is continuously evaluating and studying new hydrologic applications of satellite data. The ERTS-1 satellite provides hitherto unavailable, synoptic spectral-reflectance data on mesoscale hydrologic features such as snow, water, ice, soil, vegetation and rock.

But these features involve disciplines with which even the interdisciplinary hydrologist may not be totally familiar. Nevertheless, this exploring of new ground must be done if we are to use the satellite data wisely. The transition from aircraft remote sensing to satellite data collection is not going to be simple, nor will it be warmly embraced by the operational hydrologist until and unless the advantages are clearly revealed to him in a most convincing manner. ERTS-1 has gone a long way toward demonstrating these advantages. The chief conclusions of this study are listed below. Recommendations follow the list of conclusions:

Conclusions

Snow mapping

1. Snow mapping studies of Sierra Nevada basins have shown that maps can be produced six times faster from ERTS-1 imagery than from high altitude (20,000 m) aerial photographic surveys.

2. ERTS-1 images are most effectively used for snow mapping in moderately sized (250 - 30,000 km^2) basins, such as the American and Feather River basins in California.

3. The 80-meter ground resolution of the Multispectral Scanner Subsystem (MSS) produces unsurpassed images with excellent cartographic fidelity for snow extent measurement. ERTS-1 MSS has no peer as a snow extent mapping instrument.

4. The authors have used the ERTS-1 imagery as a check on the accuracy of the NOAA-2 VHRR imagery which is also useful for mapping snow extent (at 900 m resolution). ERTS-1 has proved to be the standard of measurement for estimating systemic errors involved in operational mapping methods using VHRR.

5. The satellite's 18-day return period plus the delay in receiving data, are adverse factors that make ERTS-1 unusable in an operational scheme. On the other hand, snow melt and snow extent/runoff curves can be compiled pass by pass and may become forecasting tools rather than interesting hindcast records, when the number of observations becomes statistically significant.

6. The cost of Sierra Nevada snow maps produced from ERTS MSS or NOAA VHRR imagery is estimated to be approximately one-two hundredths of the cost of the simplest maps made from aircraft surveys.

7. In those cases where satellite data are adequate to replace aircraft surveys, significant savings in fossil fuel consumption accrue.

8. In the Lake Ontario basin, the ERTS-1 data proved to be inadequate for basinwide snow mapping owing to the basin's large (70,000 km^2) areal extent and the cloudiness over the area. Nevertheless, by conjunctive use of ERTS-1 MSS data we consistently found that NOAA-2 VHRR data could be interpreted better and with much greater assurance and authority.

9. In thickly forested areas such as the Adirondack Mountains, snow is not observable except in clearings and on ice-covered lakes. This problem is worthy of further detailed study.

10. Visual discrimination of snowlines at small scales (1:1,000,000) is far easier than is CCT discrimination at large scales (1:15,000).

Snow surface melting

11. The reduced spectral reflectance of melting snow in band 7 was observed in the MSS data visually and also in the CCT printout data.

12. The simultaneous viewing of scenes in which the multispectral digital data may be matched spot for spot permits the gathering of unambiguous spectral information on snow reflectance and other terrain materials such as soil or rock outcrops. However, in the case of snow the low threshold of saturation of the MSS limits the usefulness of the technique.

Meltwater runoff relations

13. Although only several examples were studied, a spectral reflectance decrease factor (SRD) in high altitude subbasins was compared to daily

runoff figures. In some cases both the SRD and a drop in rate of snow cover coincided with sharp increases in runoff. Further studies of these relationships are warranted.

Albedo

14. Despite a high correlation coefficient, the relation of albedo to percent of snow cover in the American River basin is based on an insufficient sampling. Nevertheless, so little is known of spectral and total reflectance, albedo, and the relation of these parameters to snow pack conditions that even these data are of interest. Further work in both laboratory and field is highly desirable, and is planned.

Lake ice

15. Never before have scientists been able to observe the dynamics of lake ice development, migration, and dissipation with such clarity. Conjunctive use of NOAA VHRR data can meaningfully extend the ERTS data into other areas.

16. The 18-day revisit cycle for ERTS-1 is highly inadequate for monitoring ice formation, movement and breakup in the Great Lakes area.

17. Sidelap analyses of 24-hour ice movement can provide Lagrangian current information for portions of the Lakes.

18. Spectral reflectance information available from the MSS allows inferences to be made on the condition of the ice pack in the same way that spectral reflectance changes permitted us to assess the condition of the snow pack; i.e., whether the ice is melting.

Lake currents

19. Considerable information on details of lake currents can be inferred or measured from ERTS-1 data by analyzing ice fragment or algae movement and sediment patterns.

Soil moisture

20. Neither CCT printouts nor ERTS-1 MSS imagery provided a means to assess soil moisture in the vegetated farmland of the Finger Lakes region of New York State.

21. Spectral curves can be generated from densitometric measurements taken from aircraft multispectral images and used for soil moisture analysis; but unless the fields are devoid of vegetation and of the same soil type, the usefulness of such analysis is conjectural.

Flood mapping

22. Other researchers have demonstrated the usefulness of ERTS-1 MSS images

for flood inundation mapping. Most important is the surface wetness effect which persists for 10 to 12 days after the flood crest. Satellite flood mapping is fast and inexpensive, though without a quick-look capability, it is limited to a post-flood role and cannot be considered a warning system. It is especially good at scales of about 1:250,000 to 1:100,000.

Miscellaneous

23. ERTS-1 provides up-to-date information on river basin parameters and land use that affect the ecological response of the basin to hydrologic events. These data are of special importance to computer analysis that rely on parametric models.

24. Phreatophyte monitoring in the West is easily performed with ERTS-1. More importantly, the results of phreatophyte eradication projects can be evaluated.

25. Glaciers are adequately monitored with an 18-day revisit cycle. The excellent resolution of the ERTS-1 MSS makes it outstanding for glacial monitoring.

26. Groundwater cannot be directly sensed by ERTS-1; however, it may be inferred from seeps and springs and vegetation (in arid regions). The surface expression of aquifers can be mapped and their ground water potential can be estimated prior to exploratory drilling.

Recommendations

1. Although ERTS-1 is a research satellite, it can and should have a quick-look capability. This need was demonstrated during the 1973 Mississippi River floods.

2. NOAA should adopt the practice of checking operational snow-extent maps of the river basins prepared from the NOAA-3 and -4 VHRR data against the ERTS-1 MSS data to insure accuracy and to monitor the quality of the mapping technique.

3. A thermal band on future ERTS satellites would improve interpretation of satellite data. This need is extremely important to hydrology with regard to snow, ice, and soil moisture investigations.

4. NOAA and the U.S. Coast Guard should use ERTS MSS (if a quick-look capability for ERTS were established) and NOAA VHRR data for ice forecasting and shipping forecasts.

Table of Contents

LIST OF ILLUSTRATION

LIST OF TABLES

Chapter 1

INTRODUCTION

The evaluations contained in this report reflect the fact that the Earth Resources Technology Satellite-1 (ERTS-1) provided Multispectral Scanner Subsystem (MSS) data almost exclusively. The few early Return Beam Vidicon (RBV) images received prior to that instrument's shutdown are not evaluated herein. The evaluations also reflect the National Environmental Satellite Service's interest in hydrologic applications commensurate with the operational needs and responsibilities of various agencies within NOAA. In this regard, it should be obvious that imagery-type interpretation techniques are stressed because of the ease of handling and the speed and ease of comprehension. Paradoxically, computer techniques require--in the research phase--much greater planning, programming and processing time and commonly, many reruns. We believe both approaches are useful and necessary.

In retrospect, the delays in delivery of imagery and Computer Compatible Tapes (CCT) from NASA were generally confined to the earliest post-launch period. Considering the enormous amount of data handling required, the writers can only respect the processing ability of NASA's distribution force. Their responsiveness where special problems did arise was gratifying and, for the most part, commendable. The Earth Resources Aircraft Program (ERAP) should also be praised for its responsiveness to special requests that we initiated. Their performance was generally excellent.

NOAA/NESS contributed an additional aircraft survey of its own over several IFYGL test sites in New York State using airborne passive microwave scanners, multispectral cameras and 2-band thermal scanners. Selected data from these flights are published in this report.

The purpose of this final report is to evaluate the ERTS-1 data that was used to study the American River basin snow cover in California, and to evaluate the usefulness of the ERTS-1 data in the study of the Lake Ontario basin in relation to the International Field Year on the Great Lakes (IFYGL) program. During the course of these studies other opportunities for evaluation came up and the authors have also evaluated data outside of these two areas. Unfortunately, the water budget and energy budget determinations that we had hoped to obtain in the Lake Ontario basin were simply overly ambitious and beyond the state of the art. In fact, the IFYGL energy budget committee has a number of calibration problems to solve before some of the groundtruth measurements can be assimilated, collated and integrated.

As in most studies, unexpected problems plagued the project. One of these was the breakdown of the NESS' old color densitometer and the delays in receiving a new color densitometer. Furthermore, as the investigation progressed, it became apparent that other investigators were making excellent hydrologic evaluations in certain of the areas we had under consideration (for example, Mark Meier, 1973, on glaciers and Alan Strong, 1974, on lake currents). As a result we shifted our emphasis and concentrated on those areas that we felt were not getting adequate coverage, or where we could make a unique evaluation. One of our unique capabilities was the ability

to compare ERTS-1 MSS and NOAA-2 VHRR data. This proved to be remarkably and notably useful.

Acknowledgements

Many people have contributed to this study and the authors are grateful to all. Special mention is appropriate for D.G. Forsyth for his technical work on snow mapping; Michael Matson, a NOAA student trainee from Pan American University, who contributed greatly in both the snow studies and soil moisture studies; and Doran Sprecher, also a trainee from Pan American University who worked on lake ice analysis.

Dr. E. Paul McClain, Director of the Environmental Sciences Group, was instrumental in the conceptual phase of the project. John Pritchard of NESS played a key role in the use of the CCT digitization, and I.Y. Fitzgerald of NOS and the crew of the NOAA aircraft provided exceptional support and technical expertise for ERTS-related aircraft activity. Dr. E.L. Peck of NWS and his staff provided soil moisture data relative to the Scipio test site. The work of certain other groups, such as the Earth Resources Aircraft Program (ERAP) of NASA, are acknowledged within the body of the report.

Chapter 2

SNOW EXTENT MAPPING

Sierra Nevada

Snow mapping of Sierra Nevada basins is not new. Barnes and Bowley, (1970 and 1974) have mapped central and southern Sierra basins. The American and the Feather River Basins had not previously been attempted, but as they are hydrologically important yet sparsely populated areas, the need for more data was expressed by the National Weather Service River Forecast Center at Sacramento. The American River Basin, which lies on the western slopes of the Sierra Nevada Range (figure 2.1), was examined in more detail because of the better ground truth collection.

The American River is fed by the melting Sierra snowpack, a highly managed and important water resource. Remote snow readout measurements within the basin are available at Blue Mountain, and seven other sites within the basin. In addition, the Central Sierra Snow Laboratory is located immediately north of the basin. (See fig. 2.2).

The ERTS-1 orbit permitted observations of the basin once every eighteen days, weather permitting. Fortunately, despite minor orbital readjustments, this 4,890 km^2 basin was generally contained within one ERTS-1 frame of imagery. On a few occasions, the western, non-snow-covered portion was not on the frame. However, this omission fortunately had no effect on the measurement of the snow-covered portion so that all snow measurements are indeed synoptic.

The objective in the Sierra Nevada region was to evaluate the capability of ERTS-1 sensors to monitor snowmelt on an 18-day revisit cycle.

U-2 Photography

All available U-2 color-IR (0.51-0.90μm) photography of the Feather River Basin was examined to determine which images contained the best variety of snow, ice and no-snow areas. The overall clarity of the film (i.e., exposure, image contrast, absence of scratches, etc.) was also an important factor considered. Imagery from flight number 72-036 (accession number 00221) taken on March 6, 1972, was ultimately selected. Color-IR offered the best contrast between snow and no-snow areas when compared with the other spectral bands. The photographs (1:445,000) were projected individually onto a topographical map of the basin (1:250,000) by use of a Zoom Transfer Scope (ZTS). This photo-optical device allowed each image to be enlarged, rotated and stretched until the image was registered at the 1:250,000 scale. Edge distortion of the photographs was evident, and whenever possible only the central portion of the photograph was used for mapping. Twenty-three photographs were required to map the basin. It should be noted that "data holidays" in the coverage at the edges of the basin precluded 100 percent coverage of the basin.

Comparison of the snow map derived from U-2 photography with limited ground truth showed one discrepancy. French Hill had 90 cm of water content in

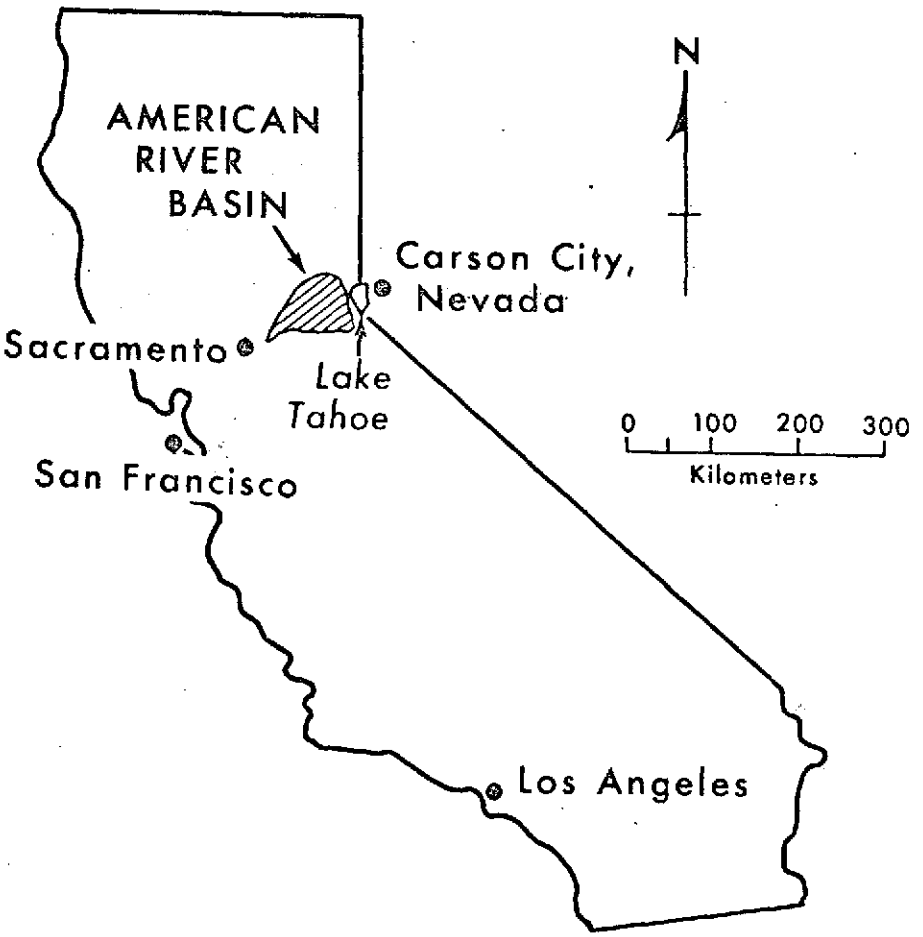

Figure 2.1 Index map showing location of American River Basin, California.

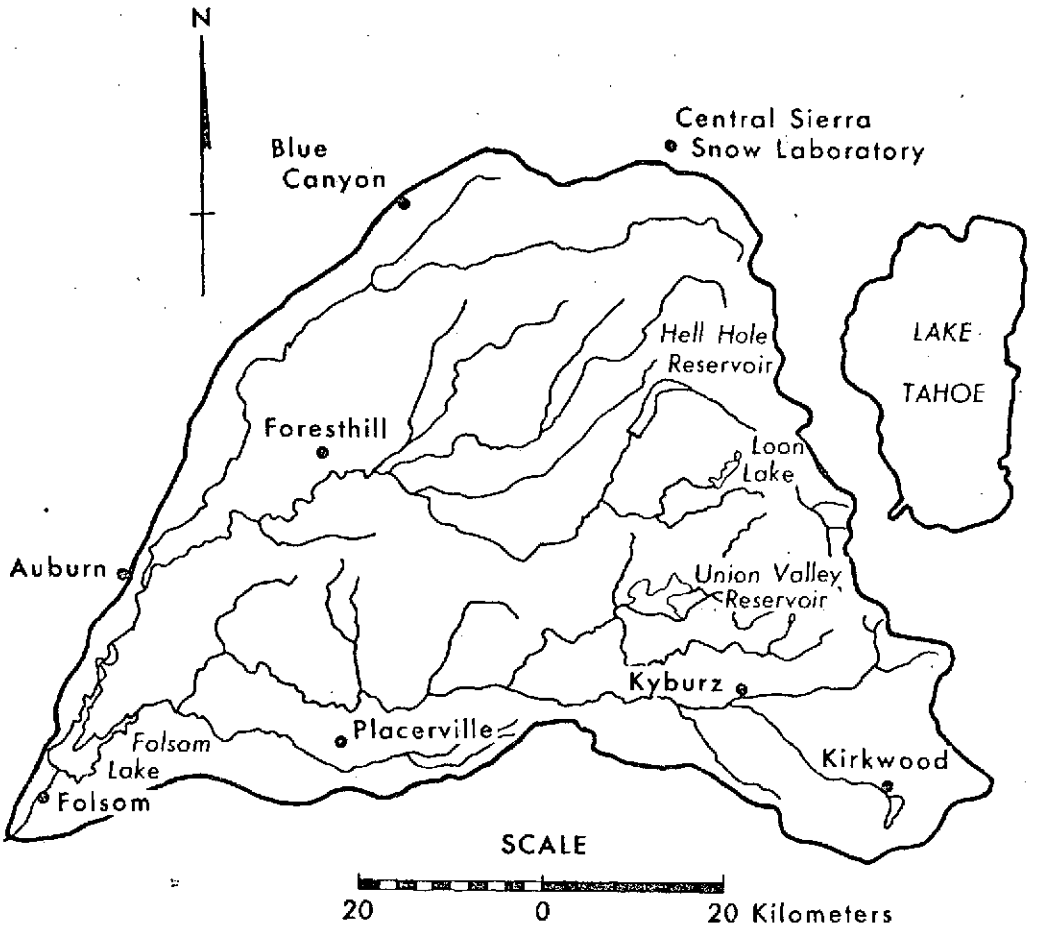

Figure 2.2 Drainage map of the American River Basin, California.

existing snow, yet the aerial photograph indicated no snow. The discrepancy has been attributed to the fact that this area lies close to the edge of two aerial photographs, hence positional error of the snowline is likely. Unless photogrammetric techniques are used, this type of error is inherent in mapping from air photographs.

The mean elevation of the snowline on south-facing slopes was determined to be 30 m lower than that on north-facing slopes. This is contrary to expectation and could be the result of the deep shadow effect in steep-walled canyons and cliffs as well as the previously described positional problems.

Production of this snow map required a total of 22 man-hours of labor, four of which were used to prepare and mount frames prior to the actual mapping operation.

ERTS-1 Imagery

ERTS-1 imagery of the Feather River Basin for November 29, 1972, January 4, 1973, and January 22, 1973 were utilized for snow-extent mapping. The 1:3,369,000-scale 70-mm ERTS chip (MSS band 5) was enlarged to 1:500,000 in the ZTS and mapped directly onto the base map in the same manner as described in the section U-2 Photography. The ERTS-1 data was much easier to handle, mount and register onto the base map. It was much quicker as well; half an hour for setup and three hours for mapping produced a finished map. This represents a 6:1 ratio in favor of the ERTS-1 snow mapping over the use of high-altitude aerial photographs in terms of man-hours saved. Furthermore, the shadow problem is greatly reduced, the positional accuracy of the snowline is much more consistent and the light forest cover tends to be less of a problem with reduced ground resolution. Six ERTS-1 images were similarly used to provide snow maps for the American River Basin (fig. 2.3).

NOAA-2 Imagery

NOAA-2 Very High Resolution Radiometer (VHRR) visible band imagery has been acquired over the Sierra Nevada daily. Thirteen cloudfree images over the American River Basin were selected for analysis, using the ZTS as described previously. Rectification in this case was much more difficult, owing to the larger distortion found in the imagery, especially at the extreme edge of the image. The images were enlarged, usually about seven times, and "stretched" to make the drainage pattern of the image fit the drainage pattern of the map.

A comparison of the NOAA-2 data and the ERTS-1 data (figure 2.4) when both data sets are plotted as snowmelt curves reveals close similarities. Note that the ERTS snow-extent measurements usually are greater than the NOAA-2 VHRR measurements. We believe that this condition is due to the outstanding geometric characteristics of the ERTS MSS, which make it literally a calibration standard for snow-extent and indeed for any type of areal-

AMERICAN RIVER BASIN
APRIL 3, 1973
SNOW COVER 49%

Figure 2.3 Snow extent map of the American River Basin prepared from ERTS-1 MSS band 5 imagery.

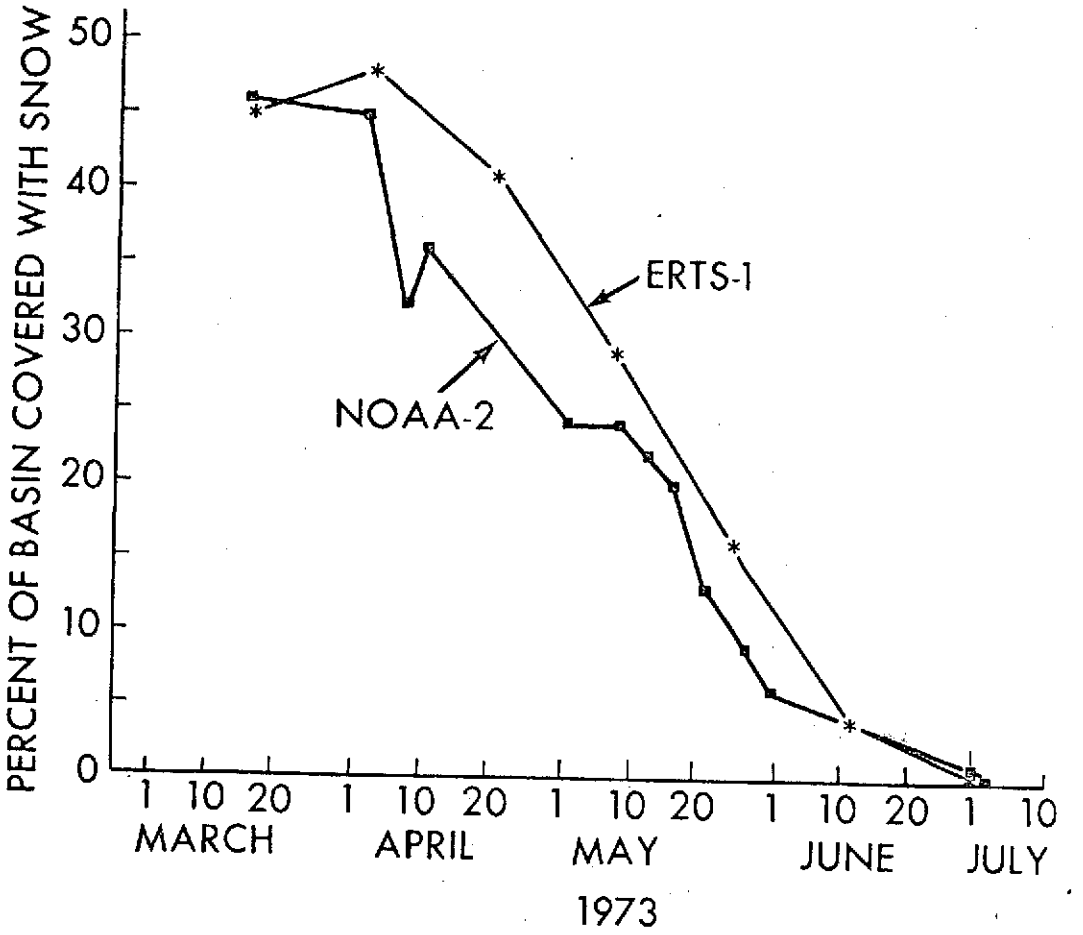

Figure 2.4 Comparison of ERTS-1 MSS and NOAA-2 VHRR snow-extent mapping in the American River Basin, 1973.

extent measurements. A color additive viewer has been used as a change-detection device to demonstrate snow meltback patterns that occur from one ERTS pass to another. By simultaneously projecting red, green, and blue light through color transparencies of three different spring images of the American River Basin it was possible to identify and record areas where the snow had completely melted away from one period to the next (figure 2.5).

At the request of the Director of the National Environmental Satellite Service, a cost/comparison figure was calculated for satellite (NOAA-2) measurement of Sierra Nevada snow cover versus conventional aircraft measurements. Assuming that 20 basins were of interest and that a simple altimeter survey by a light plane is possible, at least 40 hours would be required at a total cost of at least $20,000. Using satellite data, the entire Sierra block could be mapped in two man-days for a direct cost of about $100. This is a comparative-cost ratio of 200:1 in favor of the satellite.

Discussion

In terms of man-hours, ERTS-1 is six times faster than U-2 snow cover mapping, however, NOAA-2 VHRR snow cover mapping is almost as fast as ERTS-1, and the NOAA-2 VHRR data is timely and available more frequently. With systematic scheduled VHRR coverage (and with no clouds) daily mapping of snow cover can be accomplished. Despite its lack of timely coverage, the greater ground resolution of ERTS-1 and its cartographic fidelity make it outstanding as a snow mapping satellite. It has no peer in this respect.

From the point of view of operational snow mapping, the most significant single improvement NASA could provide is a "quick-look" capability for the snow mapping community. Resolution is much less critical to the snow hydrologist than is near-real time readout capability. Daily water level forecasts are issued; snow data one or two days old are relevant. Week-old data are probably irrelevant to the operational community.

Lake Ontario Basin

The Lake Ontario Basin occupies 70,000 km^2 in area. The best (i.e., most cloudfree) period for snow mapping was January 9-12, 1973. Even so, cloudiness in the eight frames of ERTS-1 imagery required to cover the Basin, ranged from 10 to 80 percent. Cloud contamination is a very real factor in snow-cover mapping, but the problem is relatively slight for basins that are less than 30,000 km^2 in area, because such a basin can fit within one ERTS-1 frame.

The original objective of the Lake Ontario Basin studies was to assess the ERTS data for a large temperate-region lake and its drainage basin by relating ground truth to spectral band, image density, etc., and to evaluate the effect of the 18-day cycle on hydrologic monitoring. In terms of snow cover mapping, ERTS-1 failed to furnish adequate data for synoptic snow cover maps of the basin.

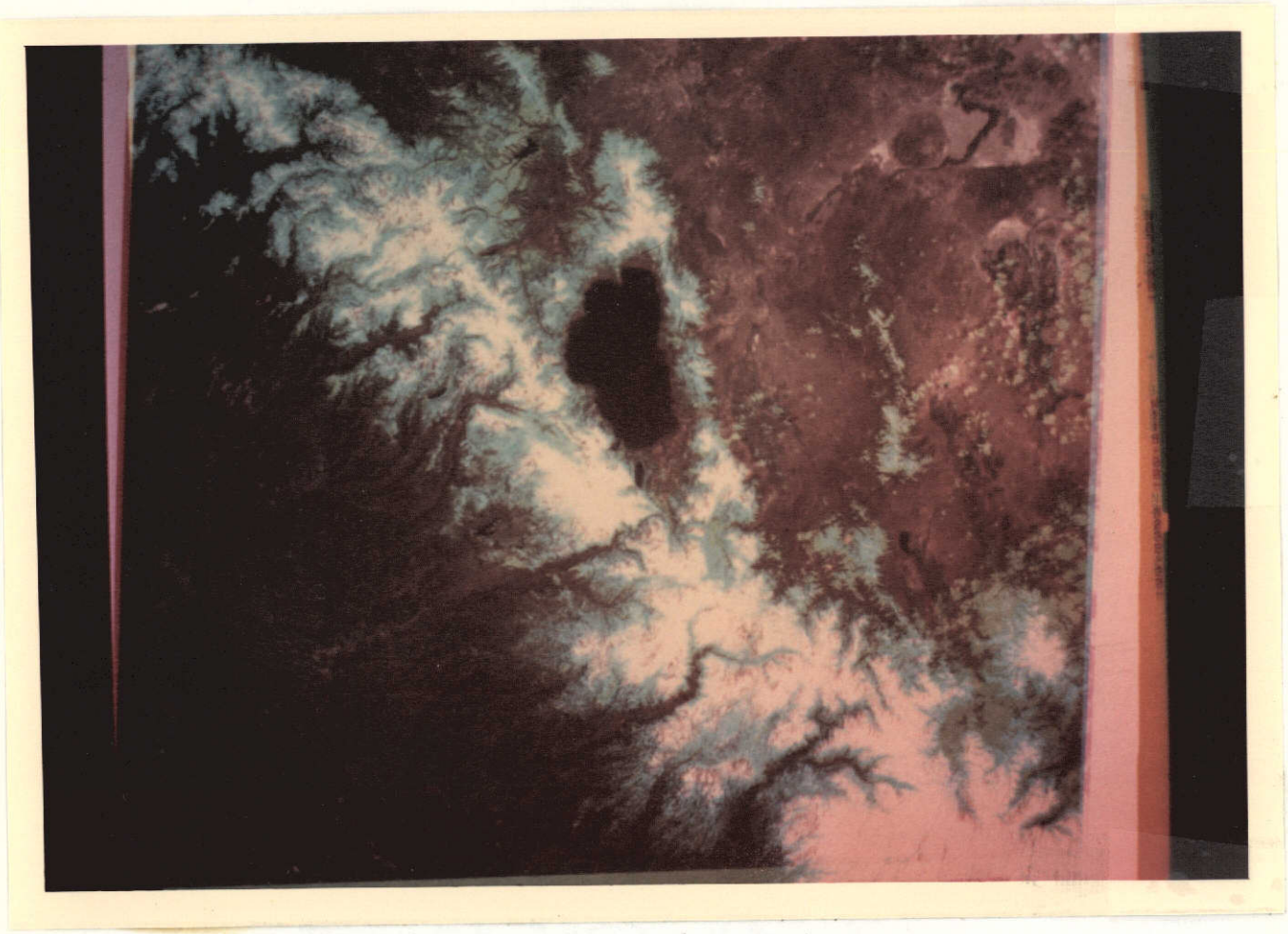

Figure 2.5 Color additive viewer prepared image illustrating the snowmelt pattern in the American River Basin and nearby Sierra Nevada basins. Using only MSS band 4, April 21 appears green, May 9 blue, and May 27 white.

The reasons for this failure are as follows:

1. The ERTS-1 orbital scan width is only 185 km; therefore it takes four days to cover the basin.

2. There was no four-day cloudfree period during the winter season.

Comparison of ERTS-1 MSS data with NOAA-2 VHRR data is meaningful in this regard. With a swath width of about 2000 km, a resolution 900 m, and a nominal orbital altitude of 1500 km, the NOAA-2 VHRR was able to secure data every day in the 0.6-0.7μm band and twice daily in the thermal (10.5-12.5μm) band. See Table 2.1.

Using an optical rectification device (a ZTS), three synoptic snow cover maps of the entire basin were prepared at a scale of 1:2,500,000. These images were selected to reveal spring snowmelt rather than early winter snow buildup. Figure 2.6 is a visible band VHRR image taken at about 0900 local time February 13, 1973. Note the small snowfree area between Toronto and Cobourg on the north shore of Lake Ontario. It amounts to one percent of the basin.

Figure 2.7 is a conventionally prepared snow cover and depth map, prepared from point source data. An operational hydrologist would wrongly assume 100% snow cover from these data. Figure 2.8 is an unusual type of map that was prepared by the Atmospheric Environment Service of Canada (Ferguson and Goodison, 1974); it shows the distribution of snowpack water equivalent for Southern Ontario for mid-February 1973 based on detailed snow-course data. Note the snowfree area corresponds rather well with the snowfree area shown on figure 2.9, the map prepared from satellite VHRR data. The extent of ice in Lake Ontario is also mapped on these three figures. Figure 2.10, March 8, 1973, was a warm day with only 32% of the basin snow covered, chiefly the northern highlands, the Adirondack Mountains and portions of the Genesee River uplands. Twenty days later (March 28), a scant 9% of the basin was snow covered (figure 2.11).

Considerable detail on the formation of ice not only in the shallow bays of Lake Ontario but also in the Finger Lakes, Lake Scugag, the St. Lawrence River, Oneida Lake and the many lakes in northern Ontario can be noted. Although we have not attempted to do so, isochrones (lines of equal time) of ice melt for the small lakes in the basin could easily have been prepared using NOAA-2 VHRR or ERTS-1 MSS data or both.

The problem of detecting snow cover in heavy coniferous areas such as the North Woods of Canada and the Adirondack Mountains of New York is indeed vexing. In general, snow in these thick coniferous forests is not observable except in clearings or on ice-covered lakes regardless of whether ERTS-1 or NOAA-2 data are used.

Table 2.1

Comparison of ERTS-1 MSS and NOAA-2 VHRR for snow extent mapping.

	ERTS-1 MSS	NOAA-2 VHRR
Altitude	900 km	1500 km
Orbital Inclination	99.1°	101.7°
Visible sensors	(Bd. 4) .5-.6μm	none
	(Bd. 5) .6-.7μm	VIS Bd. .6-.7μm
Near IR sensors	(Bd. 6) .7-.8μm	none
	(Bd. 7) .8-1.1μm	none
Thermal IR sensors	none	10.5-12.5μm
Swath width	185 km	2000 km
Resolution	80 m	900 m
Revisit time	18 days	12 hours
Cartographic fidelity	excellent	panoramic (S-curve distortion)
Design scale	1:1,000,000	1:10,000,000
Best basin size for study	$<30,000$ km^2	$>30,000$ km^2
Detect melting snow?	Yes	No
Detect new snow on old?	No	Yes[1/]

1/ Using the thermal band it is sometimes possible to determine the area of new snow on old snow (Barnes and Bowley, personal communication, 1972).

Figure 2.6. NOAA-2 VHRR image of the Lake Ontario Basin, February 13, 1973.

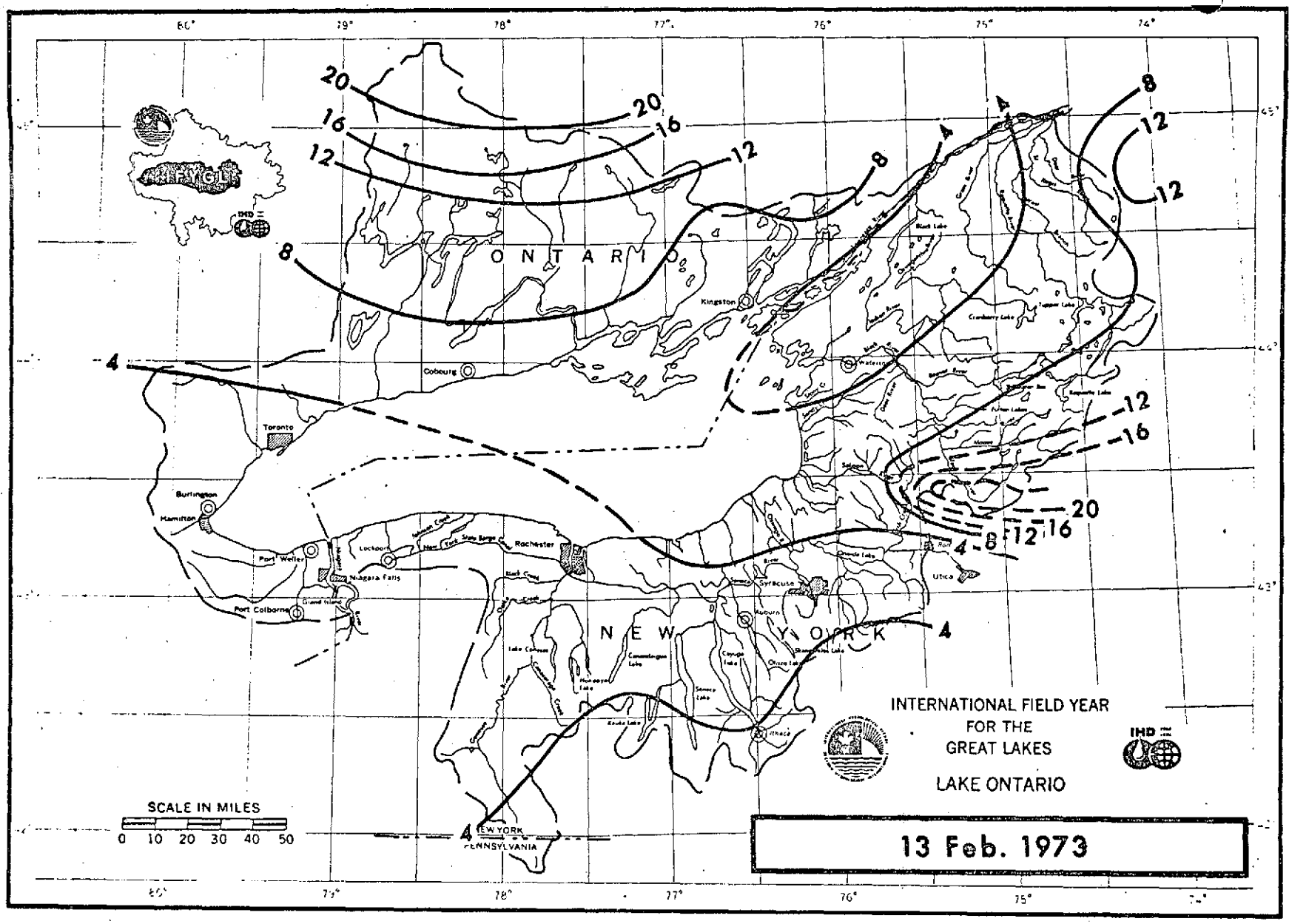

Figure 2.7 Conventional snow map showing snow-extent and depth (inches), February 13, 1973.

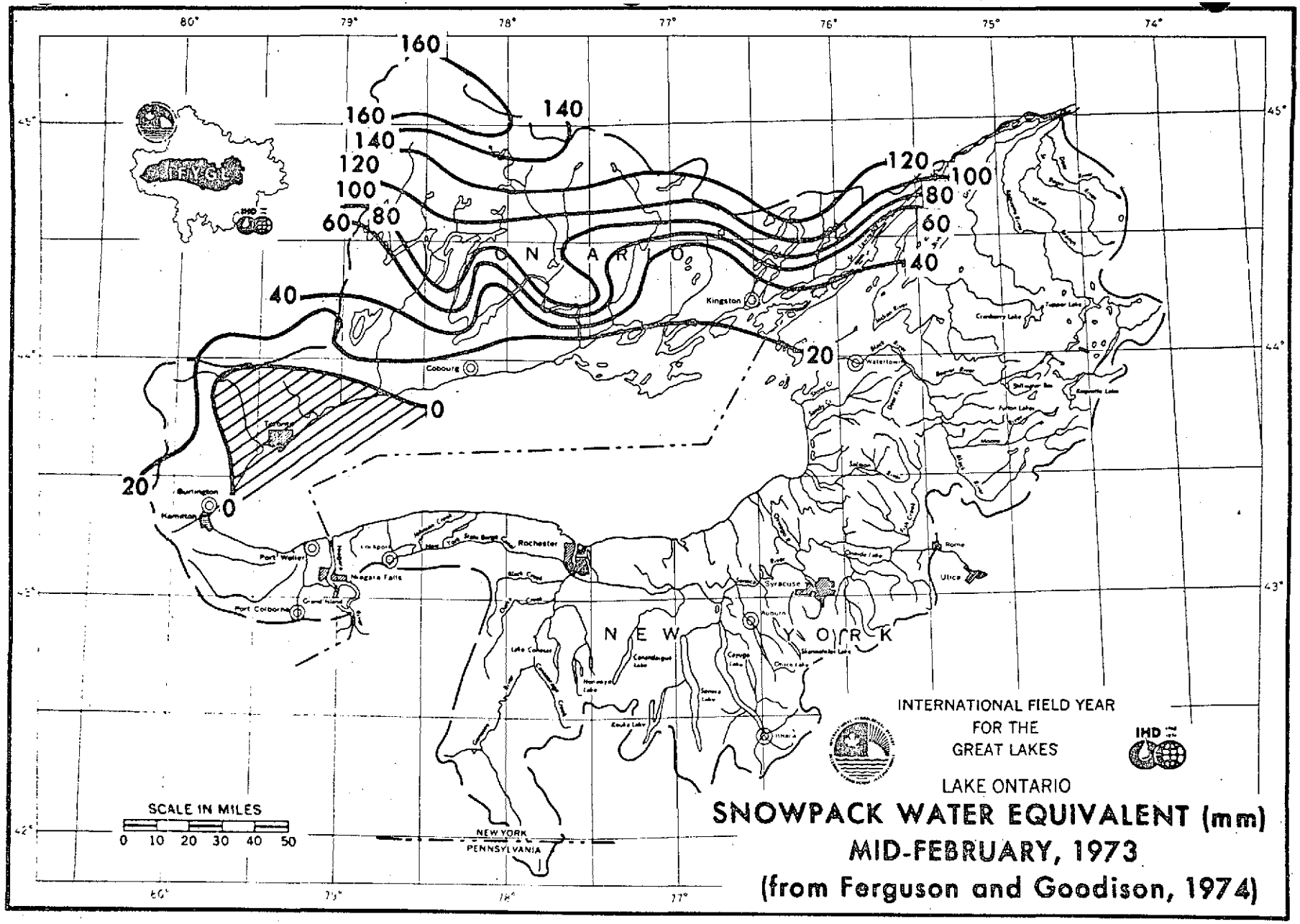

Figure 2.8 Distribution of snowpack water equivalent for northern Lake Ontario Basin, mid-February 1973 (After Ferguson and Goodison, 1974).

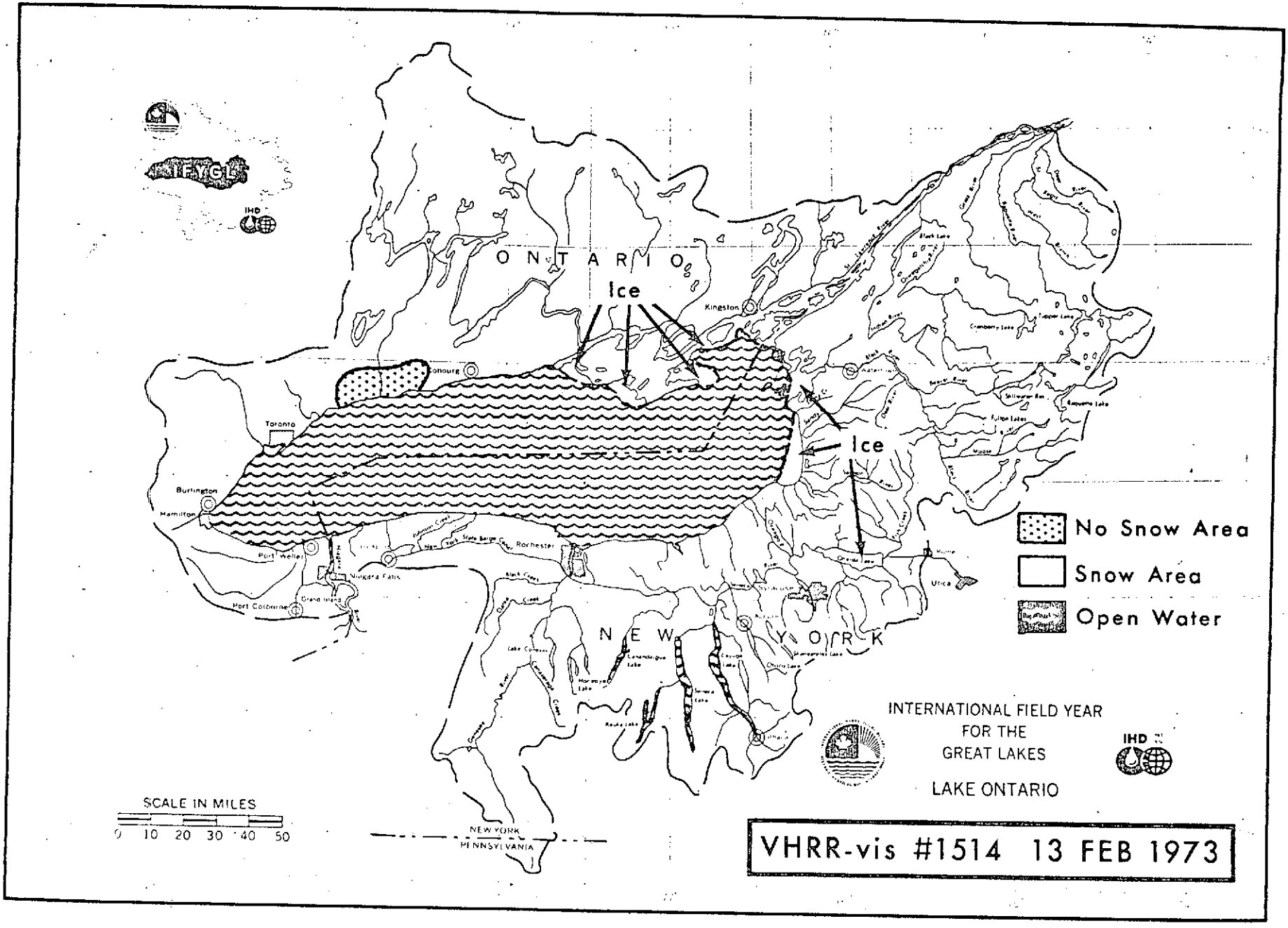

Figure 2.9. Snow-extent map of the Lake Ontario Basin prepared from NOAA-2 VHRR imagery. Basin is 99 percent snow covered. Compare with Figure 2.8.

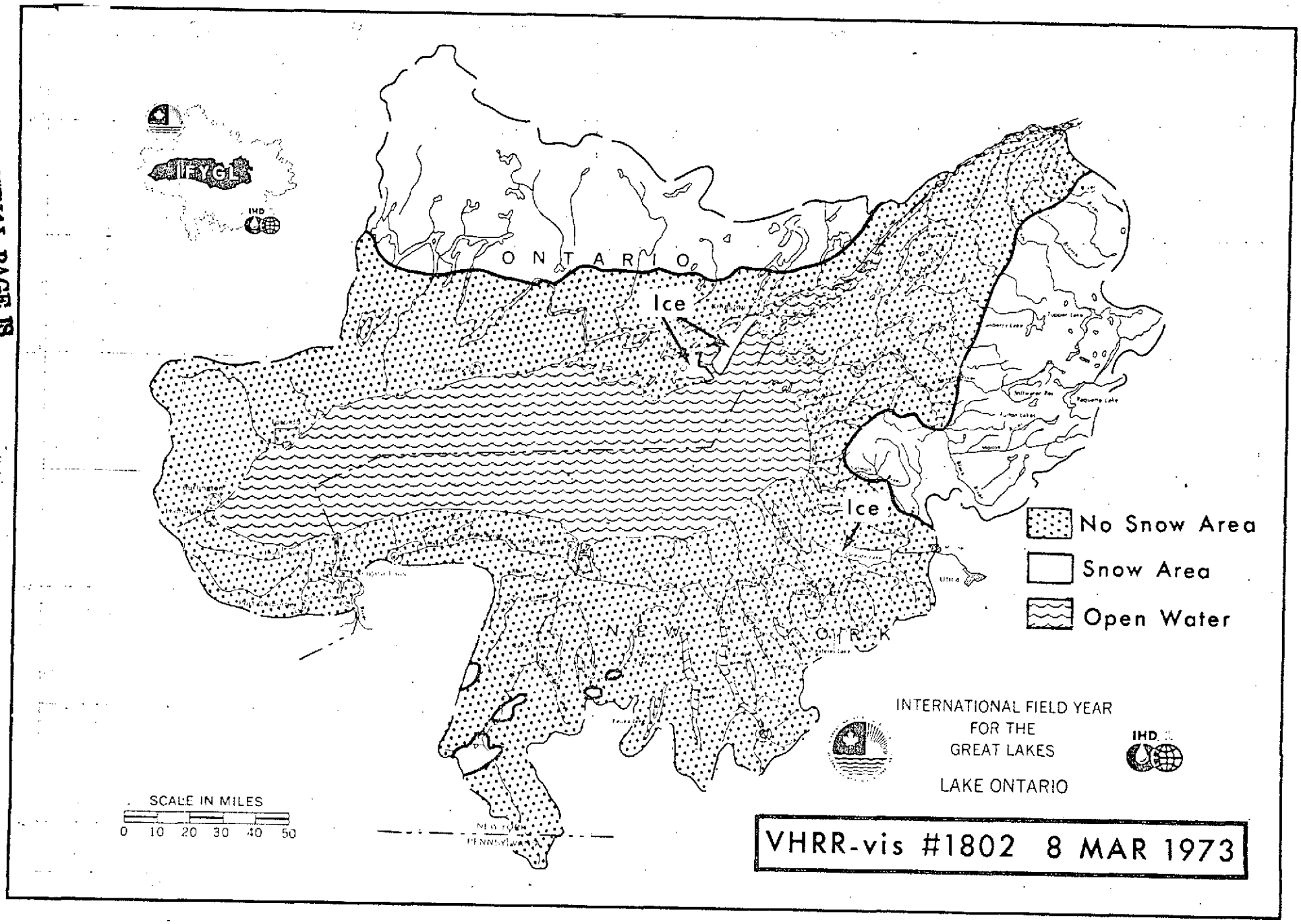

Figure 2.10 Snow-extent map of the Lake Ontario Basin prepared from NOAA-2 VHRR imagery. Basin is 32 percent snow covered.

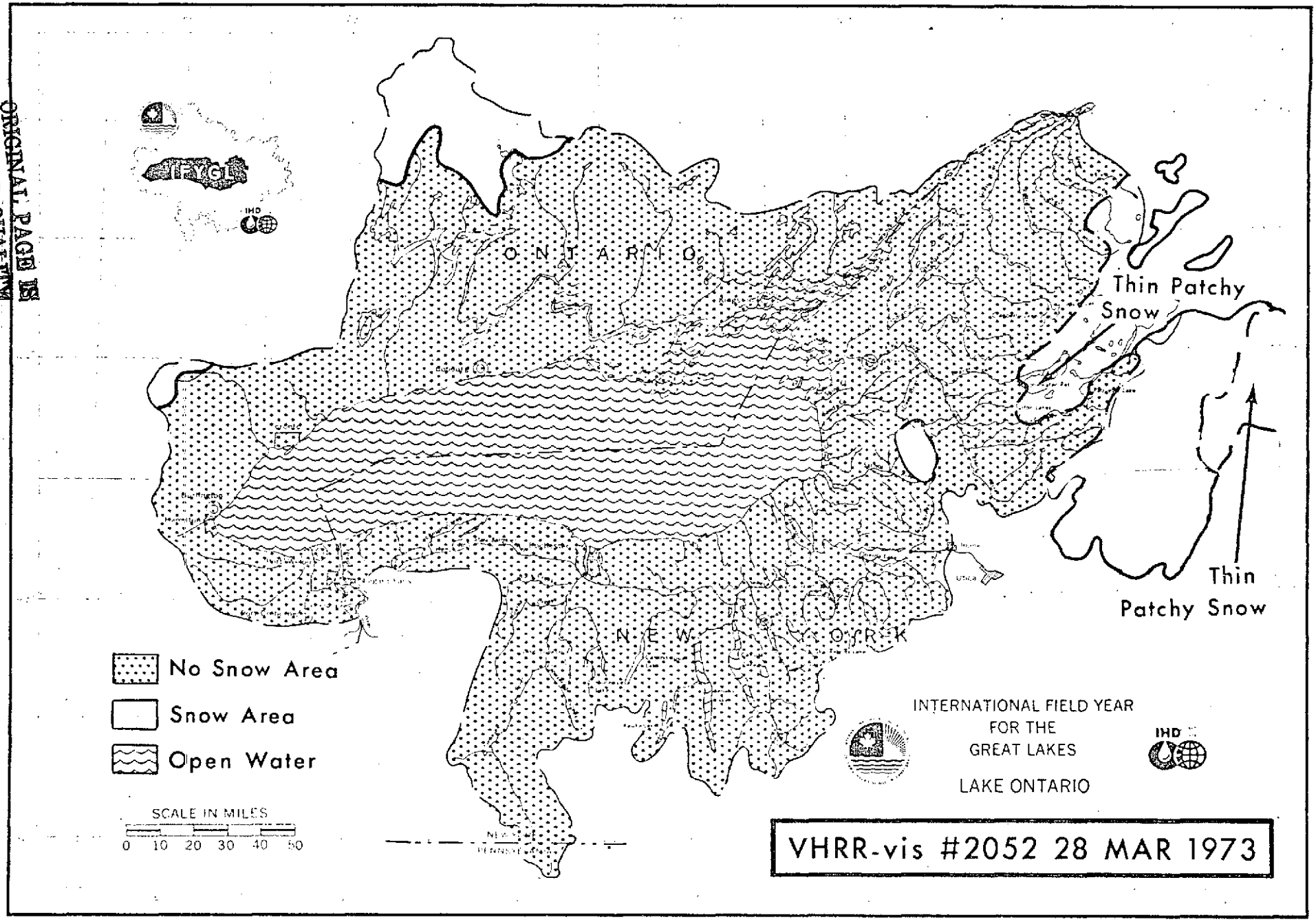

Figure 2.11. Snow-extent map of the Lake Ontario Basin prepared from NOAA-2 VHRR imagery. Basin is nine percent snow covered.

Chapter 3 SNOW SURFACE MELTING

Introduction

Previous studies by Strong et al. (1971) and McGinnis (1972) of the differential spectral reflectance of melting snow and ice using Nimbus-3 data indicate that melting snow reflects considerably less energy in the near-IR range than in the visible range of the spectrum.

A look at early ERTS-1 MSS imagery from the Cascade Mountains in Washington as well as from British Columbia tentatively supported the finding of Strong, et al. (1971) (Wiesnet, 1973). O'Brien and Munis (in press) have confirmed this satellite-observed phenomenon in their laboratory studies. Figures 3-1 and 3-2 are portions of a band 5 (0.6-0.7μm) and band 7 (0.8-1.1μm) image, respectively, which include a section of the Cascade Range. Snow-capped Mt. Eldorado (el. 2703 m) is located in the northeast corner of the images, while Snowking Mountain (el. 2267 m) and Spirepeak Mountain (el. 2517 m) are found to the south. Snow reflectance is greatly reduced in the near-IR of band 7 when compared with the visible range of band 5 in all snow areas, except near Spirepeak, indicating the probable presence of melting snow. Temperatures from meteorological stations in the Cascade area ranged from 16-29°C at 1000 PST close to the time of the satellite pass. Rawinsonde 700-mb charts place the 3280-m level temperatures near 10°C in Oregon and -3°C in northern British Columbia, confirming the presence of melting snow throughout the area.

Quantitative Studies

The possibility of detecting melting snow using satellite data has previously been accomplished by visually noting the differences in visible and near-IR images. This qualitative procedure is not necessarily reproducible and relies on individual interpretation. Quantitative spectral measurements of natural snow under laboratory-controlled aging have been conducted in cold rooms at the Cold Regions Research and Engineering Laboratory (CRREL) (O'Brien and Munis, in press). The study by O'Brien and Munis shows melting snow to be less reflective than non-melting snow from 0.8-1.4μm. "With the onset of surface melting, the near infrared reflectance decreased drastically" (p. 17, O'Brien and Munis, in press). Some of their experimental data are presented in figures 3.3 and 3.4. For the pre-melting cases, because their curves were almost identical, only one curve is shown (figure 3.3, curve A). For the same reason, only a single curve is shown for the melting and refrozen cases (figure 3.3, curve B). Curve A (figure 3.3) represents crusty old snow sifted through a food mill which produces snow very similar in appearance, texture, and physical properties to naturally wind-blown snow. This snow was first scanned at -19°C, then at -1.5 to -0.5°C and again at -19°C. The density of this snow remained 0.366 g/cm^3 during these scans. In the second series of runs, curve B (figure 3.3), the temperature was first raised above freezing (2.5 to 10.0C), then maintained at 5C for the second of the three tests. During the second run, the surface of the snow was soft and wet to a depth of approximately

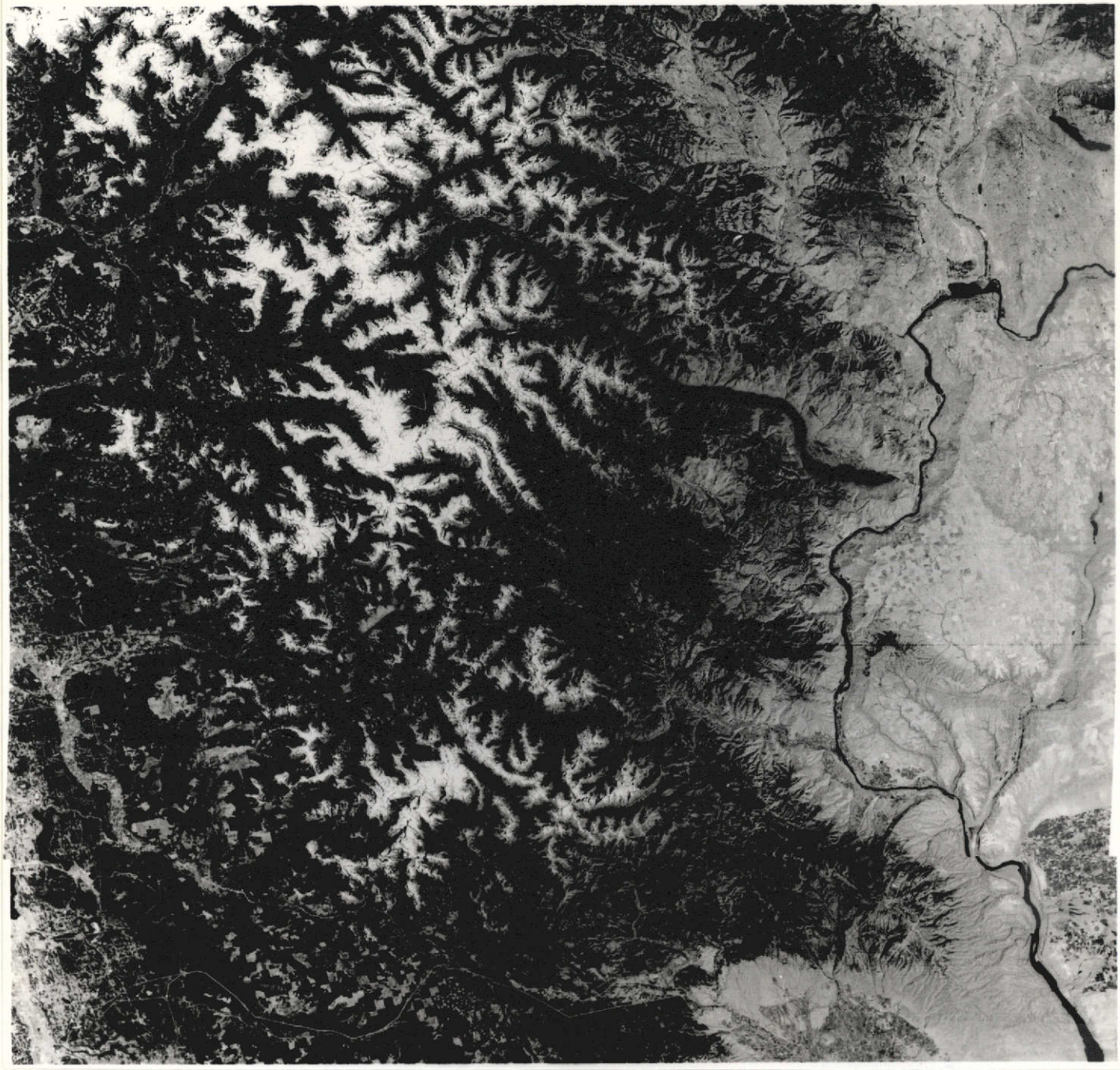

Figure 3.1. ERTS-1 MSS band 5 image of the northern section of the Cascade Range, Washington, July 28, 1972. Lake Chelan is near the center of the image.

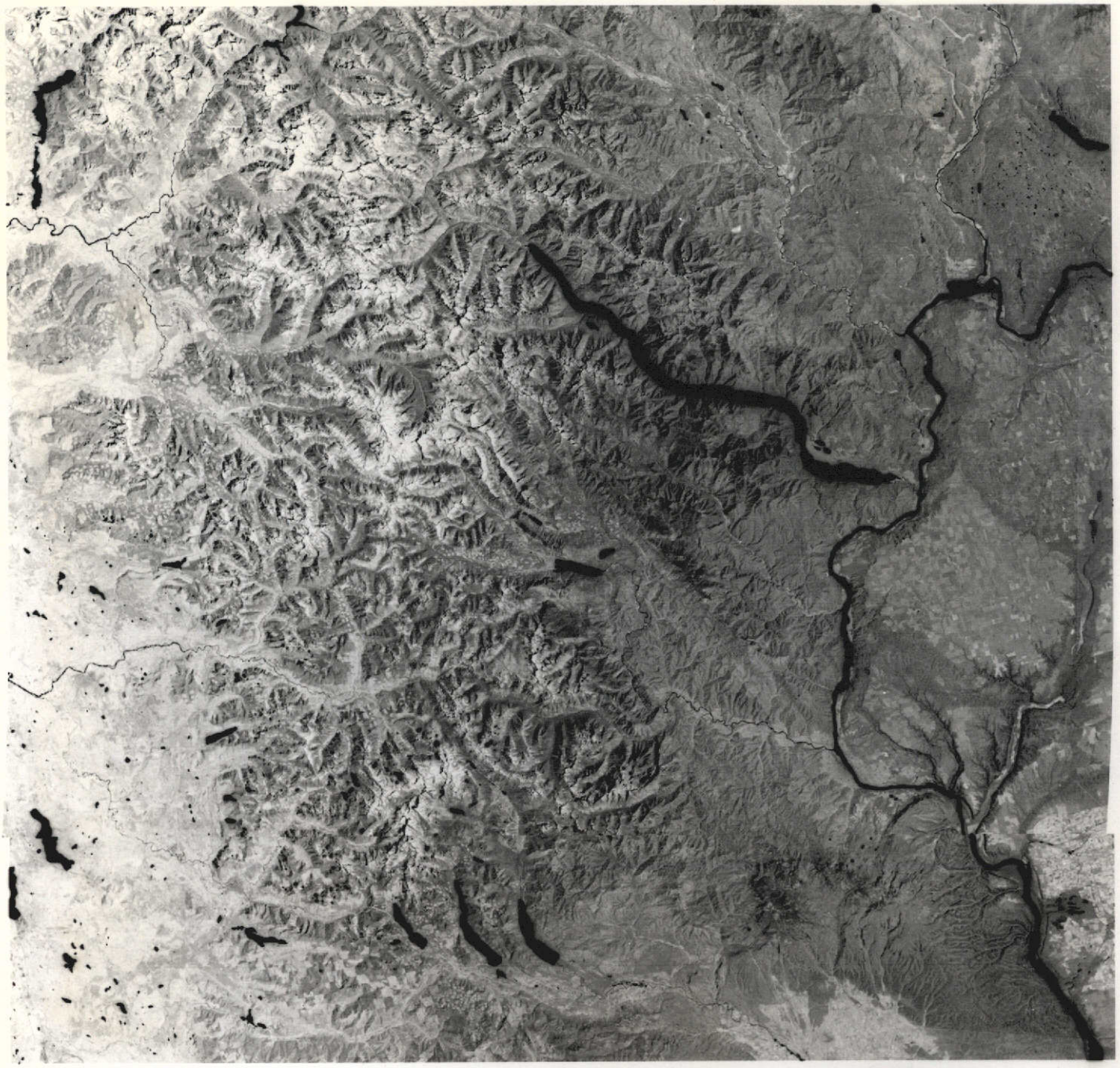

Figure 3.2. ERTS-1 MSS band 7 image of the northern section of the Cascade Range, Washington, July 28, 1972. Compare with figure 3.1.

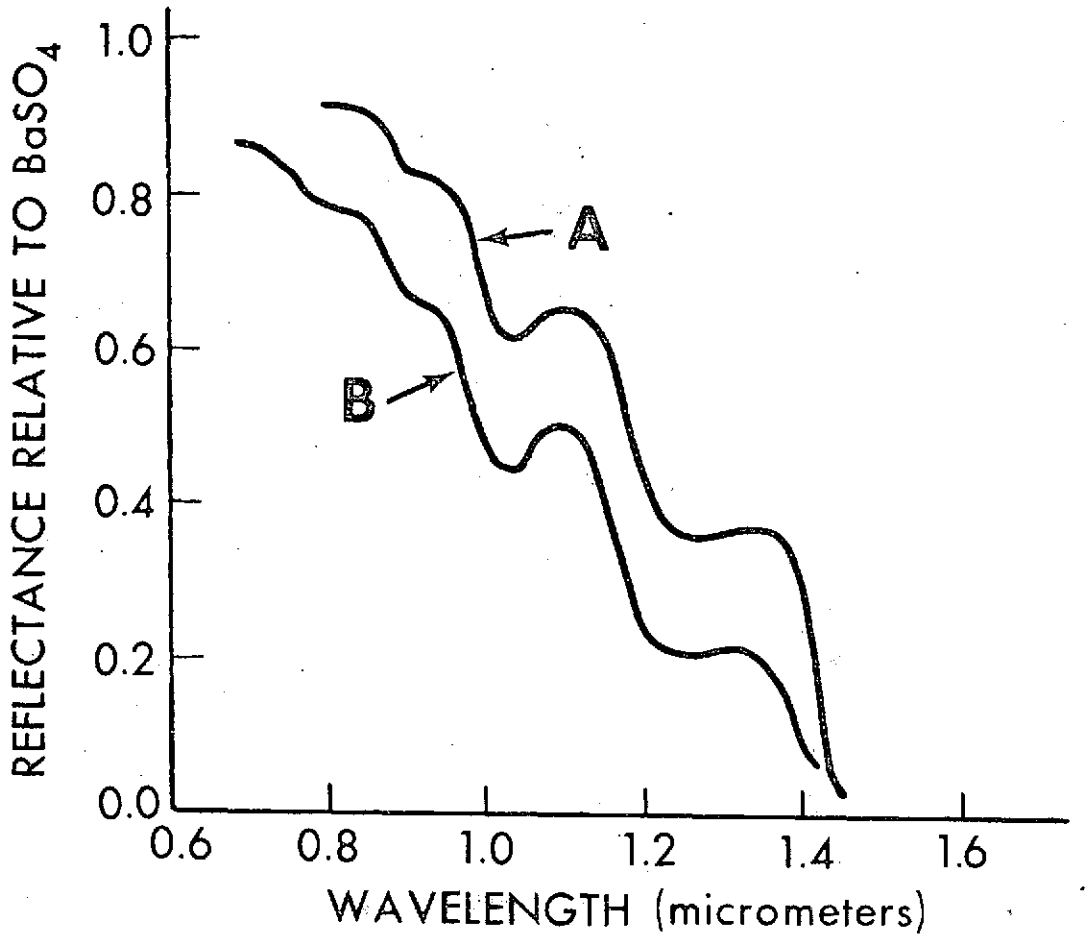

Figure 3.3. Reflectance of non-melting (A), and melting and refrozen (B) snow surfaces relative to $BaSO_4$ (After O'Brien and Munis, in press).

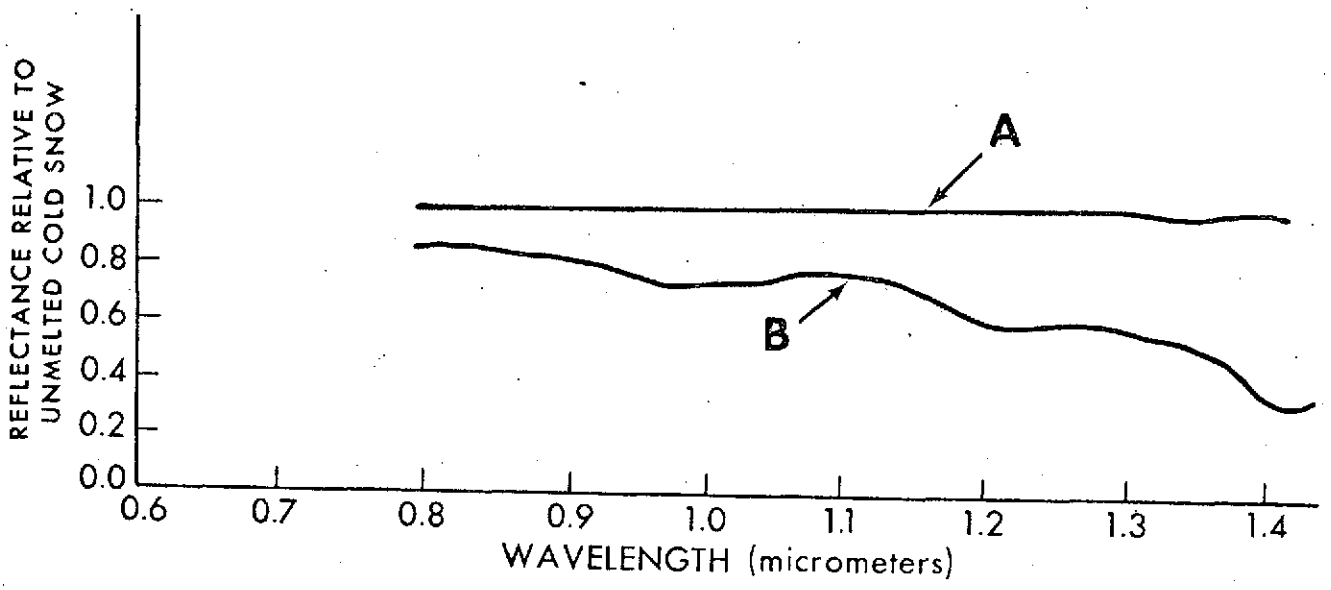

Figure 3.4. Ratio of reflectance of non-melting (A), melting and refrozen (B) snow relative to reflectance of original non-melting cold snow (After O'Brien and Munis, in press).

0.3 cm. Finally the snow was refrozen and a series of readings recorded at -5C. The density of the snow increased to 0.525 g/cm^3. Figure 3.4 presents the ratio of the reflectance of non-melting, melting, and refrozen snow relative to the reflectance of the original cold snow. For the non-melted snow (curve A in figure 3.4), the ratio remains essentially 1.0 from wavelengths 0.8 to 1.4μm. The melting and refrozen snow ratios which in this case are equal, start near 0.80 at 0.8μm (curve B) and fall to less than 0.4 at 1.4μm. These last ratios are significant in that frozen, but once melted, snow may exhibit the same reflectance properties as melting snow. Such snow surfaces (i.e. refrozen) are likely to exist in the American River Basin during the early spring when afternoon temperatures frequently exceed the freezing point, but nighttime and even late morning (ERTS-1 passage time) temperatures may still be sub-freezing.

Visual Mapping of Melting Snow

Inspection of six successive ERTS-1 70 mm images from April 21 through July 2, 1973 showed snow surfaces to be less extensive, especially during the late spring when melting is most advanced. (Table 3.1). Table 3.2 presents meteorological data at or near the time of each ERTS-1 overpass. Air temperatures were interpolated using minimum and maximum temperatures from stations within the basin. Since portions of the snow areas are at higher elevations (>2500 m), lower temperatures would be expected at those elevations at the time of ERTS-1 passage than indicated in Table 3.2.

The snow extent was mapped for each of the four MSS bands for the seven cases. There was some cloud contamination on June 14, but the effect on measurement of the percent of snow cover for that date is believed to be negligible. For each case, except July 2, 1973, when only a trace of snow remained in the basin, the percent of the basin covered with snow was observed to be less in Band 7 than in Band 5. This observation substantiates earlier studies (Strong et al, 1971; Barnes and Bowley, 1974) comparing near-IR images with those in the visible range.

Digital Analysis

Studies of quantitative satellite-derived brightness as it pertains to melting snow are unknown. Therefore, a study was undertaken using the ERTS-1 CCT's. MSS bands 5 and 7 were chosen to examine the spectral reflectance of snow in the visible and near-IR regions. These two bands are similar to the previously selected bands for pictorial assessment of melting snow (Barnes and Bowley, 1973).

ERTS-1 provides for the first time on an environmental satellite simultaneous views of the Earth in the visible and near-IR portions of the spectrum in which multispectral digital data may be matched spot for spot. Nimbus-3 (GSFC, NASA, 1969) carried similar simultaneous--but separate--sensors, thus the digital data could not be matched exactly.

A study area within the American River basin (figure 3.5), where some snow

Table 3.1. Measurement of basin snow cover.

	3/16/73	4/3/73	4/21/73	5/9/73	5/27/73	6/14/73	7/2/73
Band 4	46	49	40	26	16	4	T
Band 5	45	48	41	29	16	4	T
Band 6	45	44	38	28	15	2	T
Band 7	42	43	36	26	12	2	T

Table 3.2. Meteorological Conditions at or near satellite passings.

	1800 Z Surface Conditions		850 mb Temp °C		700 mb Temp °C	
	Air Temp °C	Cloud Cover in tenths	1200Z	0000Z	1200Z	0000Z
3/16/73	-1	0	6	6	-2	-3
4/3/73	1 - 3	1	5	7	-5	-3
4/21/73	3 - 4	0	4	8	-5	-1
5/9/73	8 - 10	0	13	19	5	5
5/27/73	8 - 10	0	12	20	5	8
6/14/73	8 - 10	3	10	11	-1	-2
7/2/73	26	0	19	25	9	12

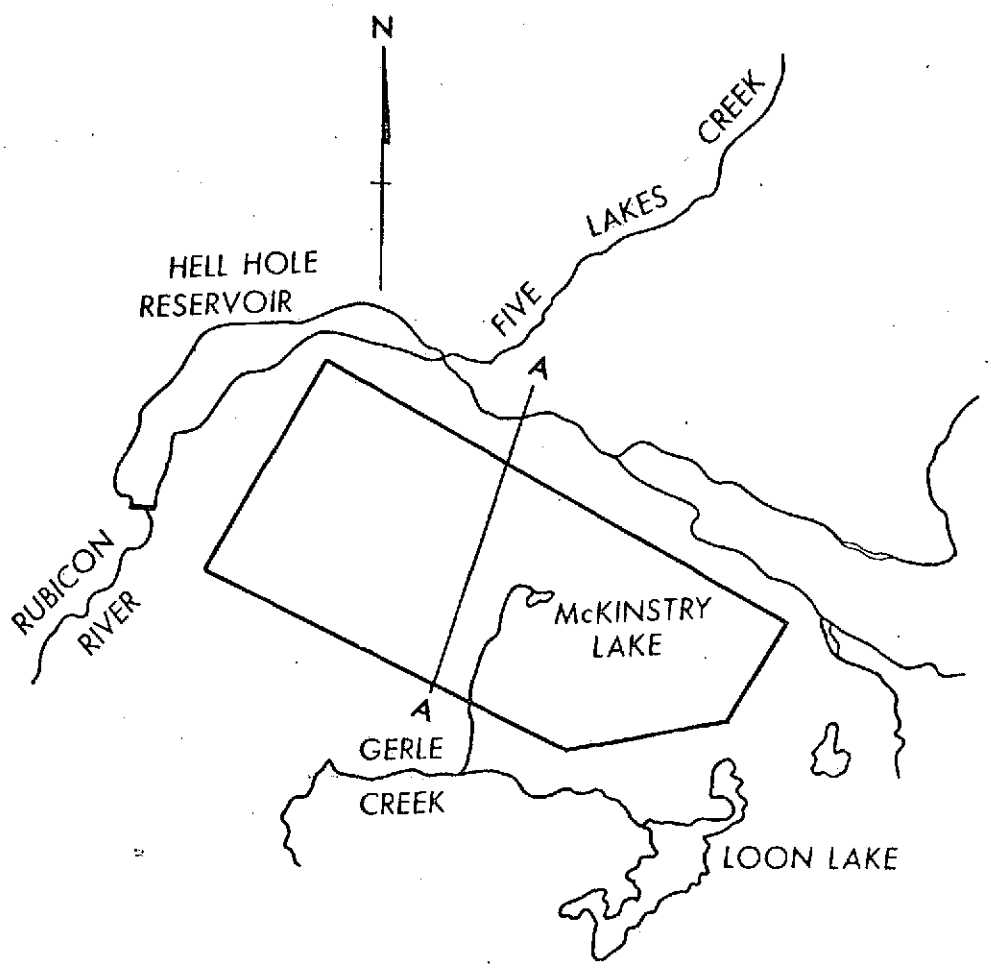

Figure 3.5. Study area for digitized analysis of snowmelt within the American River Basin.

remained until the July satellite observation, was selected for examination. CCT data for the area in band 5, band 7, and band 5 minus band 7 were displayed in 32 x 32 grids (approximately 2.6 x 2.6 km).

Each digital display, at a scale of approximately 1:15,000, was contoured at 8-step intervals from 0 to 120. The range of the gray scale is 0-127 in band 5 and 0-126 in band 7. Color schemes were applied at 16-step intervals, viz., 0-23 blue, 24-47 green, 48-71 yellow, 72-95 orange, 96-119 red, while values exceeding 120 were left uncolored. It was thought that such a grouping by colors would enhance snow boundaries in band 5 and, more importantly, separate melting from non-melting areas of snow in band 7. Figures 3.6 and 3.7 show examples of the contouring for bands 5 and 7 respectively, on May 27, 1973.

Detection of the snow boundary in band 5, however, proved somewhat difficult at a scale of 1:15,000. A smaller scale would allow the snow boundary to be located more precisely. Nevertheless, a value of 70 or greater appeared to lie within the snow area, while values less than 50 were designated as snow-free.

Snow patterns (i.e. contour shape) in band 7 were very similar to those in band 5. Brightness differences between band 5 and band 7 range from 1 (areas of saturation) to approximately 40 along the snow boundary, running near 20 in areas between saturation and the snow boundary. This range in brightness difference remained essentially unchanged throughout the snowmelt season. No apparent threshold level in band 7 could be found that separated melting from non-melting snow, which is not surprising in view of the findings of O'Brien and Munis (1974) that the reflectances of melting and refrozen snow surfaces are almost identical for visible and near-IR wavelengths (see figure 3.3, curve B).

A disturbing feature of both digitized MSS bands was the low threshold of saturation, particularly in band 5. During the early melt season, more than 75 percent of the snow in the study area had brightness values at saturation (i.e. 127). In band 7, 25 percent of the values reached saturation. The designed upper limits of 2.00 milliwatts/cm^2-steradian and 4.60 milliwatts/cm^2-steradian for bands 5 and 7, respectively, are much too low for monitoring bright snow surfaces. It should be remembered that ERTS-1 was designed for earth resource surveys and not for meteorological purposes. Mention was made (General Electric Corp., 1972) that clouds may often saturate the MSS; unfortunately, snow has similar high brightness values.

A north-south transit through the study area (figure 3.5) was selected in search of a relationship between band 5 and band 7 data and snowmelt. Data for two dates, one before the melt season (March 16, 1973) and one during extensive melting (June 14, 1973), are plotted in figure 3.8. In the early case, brightness values for band 5 exceed the corresponding values in band 7 by 30 to 55 in unsaturated snow areas, but were similar at saturation. Differences for the June 14 case fall in the same range

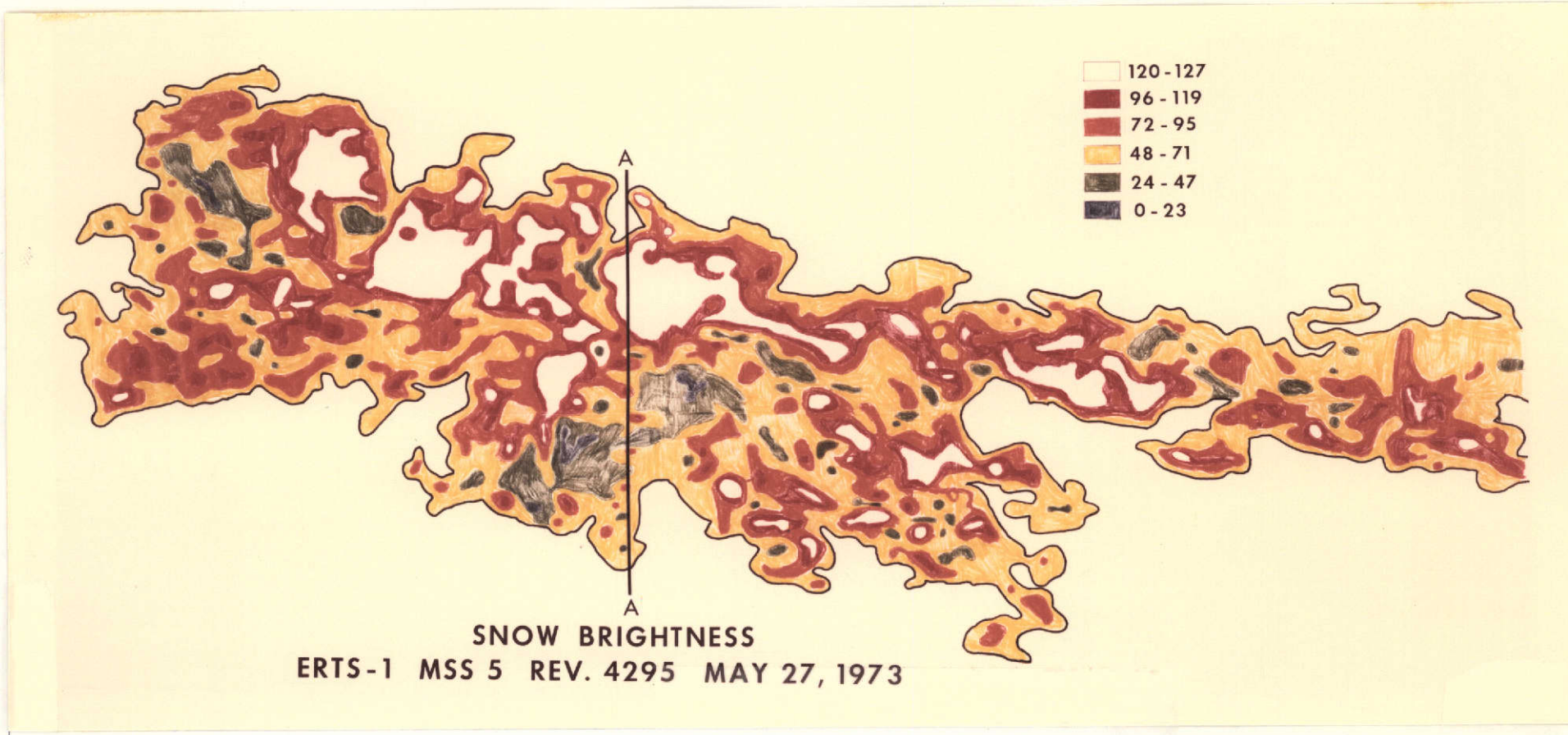

Figure 3.6 Example of digital data for study area on May 27, 1973, Band 5.

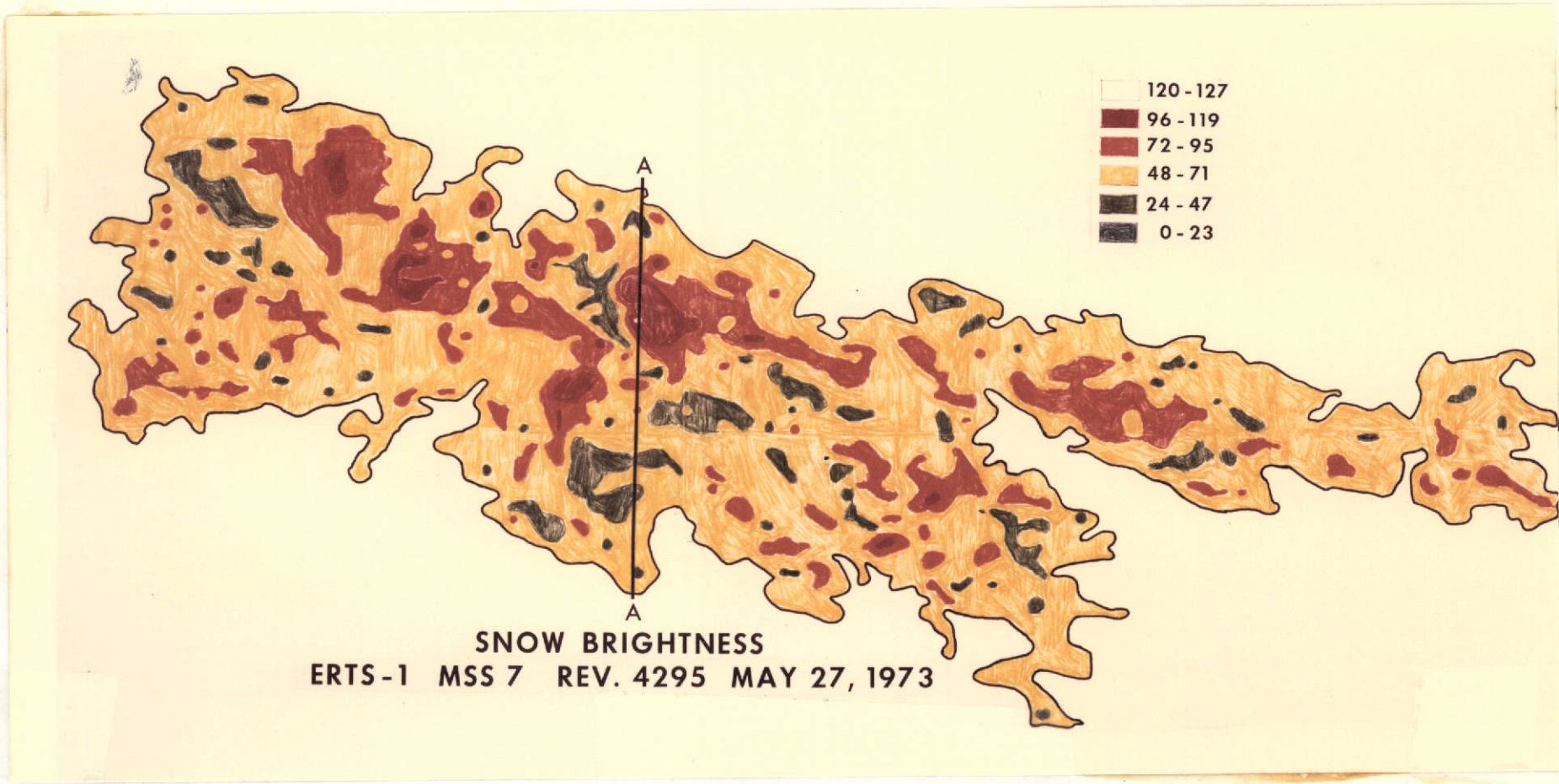

Figure 3.7 Example of digital data for study area on May 27, 1973, Band 7.

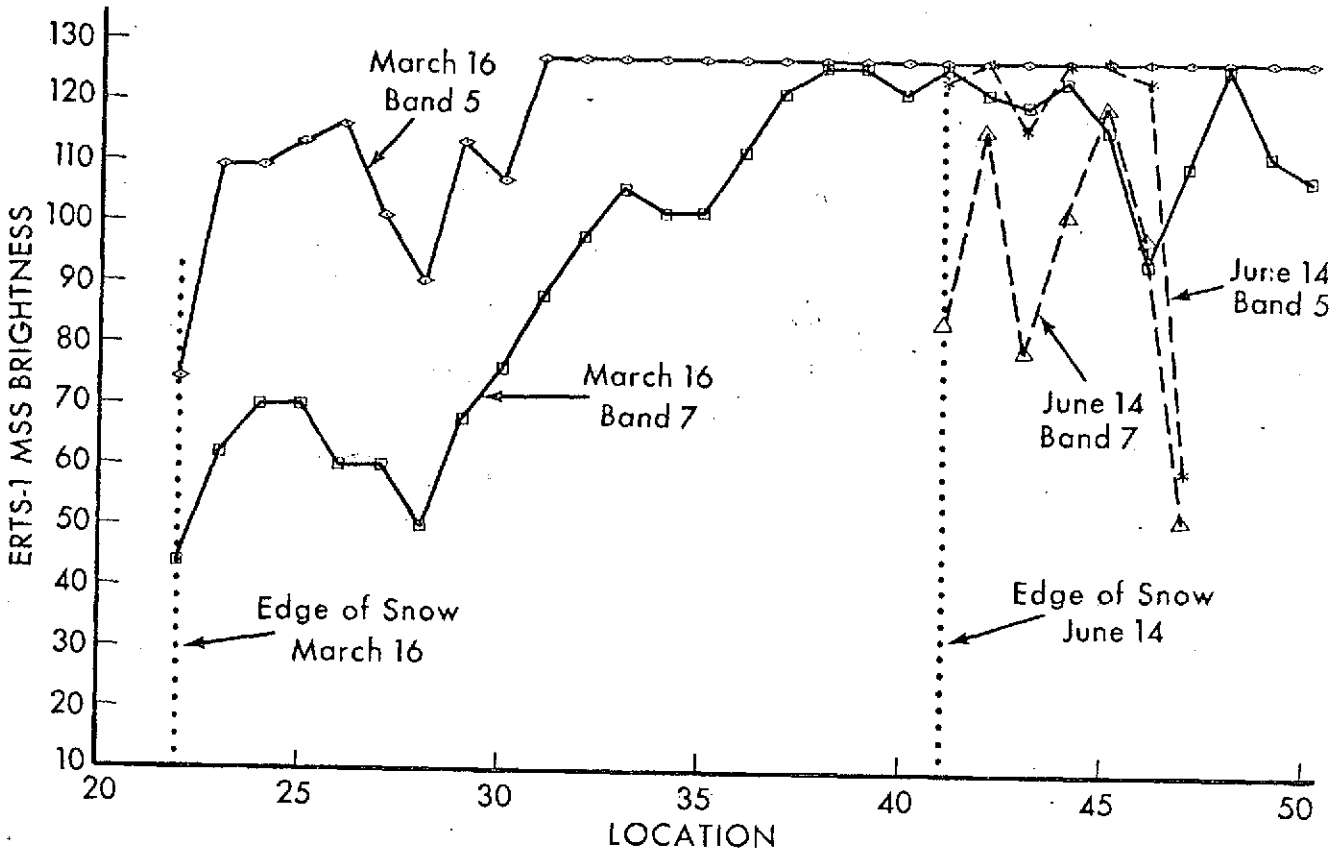

Figure 3.8. Brightness values for bands 5 and 7 for a selected transit through the study area.

(30 to 55), with three pairs of values (at location 42, 45, and 46 for both band 5 and band 7) being almost identical to the early non-melting values. No conclusive results are noted that would allow separation of areas of non-melting from melting snow.

The main difficulty in applying digital data to search for melting snow is the low saturation limits of the MSS sensors. This imposed upper bound on snow brightness precludes the determination of true differences between bands. Furthermore, examining the digital data at full resolution is too close a view at which to assess this phenomenon. Imagery, on the other hand, at a much smaller scale of 1:1,000,000, provides an averaging and integration of the data that is further refined by the human eye. The eye is merely looking for the edge of the bright snow boundary--an edge that may or may not be related to a specific gray level.

One way to examine snowmelt using digital data from ERTS-B would be to raise saturation values on the MSS, thus permitting assessment of spectral differences over a wider brightness range. Extending the upper spectral limit of band 7 to 1.3 or 1.5μm would be helpful by providing a greater contrast between melting and non-melting snow in band 5 and band 7.

Meltwater Runoff Relationships

The relationships between river basin discharge, satellite-determined snow cover and the decrease in areal snow cover, as observed between MSS bands 5 and 7, of four watersheds within the American River Basin were examined. Each basin differed in area, elevation, and maximum extent of snow cover. Discharge, snow cover, and basin spectral reflectance decrease (SRD) data were graphed and compared. Also, SRD data were compared to the snowmelt component of the daily hydrograph for one of the four watersheds.

Drainage Basins

Various stream gaging stations were selected to represent a variety of drainage basins (figure 3.9). The basins range in size from 231 to 1743 km^2 and are at various elevations (see Table 3.3). They were chosen to minimize artificial regulation effects on the discharge hydrograph; total elimination of the effect of stream regulation was not possible owing to the highly regulated nature of the Sierra Nevada runoff. The gaging stations' coordinates were obtained from the USGS "Index to Surface Water Stations" (USGS, 1969), then located on 1:250,000 scale USGS topographic maps (Chico and Sacramento quadrangles). Using the map contours, the drainage area for each station was carefully outlined. A zoom transfer scope was used to transfer the basin outlines onto a smaller map, viz., the same base map used for previous American River snow-extent mapping (see chapter two). The drainage network outline was then transferred to tracing paper for each day of satellite image.

The corresponding basin discharge data were obtained from the Sacramento office of the Geological Survey. The daily discharge data for mid-March through mid-June were plotted. Various scales were selected to best

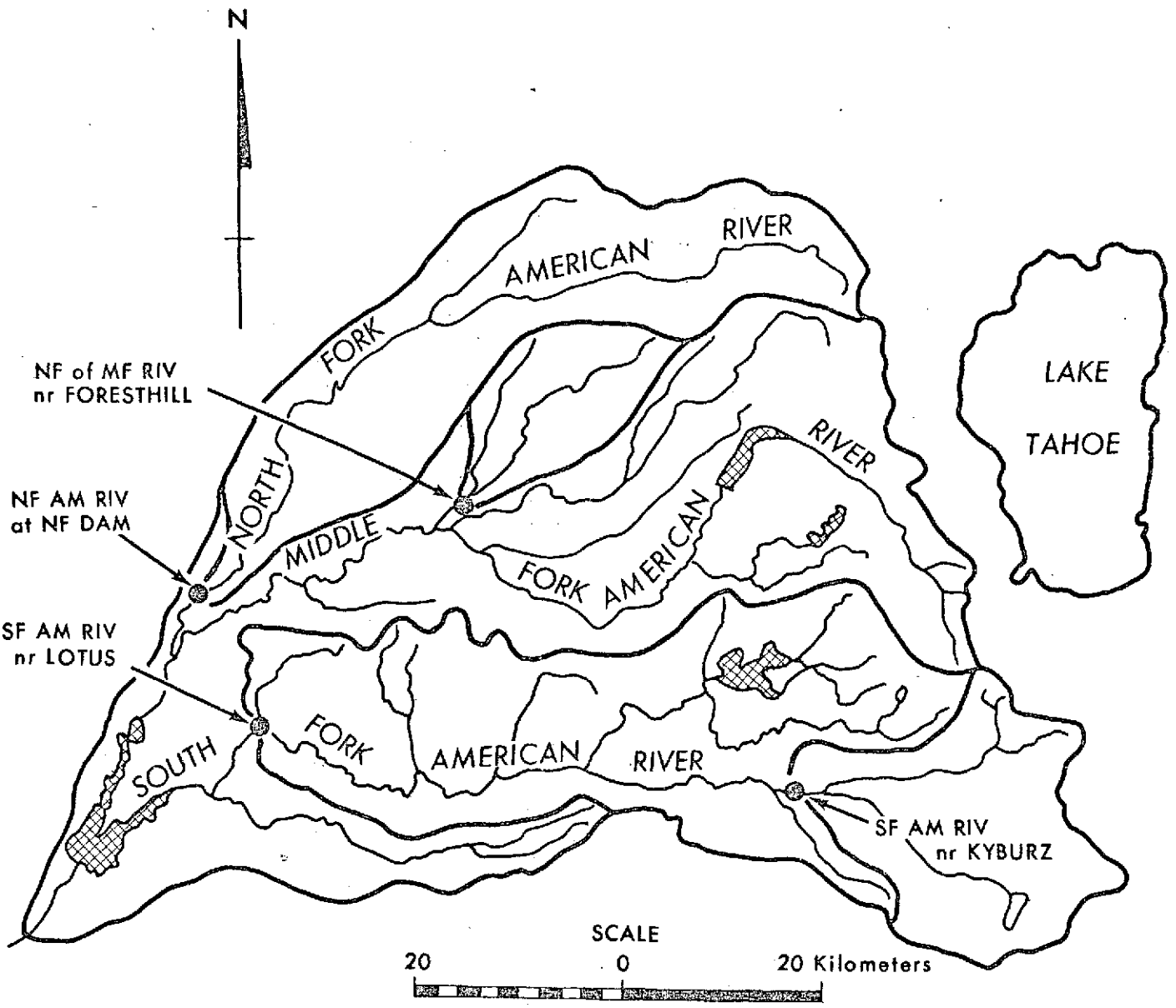

Figure 3.9. Drainage map of American River Basin with subbasins.

Table 3.3

Characteristics of subbasins within the American River Basin.

OWDC Site Number	River Basin Gage	Drainage Area	Mean Daily Discharge May 1973	Percent of Basin Above 1500 Meters
11-4455	SF AMERICAN RIVER NEAR LOTUS	1,743 km^2	80.9 cms	50%
11-4270	NF AMERICAN RIVER AT NF DAM	886 km^2	56.4 cms	35%
11-4395	SF AMERICAN RIVER NEAR KYBURZ	500 km^2	56.3 cms	95%
11-4332.6	NF OF THE MF AMERICAN RIVER NEAR FORESTHILL	231 km^2	11.2 cms	40%

illustrate the discharge characteristics. All discharge data are from preliminary USGS records and are subject to revision. Precipitation data for the stations nearest the individual basins were obtained from the monthly Climatological Data Summaries for California (NOAA, 1973).

The drainage network outline was placed over the snow-extent maps previously compiled (chapter two) so that the snowlines could be traced. MSS bands 5 and 7 were selected for use. The area of each basin and the basin snow cover were then planimetered for each day of satellite observation. The area of band 5 snow cover was considered the best representation of the actual snow cover. This area, expressed as a percent of total basin area, was plotted on the corresponding stream discharge graphs (figures 3.10 through 3.13). Note that the snow cover curve shows only the general trend between satellite observations. No attempt was made to estimate the probable values during the 18-days between observations.

Spectral Reflectance Decrease (SRD)

The planimeter was next used to measure the area of snow-extent in MSS band 7 (A_7). This value was subtracted from the band 5 area (A_5) yielding the area of decreased reflectance. This difference in area, expressed as a percent of total snow-extent (A_5), was plotted to produce the third element of the previously mentioned graphs. That is,

$$\frac{A_5 - A_7}{A_5} \times 100 = \text{SRD\%} \qquad (1)$$

Again, note that the SRD curve shows only the general trend between satellite observation dates.

For example, on May 27, 1973, satellite images indicated the South Fork of the American River basin near Kyburz was 64% snow covered in band 5 ($A_5 = 64$). Similar interpretation of the simultaneously acquired band 7 image indicated only 45% of the basin was snow covered ($A_7 = 45$). Therefore on May 27, substituting in (1) we obtain

$$\frac{A_5 - A_7}{A_5} \times 100 = \frac{64 - 45}{64} \times 100 = 30\% \qquad (2)$$

or 30% of the basin snow covered exhibited a significant spectral reflectance decrease (SRD) between MSS bands 5 and 7.

Daily Snowmelt

During the course of the investigation, bihourly stage-height data for the North Fork of the Middle Fork American River (NFMFAR) near Foresthill became available from the Pacific Gas & Electric Company. It was then decided to compare the satellite data with an analysis of the snowmelt hydrographs as described by Garstka, et al. (1958) in Chow (1964).

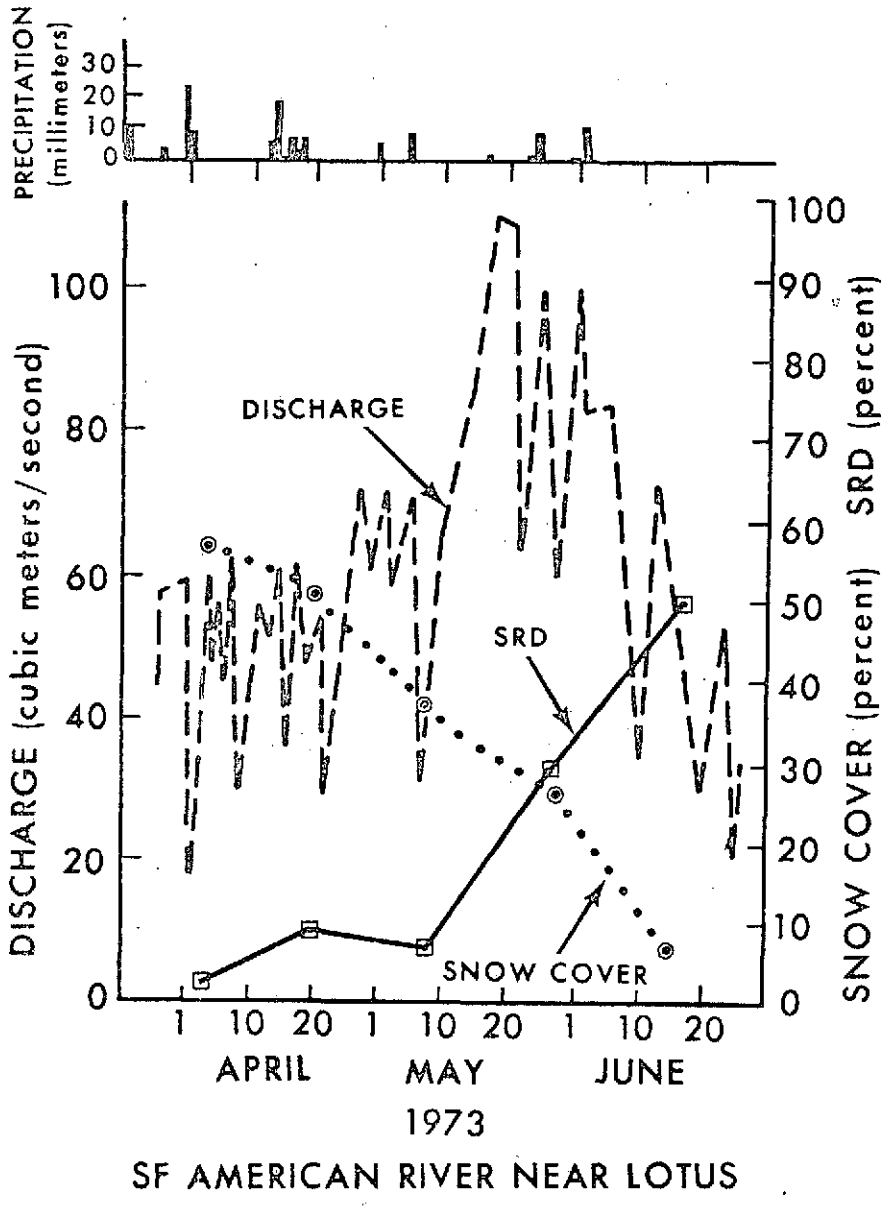

Figure 3.10. Graph of discharge, snow cover and SRD for the South Fork, American River near Lotus.

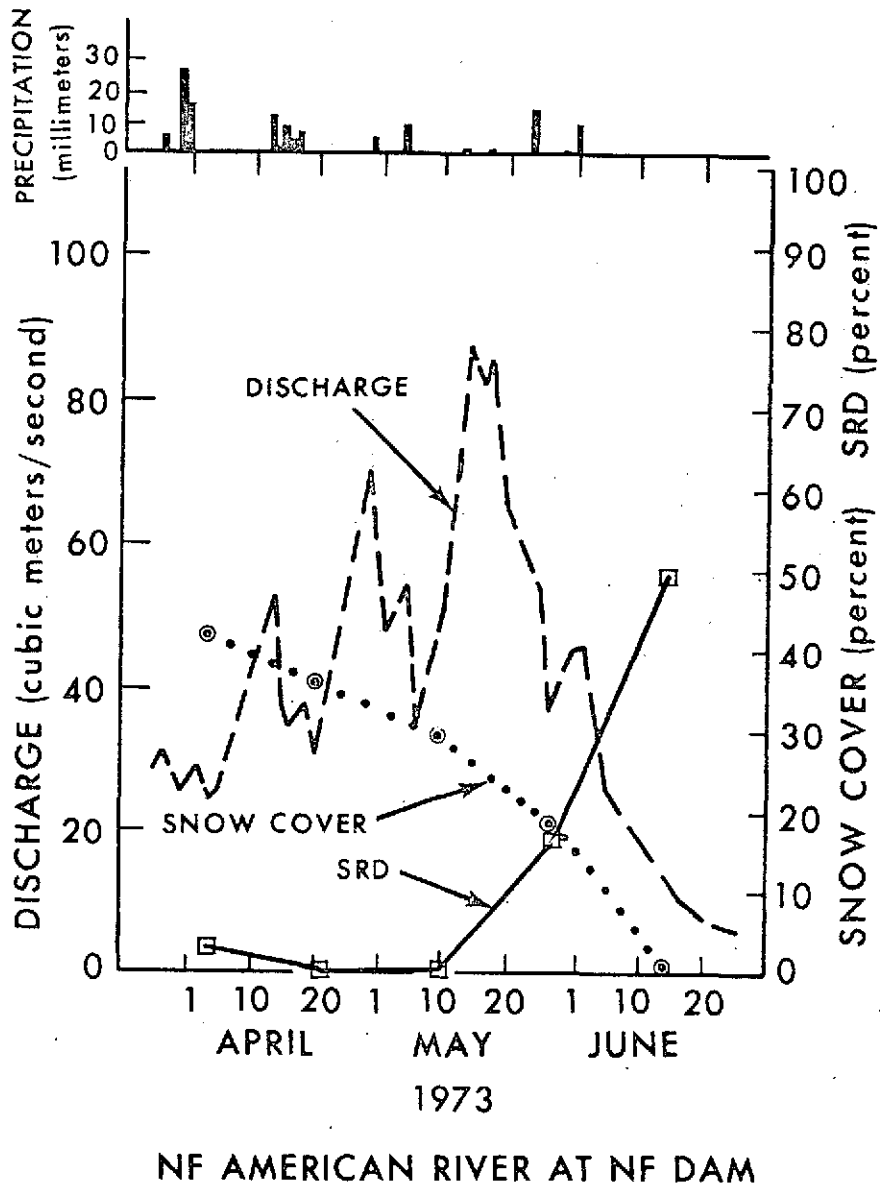

Figure 3.11. Graph of discharge, snow cover and SRD for the North, American River at North Fork Dam.

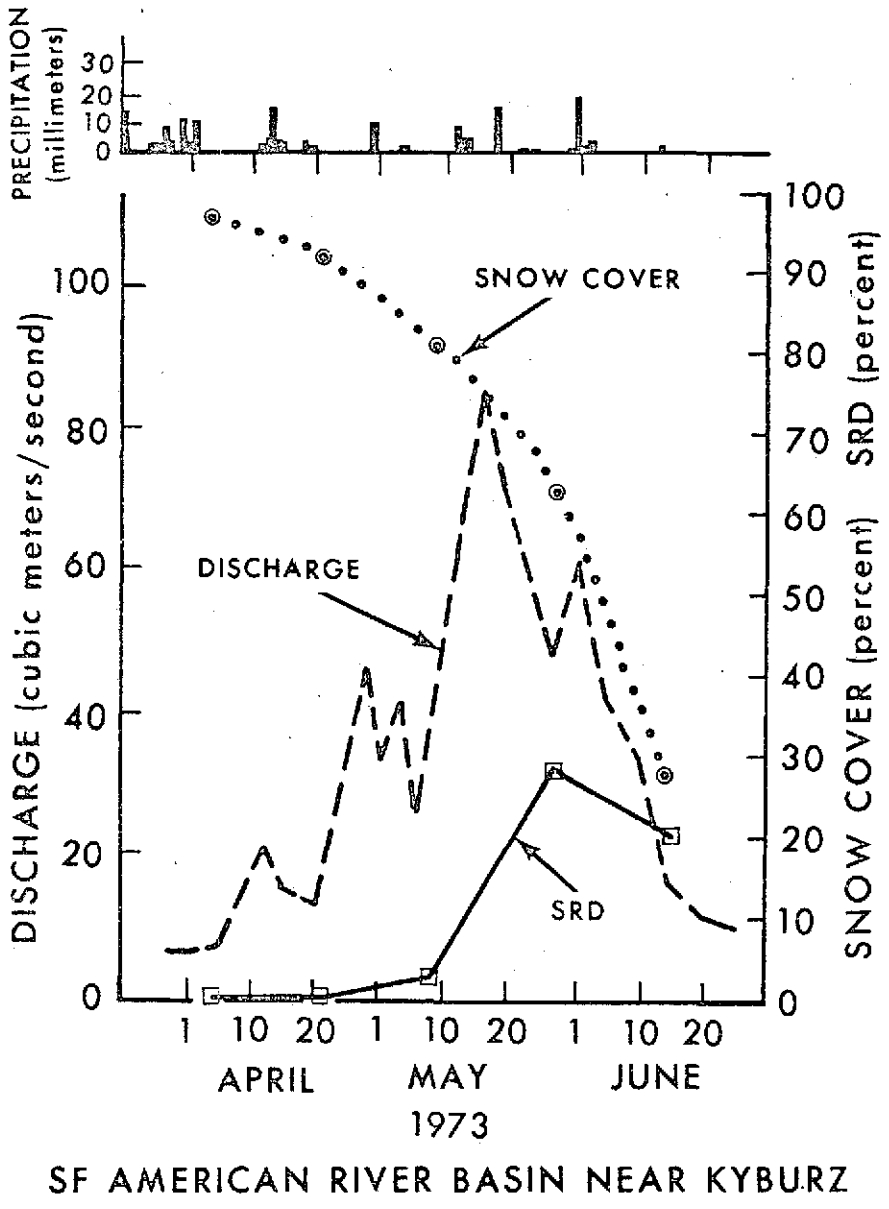

Figure 3.12. Graph of discharge, snow cover and SRD for the South Fork of the American River Basin near Kyburz.

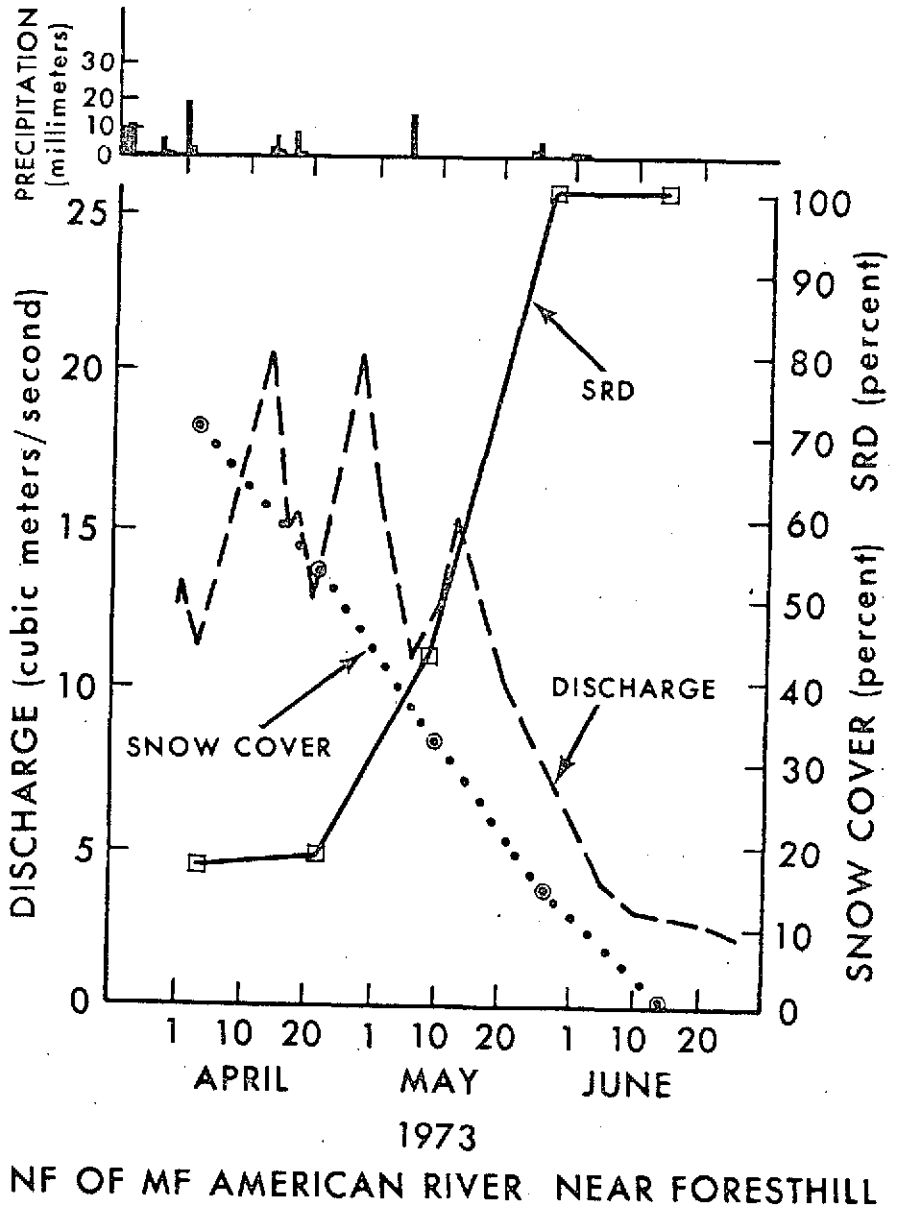

Figure 3.13. Graph of discharge, snow cover and SRD for the North Fork of the Middle Fork American River near Foresthill.

Garstka, et al., had observed that in forested areas there is little basin-wide surface runoff from snowmelt. Practically all snowmelt runoff enters stream channels as a combination of subsurface and groundwater flows. They reasoned, therefore, that each day's snowmelt contribution to the total flow should be characterized by the hydrograph recession during the snowmelt season.

To obtain the recession factor K_r for the NFMFAR, daily mean discharges were plotted against the daily mean discharges for the preceding day for the months of April through mid-June, 1973 (figure 3.14), falling discharges only. The recession factor is then the slope of the linear equation best fitted to the data points. Using a least-squares program on a desk calculator, the recession factor for discharges greater than 5.5 cms was determined to be 0.900 (r^2 = 0.973 with 34 data pairs); for discharges between 2.8 and 5.5 cms, K_r = 0.860 (r^2 = 0.998 with 12 data pairs). A flow of 2.8 cms, for this study, was considered to be a groundwater base flow which could not be further separated.

The volumes constituting a given day's contribution to the snowmelt hydrograph are illustrated in figure 3.15 for each day for which there was a satellite image. The recession portions of the hydrographs are extended by curves based on the equation originally proposed by Barnes (1942):

$$Q = Q_o K_r^t \qquad (3)$$

where Q is the flow in cms at time t in days, Q_o is the flow in cms at the beginning of the computation period or when t = 0, and K_r is the daily runoff recession coeffcient. Each day's contribution therefore consists of two areas: area 1, which is the volume of the day's snowmelt runoff appearing between troughs of two successive days, and area 2, which is the recession flow.

Area 1 was determined by planimetering the graph and converting to appropriate units. Area 2 was computed mathematically on the basis of the above equation.

Discussion

As mentioned in previous chapters, one major disadvantage in using ERTS-1 data to study relatively short-lived phenomena is the 18-day revisit cycle. The snowmelt season in the American River basin usually lasts from April 1 to June 30. A maximum of six images could then be expected during those 91 days, assuming cloudfree conditions. For the 1973 snowmelt season, five images of the river basin were available for analysis.

The most interesting watershed examined during this study was the South Fork of the American River near Kyburz. Over 90 percent of the basin area lies above 1500 meters; Rantz (1972) has stated snowmelt is a significant factor in runoff if 30 percent or more of the basin is above this elevation. In this basin (figure 3.12), snow cover decreased almost exponentially; the discharge increased until the middle of May. A secondary increase in

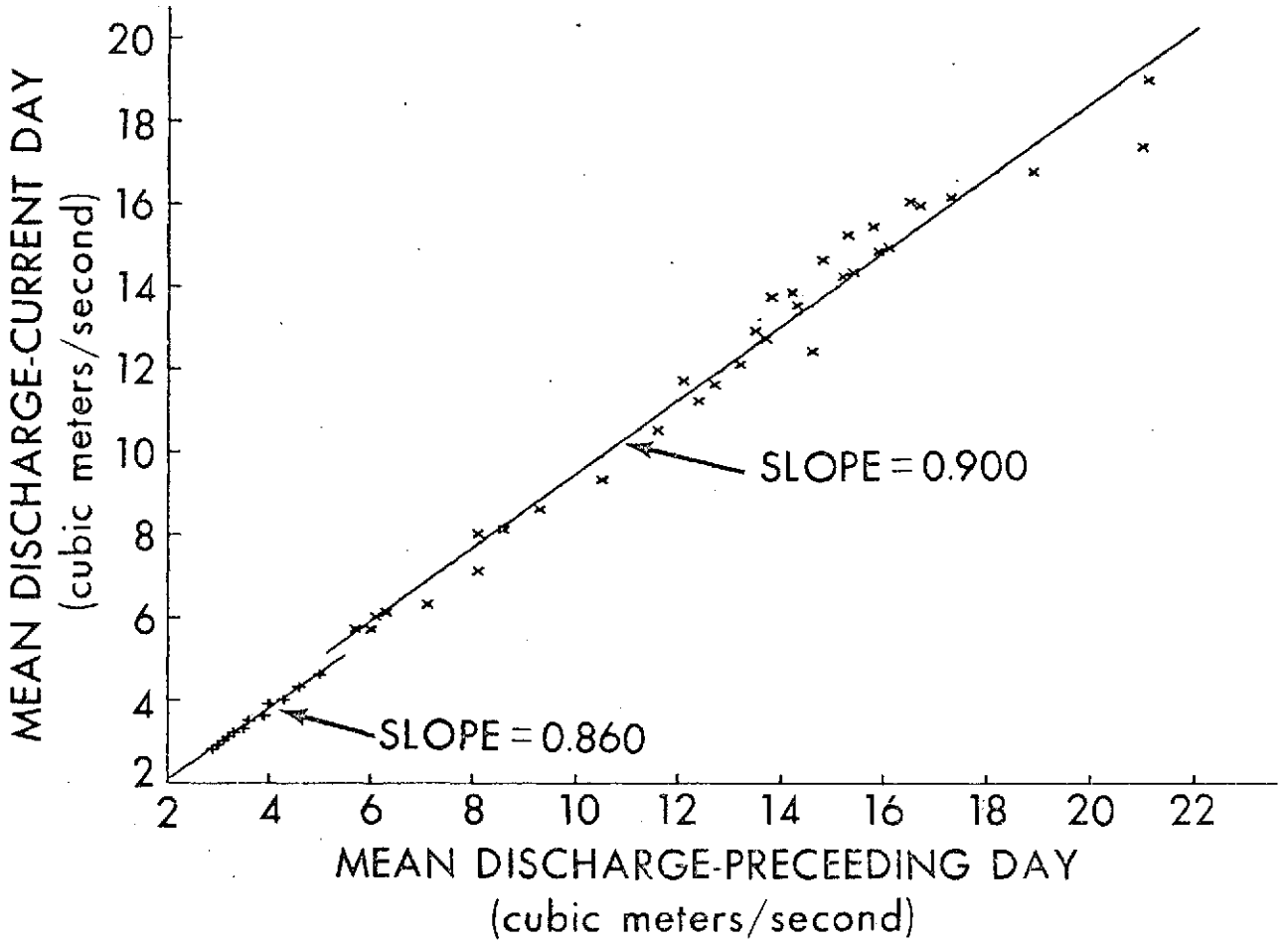

Figure 3.14. Derivation of the snowmelt recession factor for the North Fork of the Middle Fork American River utilizing falling discharges only, for April through mid-June, 1973.

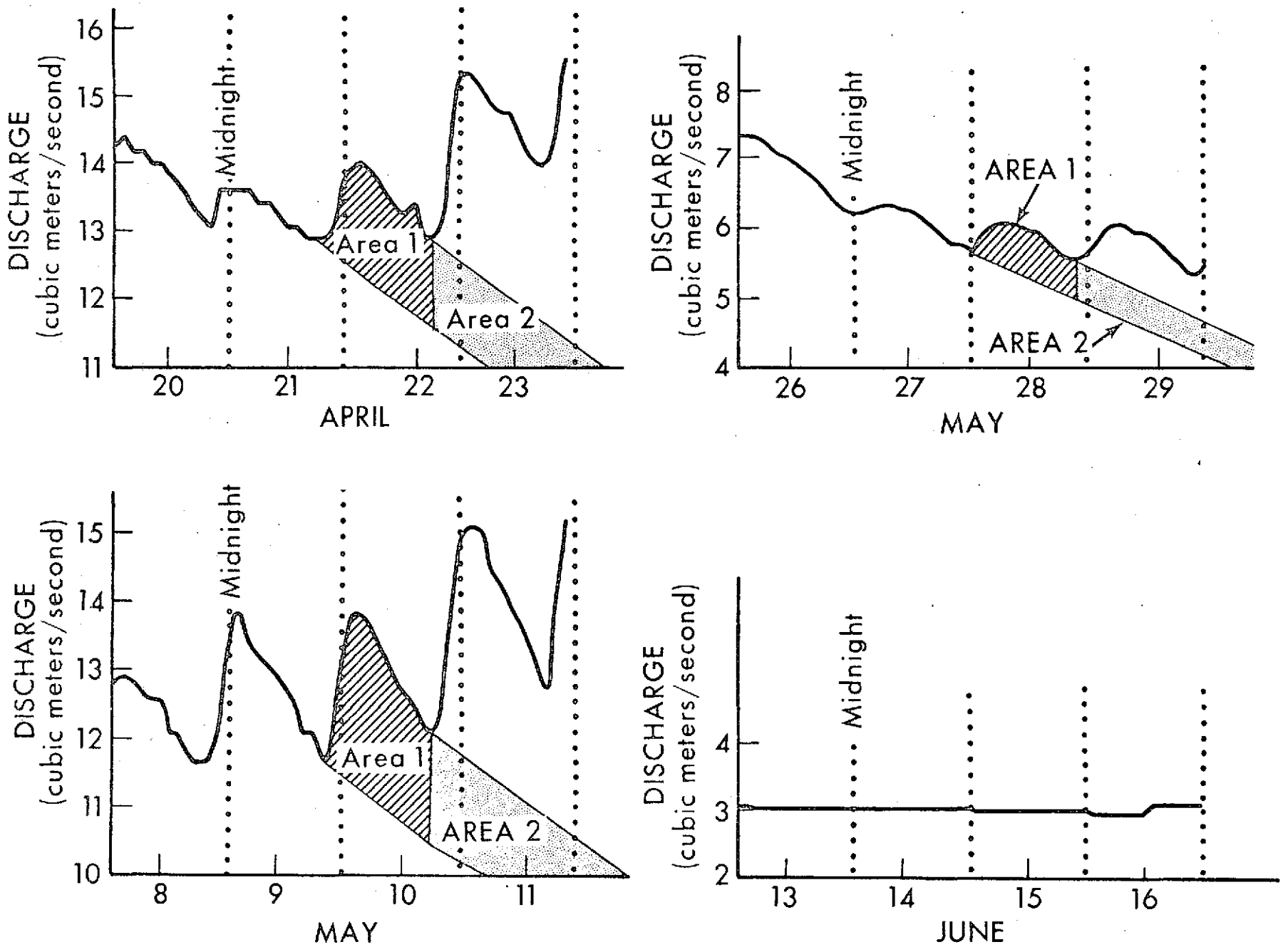

Figure 3.15 Runoff volumes due to snowmelt for the North Fork of the Middle Fork American River Basin near Foresthill.

discharge, which occurred in early June, coincides well with the sharp drop in snow cover from May 27 to June 14 (64% to 14%). The SRD curve appears to agree with the discharge pattern rather well for this period. The large rise in discharge from May 6 to 16 is similarly reflected in the SRD data. This response would be expected if the spectral reflectance decrease between bands 5 and 7 were related to melting snow. The decrease in the SRD value for June 14 does not appear to be consistent with this hypothesis: the difference between bands of areal snow cover should generally increase throughout the melt season as the snowpack ripens. This anomaly may result from the fact that on June 14 snow covered a mere 11 percent (55 km^2) of the basin, which approaches the limits of this type of measurement.

The results of this preliminary analysis, though encouraging, are limited by several factors. First, the 18-day cycle of the satellite restricted the number of possible observations to five; second, a malfunction of the recording device at the North Fork of the Middle Fork American River near Foresthill gaging station for the first week of April (J. Blodgett, U.S. Geological Survey, Sacramento, personal communication) further restricted the data to four days; and third, most of the snow cover in the NFMFAR had melted by June 14, the day of the last possible ERTS orbit for the 1973 snowmelt season.

The data for the remaining three days of satellite observations (Table 3.4) indicate there may indeed be a correlation between areal measurements of spectral reflectance decrease between ERTS-1 bands 5 and 7 and daily snowmelt discharge. However, no conclusions should be drawn on the basis of this preliminary study. A more comprehensive study is now underway which will explore this possible correlation more fully.

Albedo

The portion of the total incoming radiation reflected to space is called the albedo. The decrease in surface albedo of an aging snow pack has been documented by the Corps of Engineers, 1960. The causes for such a decrease in albedo are many--some relating to the changing physical properties of the snow itself, others to outside influences such as contamination of the snow surface from falling pine needles.

The correlation between percent of satellite-determined basin snow cover and albedo is also of interest. Although a generally positive correlation would be expected between these two variables, large, short-lived increases in albedo, resulting from fresh snow falls, would also be expected in the beginning of the snowmelt season. Early spring snowfalls as small as a few centimeters can renew the high reflectance of an aging snowpack surface.

The Central Sierra Snow Laboratory (CSSL) at Donner Summit (a few miles from the northeast extremity of the American River Basin) provided hourly albedo measurements for each day of ERTS-1 overflights through May 27, 1973.

Table 3.4

Snowmelt components of daily hydrograph.

Date 1973	24-Hour Snowmelt	Snowmelt Recession Flow	Total	SRD	Snowcover as a Percent of Initial
April 3	Recorder Malfunction			17	100
April 21	0.105 hm^3	0.958 hm^3	1.063 hm^3	18	73
May 9	0.147 hm^3	1.101 hm^3	1.248 hm^3	43	46
May 27	0.040 hm^3	0.281 hm^3	0.321 hm^3	100	20
June 14	Snowmelt Component Negligible			-	0

No snow cover existed at the Laboratory on June 14, 1973, or July 2, 1973. Table 3.5 shows albedo readings from an Epply pyrheliometer and the satellite-determined snow cover for the entire American River Basin as well as the subbasin upstream from the North Fork of the American River at North Fork Dam - the subbasin nearest the Donner Summit. The spectral reflectance decrease (SRD), seen in Meltwater Runoff relationships section is also shown. Correlation coefficients for a parabolic best fit between albedo and snow cover and SRD are given at the bottom of Table 3.5.

Data from Table 3.5 are plotted in figure 3.16. The high direct correlation between albedo and total basin snow cover, though logical, is based upon only the six data pairs available for regression analysis. The limited number of degrees of freedom in such a regression lowers the statistical significance of these high correlation coefficients and widens the confidence limits. The high correlation between albedo and SRD (figure 3.17) is rather misleading in one respect. The decrease in SRD as the albedo increases during the melt season is expected; however, the increase in the SRD as albedo increases above 50% is unrealistic. With additional data from the 1974 and 1975 snowmelt seasons, a hyperbolic relation may result with the X-axis (SRD=0) as a horizontal asymptote.

The authors recognize the speculative and inconclusive nature of the curves shown here. They also realize that the data sample size is extremely small. Nevertheless, these data, though sparse, constitute the initial results of the project. Additional values from 1974 and later snowmelt seasons will be added to the existing data set to permit a further exploration of this relationship.

Table 3.5

Albedo, snow cover and spectral reflectance decrease (SRD) values in the American River basin.

Date 1973	Albedo 1000 PST C.S.S.L.	Percent Snow Cover Total Basin	Percent Snow Cover NF Amer. Riv. at NF Dam	Spectral Reflectance Decrease Total Basin (Band 5-7)/Band 5
3/16	65	47	40	7
4/3	67	49	42	19
4/21	53	43	36	12
5/9	49	29	30	10
5/27	12	17	18	25
6/14	(est) 0.001	4	4	50
Parabolic Best Fit		**0.95**	0.97	0.92

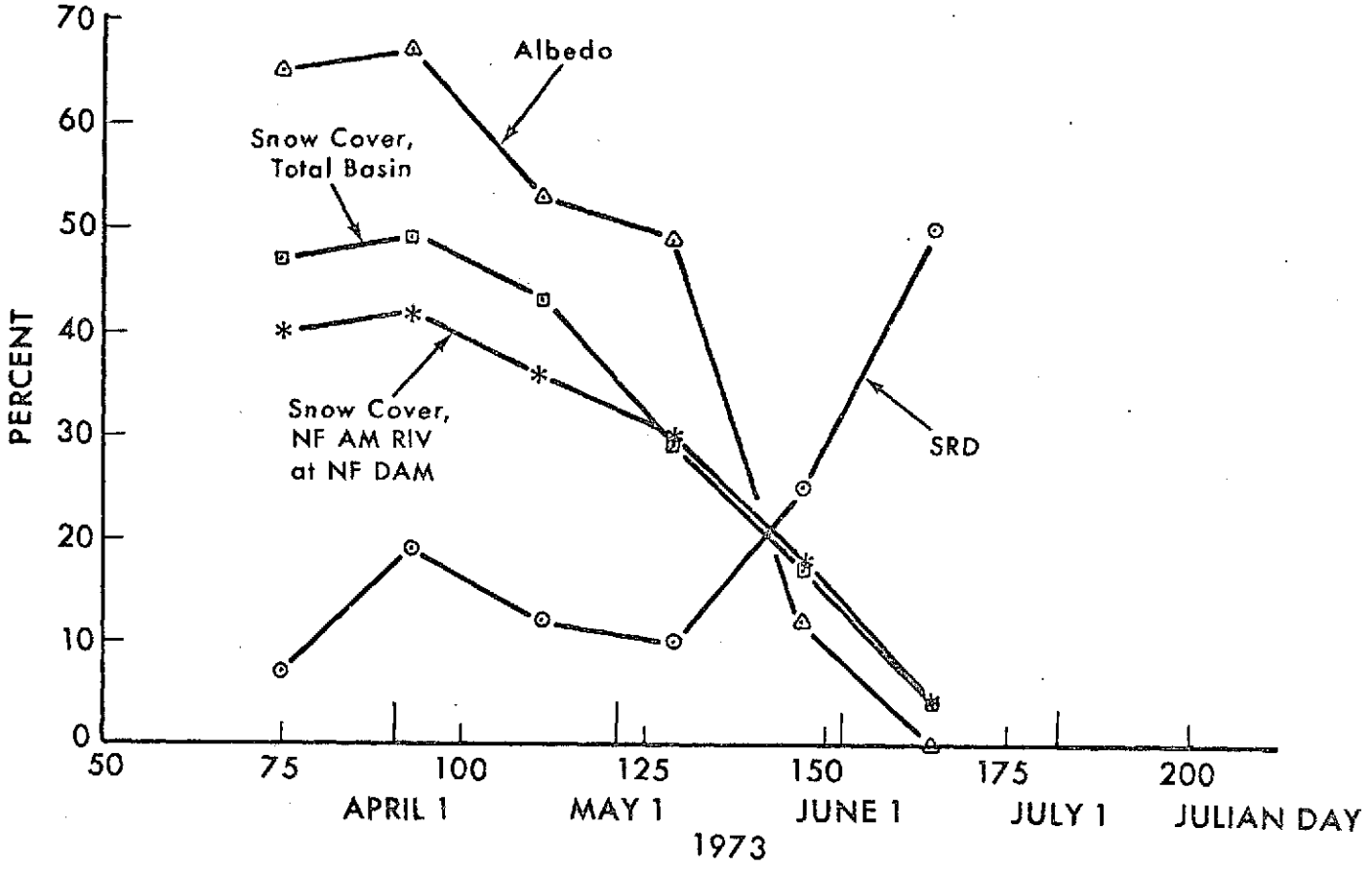

Figure 3.16 Graph showing albedo, snow cover and SRD in the American River Basin as a function of time.

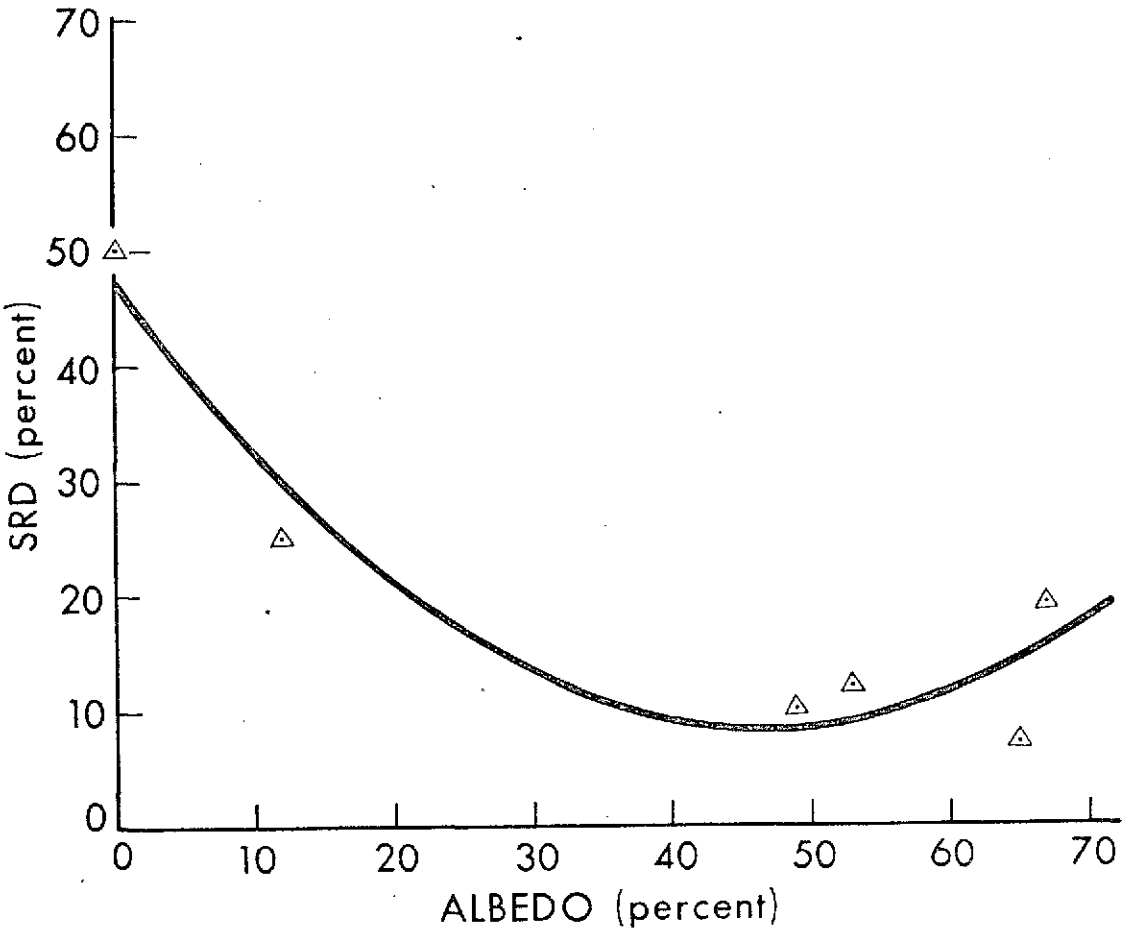

Figure 3.17 Graph showing SRD in percent as a function of albedo.

Chapter 4

LAKE ICE

Lake Ontario

Lake Ontario, the lowest (75 m msl) and one of the deeper (245 m) of the Great Lakes (figure 4.1), was a poor choice for ice studies in the sense that the lake is generally 85% icefree in a normal winter, and only twice in the last 100 years did the lake completely freeze over (Phillips and McCulloch, 1972). Ice can be observed more frequently in Lake Erie and is much more extensive there than in Lake Ontario. (See section on Lake Erie ice.) It was for this reason that the project area was designed to include Lakes Erie and St. Clair as well as Lake Ontario.

An excellent image of Lake Ontario ice was taken on February 17, 1973 (figure 4.2). It was the coldest day of the year and the satellite MSS image indicates a great deal of ice forming along the northern side of the lake. The northerly winds blowing out of a high pressure center had pushed the ice offshore where it tended to melt owing to thermal energy stored in the lake. Note the melting stringers oriented N-S. Note the solid ice forming at the shore's edge and the intermediate area where wave action has broken up the newly formed ice. In the southern part of the lake many small fractocumulus clouds have developed. Their cumuliform shape and their shadows identify them as clouds.

Rondy's (1969) work on Great Lakes ice is both authoritative and comprehensive. Prepared from ground-based data, it provides a standard that was much needed and deserves high praise. Nevertheless it also serves to illustrate the incalculable value of the satellite's vantage point from space. For example, from NOAA-2 daily satellite observations, we know that Lake Ontario's maximum ice cover--25%--occurred on February 17. Rondy's (1969) data list 25% ice cover for Lake Ontario as occurring during a severe winter. Overall the 1972-73 winter was very mild, (Boyce, 1973), but the response of Lake Ontario to the Arctic air mass and its subzero temperatures was prompt and was recorded by the ERTS-1 and NOAA-2 satellites. To the same Arctic blast, Lake Erie responded by extending its ice cover to 99+% (a small hole off Long Point refused to close). We stress that this took place during a "mild" winter during which, according to the ground-based statistics, one would expect a 50% ice cover on Lake Erie.

The point made here is not that generalized statistical data can be incorrect under special or unusual events, but that ERTS-1 and NOAA-2 were able to record precisely what happened to the ice cover and precisely when it happened. The satellite observational vantage point permits detailed analysis of the effect of winds, ice type, depth, currents, temperature, etc. on the formation and migration of lake ice. Never before have scientists been able to observe with such clarity the dynamics of lake ice development, migration and dissipation.

No single tool would be of more value to ice forecasters than a quick-look ERTS image of the Great Lakes, especially if it could be available much more frequently than every 18 days. We predict that ultimately ERTS-type data will be used by the Ice Forecast Center in Cleveland, and by

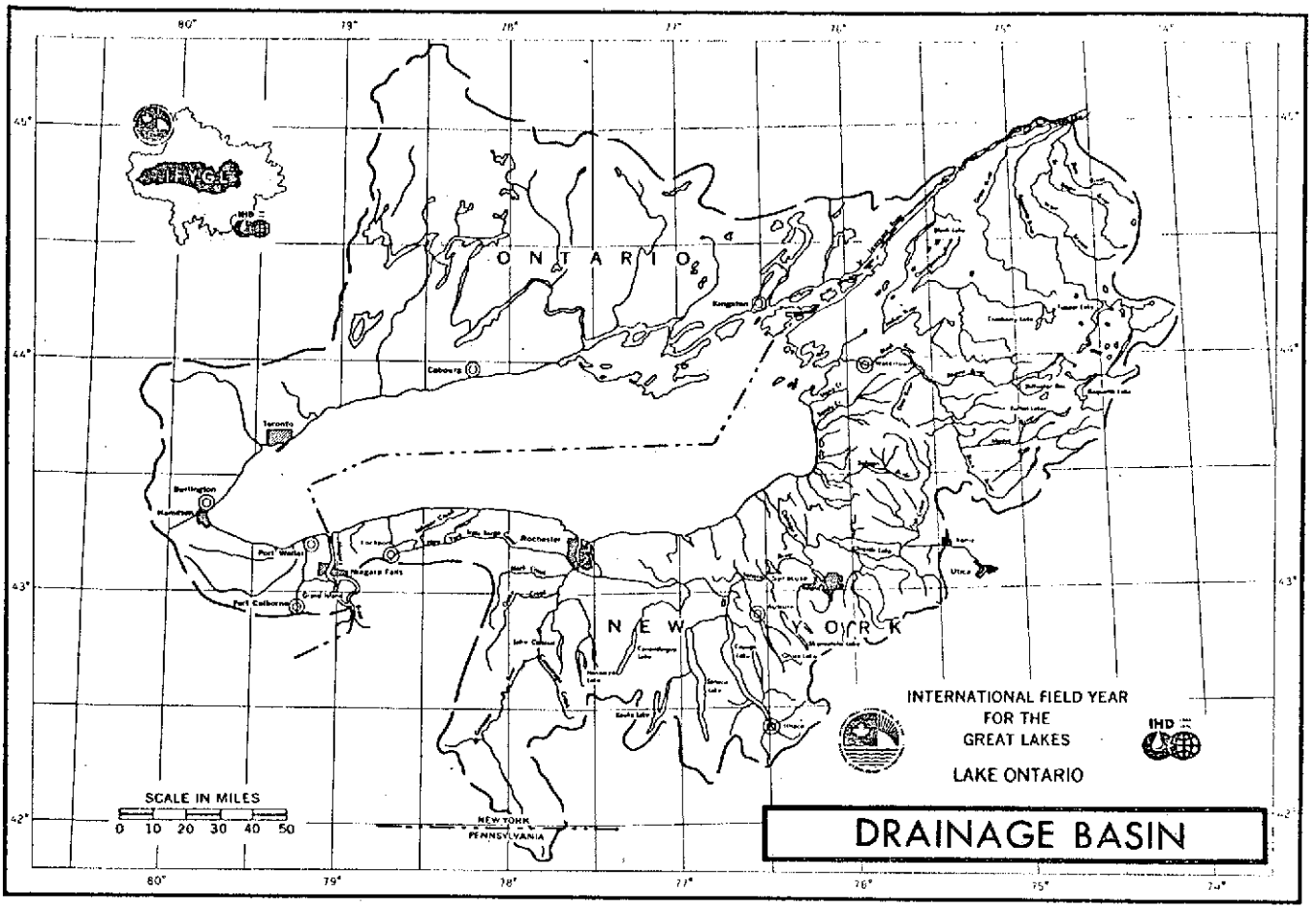

Figure 4.1. Lake Ontario drainage basin.

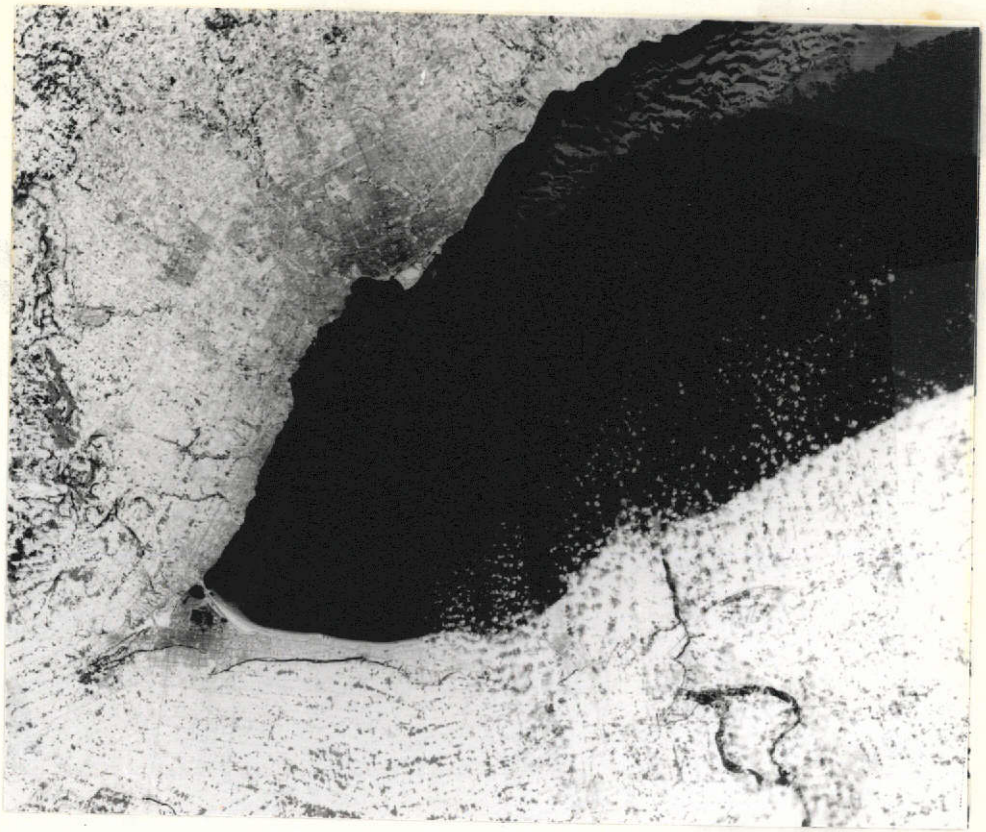

Figure 4.2. ERTS-1 image of the western end of Lake Ontario showing ice features, February 17, 1973.

operational elements of the U.S. Coast Guard, not only to forecast conditions but to route shipping and to control the activity of their ice breakers and helicopters. Ice prediction schemes based on climatology and statistics such as Snider's (1971) will give way to more advanced parametric models based on antecedent meteorological conditions and synoptic satellite observations.

As mentioned above, ERTS-1 as an ice observation satellite is severely limited in one respect: the revisit period is far too long. It should be obvious that the best technique now available for ice study is a combination of ERTS-1 and the current NOAA operational environmental satellite. In this way frequent observations can reveal the rate of response of the water/ice to meteorological conditions. ERTS-1 can provide the detailed identification, and the VHRR aboard the NOAA spacecraft can provide the more frequent spatial and temporal coverage required.

In terms of energy use, shipping by water is historically the cheapest and most efficient method of transportation. To extend the shipping season on the Great Lakes is worth literally millions of dollars and the savings of huge amounts of energy to the U.S. economy.

Lake Erie

As the shallowest of the Great Lakes, Lake Erie is subject to more extensive freezing and ice formation than any other of the Great Lakes. Freeze-up tends to be much more sudden than break-up and melting, which however, can also be rather dynamic. For monitoring ice conditions, ERTS-1's 18-day revisit cycle again presents problems as ice formation, movement and break-up may all take place within very short time thus possibly go totally unrecorded by the ERTS-1 sensors.

Despite this possibility, excellent images of Lake Erie ice were recorded on February 17-18, 1973, and again on March 8, 1973. Strong (1973) has already reported on an analysis of ice movement from changes noted on the sidelap portions of images taken on the 17th and 18th. A mosaic of these two days is shown in figure 4.3

In cases where bad weather eliminates the possibility of sidelap analysis of movement, an analysis of fracture patterns will sometimes provide good estimates of ice movement (Wiesnet and McGinnis, 1974). Antecedent meteorological conditions are vital to such an analysis, as they are an overriding factor in determining the physical conditions and movement of the ice. As an example, imagery of the lake adjacent to the Cleveland area was analyzed by measuring the displacement of a series of characteristic ice edges which had broken from shorefast ice within the preceding 24 hours. Preliminary estimates of the ice movement made from the analysis of fracture patterns range from 0.3 km/hr to 0.8 km/hr (0.2-0.4 knots) to the west. Strong's sidelap analysis of motion yielded figures ranging from 0.5 km/hr to 1.5 km/hr (0.3-0.8 knots). Considering the fact that the onset time of motion is not precisely known, and was assumed to be 24 hours, the figures from the ice-displacement (one image) method agree

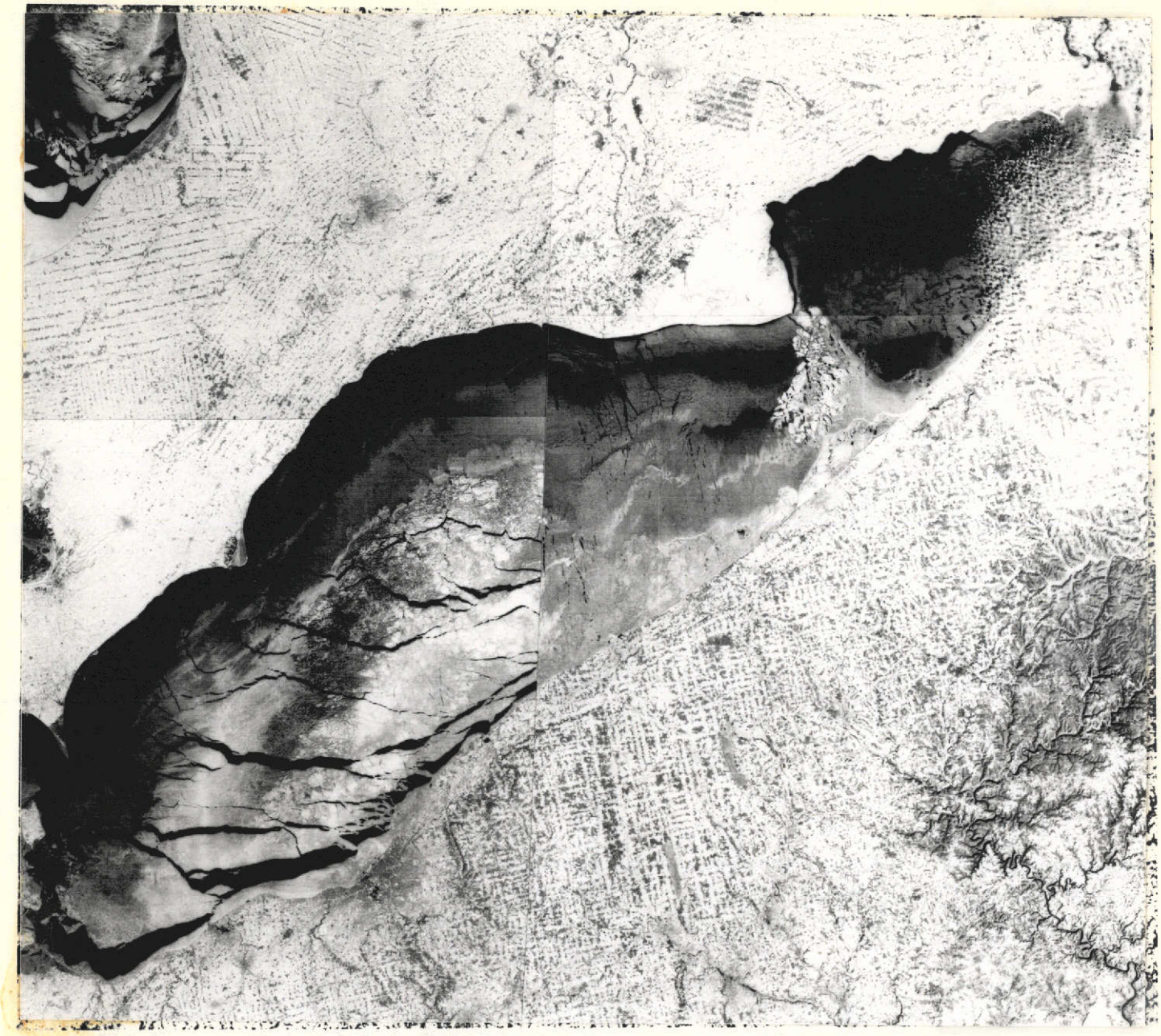

Figure 4.3. ERTS-1 MSS-7 mosaic of Lake Erie ice from images taken on February 17, (eastern half) and February 18, (western half) 1973.

rather well with the more precise sidelap (two-image) method. The 80-meter resolution of ERTS-1 provides outstanding data on synoptic ice pack conditions, but it is severely constrained by the poor (18-day) temporal coverage. Crowder et al. (1974) have reported on deformation and sequential strain array analysis of ERTS-1 images in the Arctic ice north of Pt. Barrow in a paper noteworthy for its quantitative aspects.

Thermal Map of Lake Erie Ice

Although the most immediate type of satellite data display is an image, the data as received from the satellite are in an analog format. These data can be converted to a digital state, and the digitized data tapes can then be manipulated in the computer to provide digital data printouts, contoured maps, enhanced images, etc. The digital printouts reveal the immense data-gathering ability of the satellite sensors. A digitized printout of NOAA-2 VHRR-IR data was used to prepare a thermal map of Lake Erie at a scale of 1:2,000,000. (Publication scale is less.) This map (figure 4.4) was contoured by hand to show the temperature distribution of the ice surface of the lake. Four cross sections illustrate representative temperature across the lake. The temperatures shown here are believed to have an absolute accuracy of 2°C and a relative accuracy of 1°C.

Since this map was prepared, programs have become available in NOAA/NESS to correct for variable path lengths through the atmosphere and to compensate for the atmospheric water vapor attenuation along the path length. These corrections were not applied to this set of thermal data; however, they are small in comparison with the wide range of temperatures shown in figure 4.4.

Surface temperature of ice is affected by many factors, e.g., air temperature, water temperature, thermal conductivity of ice, ice thickness, and surface emissivity. In turn, snow cover and wind speed also affect some of these variables. The four cross sections in figure 4.4 clearly show the warming effect of the lake water on the ice temperatures. It is interesting to speculate on the causes of the temperature variation. Sections A-A' and B-B' cross a warm zone on the north side where the ice is new, dark, and thin. Northerly winds had pushed the brittle ice sheet to the southern shore. The ice was thrust into thick accumulations between Sandusky and Erie presumably influencing the surface temperature in B-B' by building up the ice thickness thereby reducing the effect of the warmer water below the ice. B-B' in figure 4.4 shows a pronounced cooling trend from northwest to southeast.

At C-C' the highest ice temperatures coincide with the deepest portion of the lake along that section, and D-D' shows a similar condition with remarkable temperature stability over the deep eastern third of the lake.

Although Webb (1974, p. 209) has pointed out that thermal data for the ice-covered surfaces of the Great Lakes, especially Lake Erie, have not been available previously, figure 4.4 demonstrates that these data are now

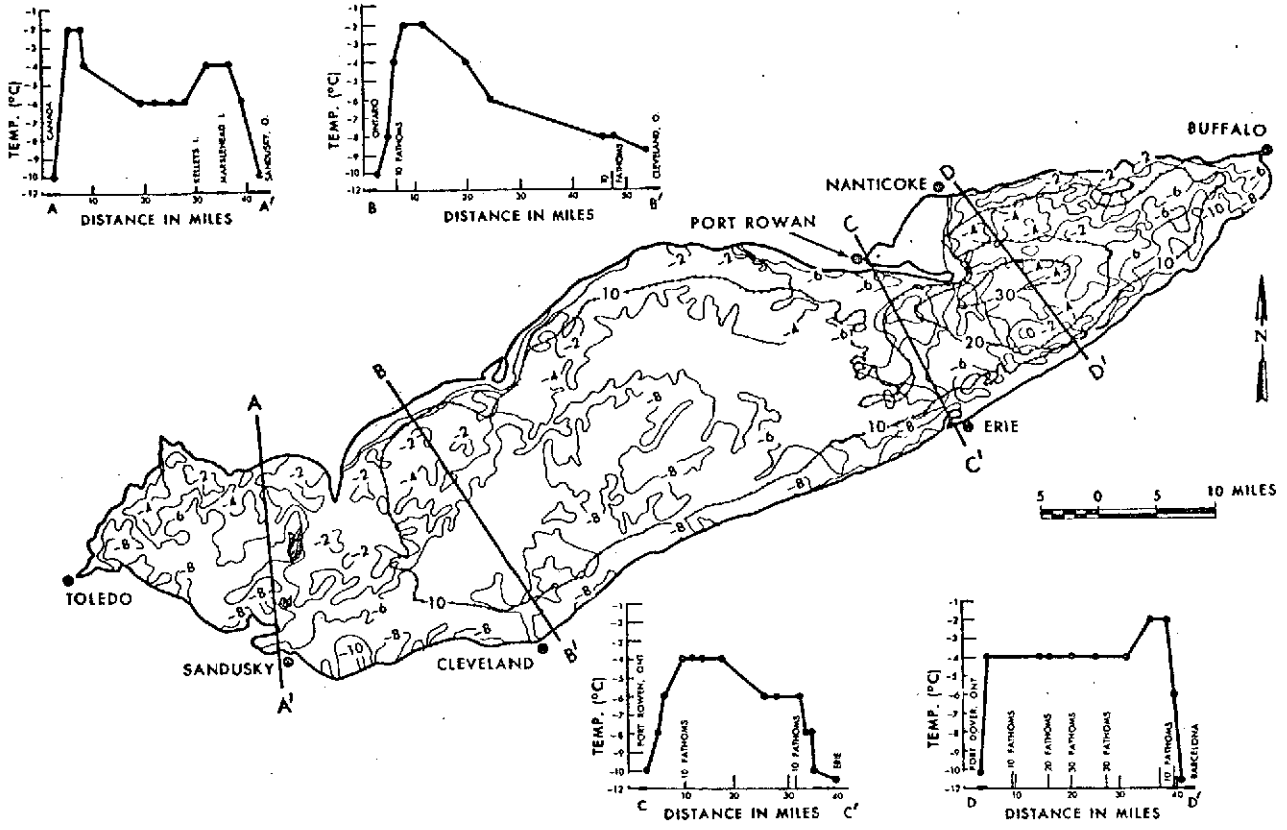

Figure 4.4 Thermal map prepared from digitized data printout of February 17, 1973, from NOAA-2 VHRR (10.5-12.5μm) and rectified to base map of the lake. Compare with Figure 4.3.

available for Great Lakes studies of local winter weather effects, energy balance, ice formation, evaporation, effluent dilution, and transportation and industrial problems.

Melting Lake Ice Detection

The use of ERTS-1 MSS bands 5 and 7 in an attempt to identify melting snow was discussed in Chapter 3. Similarly, ERTS-1 MSS images over Lake Erie (figures 4.5, 4.6) were examined for melting ice. The ice field in band 5 exhibits a highly reflecting but "lacy" appearance resulting from many thaw holes, a characteristic of "rotten" ice, i.e., deteriorating under warm temperatures. A great decrease in apparent reflectivity in band 7 as compared to band 5 also indicates melting conditions in agreement with the experimental results of O'Brien and Munis (in press) (See figure 3.3, curve B). Table 4.1 shows the air temperature and wind data for stations over Lake Erie before and after the ERTS-1 pass (1542 GMT). Note that no station reported subfreezing temperature.

Because it was apparent that ERTS-1 prints in bands 5 and 7 had been developed and processed differently, we attempted to treat the two negatives in a uniform fashion to obtain a more realistic interpretation of the difference in reflectivity. Figure 4.6 shows two MSS images of the melting ice field that were exposed and developed simultaneously under the same photographic constraints. Note the identical calibration of the step wedges at the bottom of each image. The decreased reflectance in the near-IR (band 7) is rather pronounced under equal development conditions. However, the original negatives were developed by NASA, GSFC, and were undoubtedly processed differently in the two bands owing to contrast and tonal differences.

Identification of Ice Types

ERTS-1 MSS imagery over Lake Erie (figure 4.5) has been examined and the following features tentatively identified on this image are: grounded ice west of Pt. Aux Pins, Ont.; an icefoot near Marblehead, Ohio and along the east edge of Pt. Pelee, Ont.; a compacted ice edge of the southern edge of the icefield northwest of Cleveland, Ohio; a young ice-snow sheet broken up by wave action east of Pt. Aux Pins; and brash belts oriented almost N-S between Painesville and Astabula, Ohio.

The following ice features have been tentatively identified from the February 17-18 and March 8, 1973, ERTS-1 MSS images of Lake Erie and Lake Ontario (Note that ground truth is not available for verification.): Shuga, light and dark nilas, fast ice, icefoot, ice breccia, brash ice, fracturing, ridging, rafting, sastrugi, thaw holes, rotten ice, ice floes, dried ice puddles, hummocked ice and leads. These terms are defined in WMO Sea-Ice Nomenclature WMO/OMM/BMO No. 259 TP 145.

Figure 4.5 ERTS-1 MSS band 5 image of melting ice features on western Lake Erie, March 8, 1973.

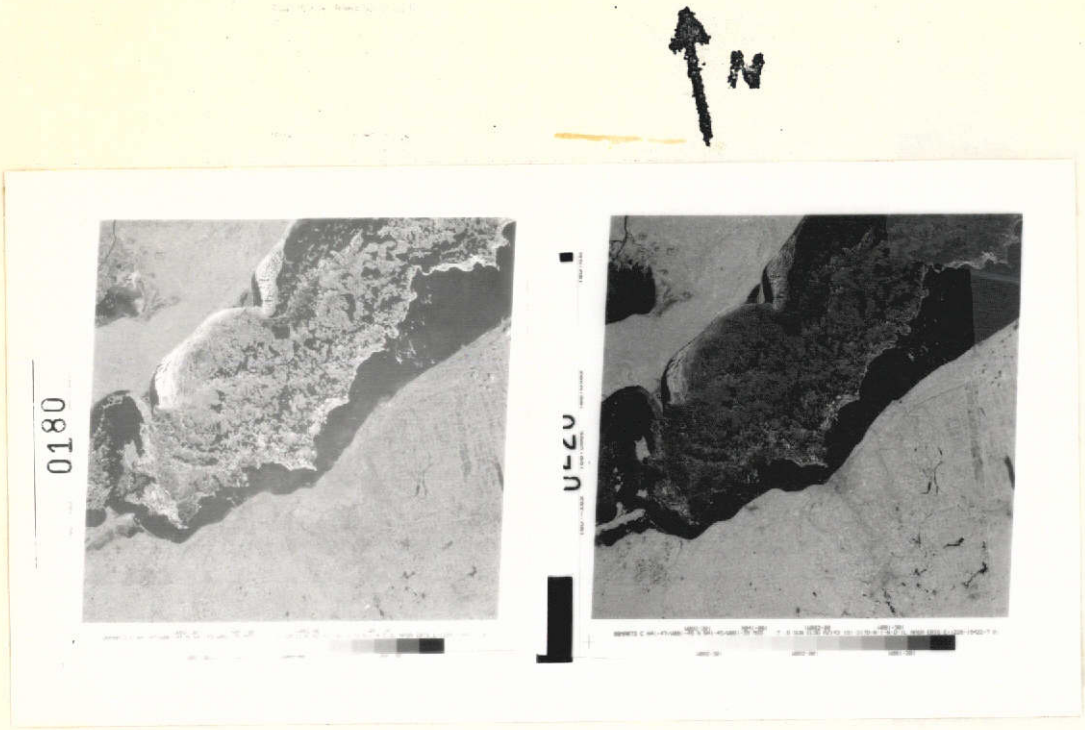

Figure 4.6 Two ERTS-1 images of Lake Erie ice simultaneously exposed and developed, March 8, 1973. Note the decreased reflectance of ice in MSS band 7 (right) compared with MSS band 5 (left).

Table 4.1

Meteorological data before and after the ERTS pass on March 8, 1973.

Station	TEMPERATURE (°C)			WIND (km/h)		
	1200Z	1500Z	1800Z	1200Z	1500Z	1800Z
Erie	7	12	13	SW 18	SW 18	NW 37
Cleveland		13	16	SW 9	SW 9	W 18
Toledo	4	11	16	S 18	W 9	W 18
Detroit	3	10	14	SW 9	SW 9	SW 37
London, Ont.	3	8	11	SW 9	W 28	W 37
Buffalo	6	9	12	SW 9	SW 28	W 37

Chapter 5 LAKE CURRENTS

The determination of current direction and current speed in large lakes is commonly accomplished by extensive and expensive ground truth surveys. Point measurements are obtained by rather sophisticated current meters. Such point measurements are termed "Eulerian." Other measurements are made by drogues or floats which can be tracked, thus providing a planned view or map type of current flow determination, termed "Lagrangian." The use of ERTS-1 data in detecting lake currents by using current indicators is neither Lagrangian nor Eulerian but is more appropriately called "synoptic."

Synoptic methods are here defined as remote-sensing methods that record from an airborne or space platform, one or more parameters of large areas of the sea surface known to be related to current speed or direction. Examples of such remote sensing methods are: aerial photography, passive microwave, radar and infrared imagery.

Strong (1973) first pointed out the value of using ERTS-1 sidelap images of Lake Erie ice as current indicators by observing the 24-hour shift in ice fragments in the sidelap portion of two ERTS-1 images taken on adjacent orbits. (See also Chapter 4.) This method, however, is Lagrangian. Distinctive and identifiable ice fragments suitable for tracking are shown in figure 5.1.

Wiesnet and McGinnis (1974) demonstrated that even a single ERTS-1 frame can be used to determine current motion in those special cases where the ice can be related by its shape to shore-fast ice--again, a Lagrangian approach.

Turbidity patterns on satellite imagery yield information on current patterns but in general only current directions can be mapped (figure 5.2). This technique of charting current directions from synoptically gathered imagery is the synoptic method referred to earlier. The current indicators may be turbidity (sediment or algae), ice cracks, ice fragments or thermal patterns. (A thermal channel will be available on ERTS-C.) For an example of thermal patterns, see figure 5.3. Care must be exercised so that linear features in the lake bottom such as submerged bars are not inadvertently mapped as currents. Strong and Stumpf (in press) provide numerous examples of current patterns from ERTS-1 images in the Great Lakes.

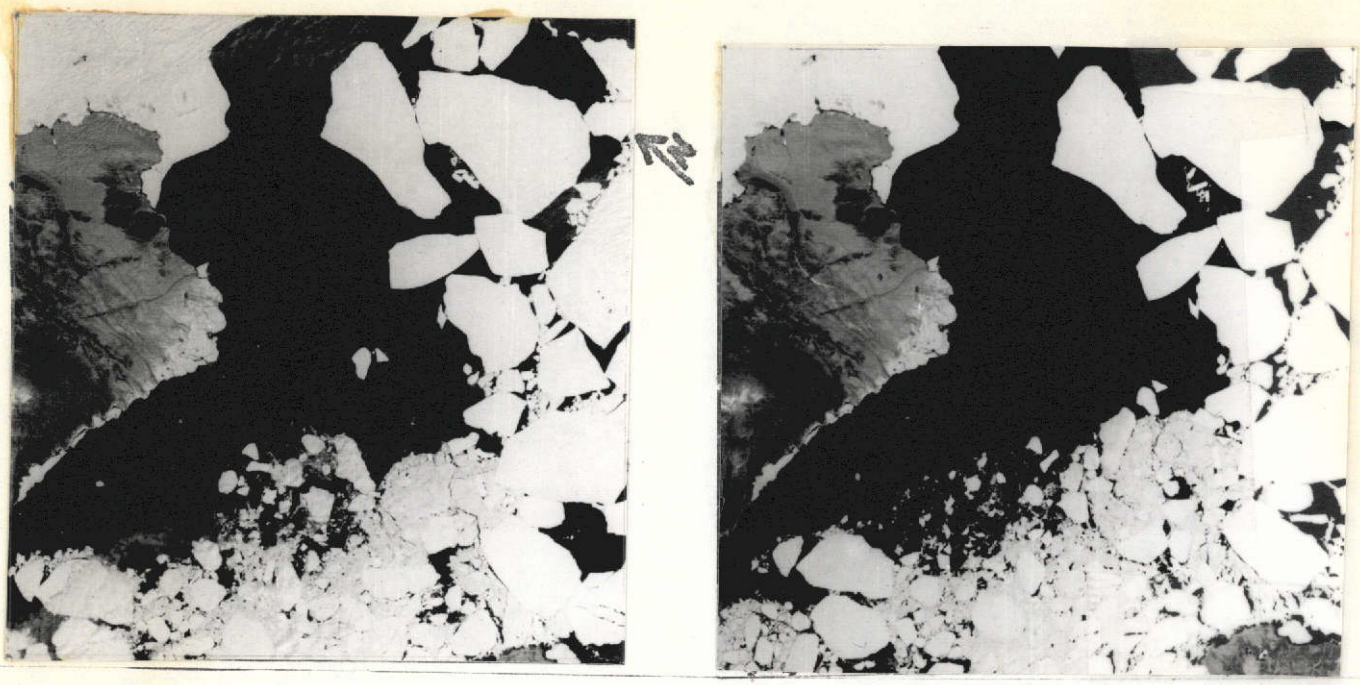

Figure 5.1. ERTS-1 images taken on August 23, 1972 (Figure 5.1A) and August 24, 1972 (Figure 5.1B) east of Cornwall Island. Current can be derived from the movement of distinctive ice fragments from one day to the next. Two small separated ice fragments in figure A moved approximately 3.8 nautical miles in 24 hours 8./cm/sec indicating current motion of 16 knots to the SSE.

Figure 5.2. ERTS-1 MSS band 5 image of Lake St. Clair and western Lake Erie useful for Lagrangian current measurements using turbidity, April 14, 1973.

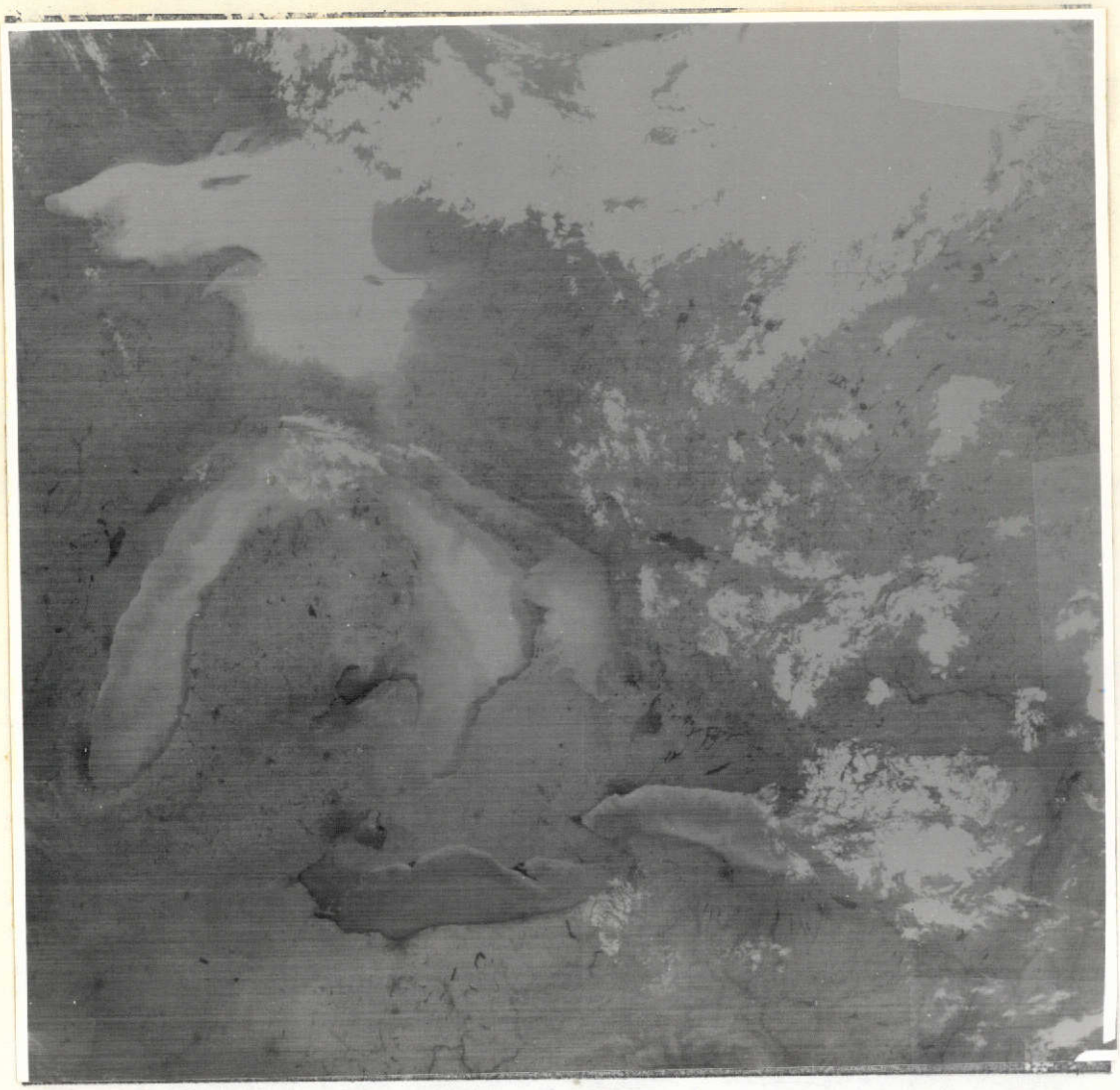

Figure 5.3. NOAA-2 VHRR-IR image of the Great Lakes showing thermal current motions, June 13, 1973.

Chapter 6

SOIL MOISTURE

The ability to make even semiquantitative estimates of soil moisture (i.e. saturated, moderate, or dry) from a satellite would provide the operational hydrologist with new information that would improve the accuracy of water level forecasts, especially flood forecasts. The agricultural community would find that soil moisture monitoring via satellite would generate forecasts valuable for planting and harvesting, NOAA's primary interest in soil moisture is in evaluating the amount of precipitation that can infiltrate the soil so that flood runoff can be computed more accurately.

Three facts should be stressed: 1) Soil moisture data are not routinely collected in the U.S.; 2) The effect of incorrect soil moisture values on computerized flood modeling can be devastating; 3) At present, soil moisture is estimated on basis of sparse rainfall network data.

The ERTS-1 MSS offers the hope that multispectral data will provide an indication of soil moisture. Condit (1970) had obtained spectral reflectance curves (0.32 to 1.00μm) for 285 soil samples from 36 states in both wet and dry conditions. He developed three typical curves on the basis of these data. Earlier, Angstrom (1925) and Planet (1970) offered explanations of the physical basis for the decreased reflectance of wet soils. An excellent review of soil mapping problems using aerial photography methods is available (Curtis, 1973).

NOAA Test Sites

As mentioned earlier, ground determinations of soil moisture are relatively rare. At a NOAA test site in the Finger Lakes region of New York State, (figure 6.1) we decided to take advantage of an ongoing NOAA aircraft experiment under the sponsorship of Dr. E.L. Peck, National Weather Service/ Office of Hydrology. In this experiment a crew of soil scientists took soil samples and then had them measured gravimetrically in the laboratory to determine soil moisture. Peck et al., (1971) was engaged in an attempt to test a gamma-ray technique for measuring snow depth as a function of suppressed radioactivity. The technique requires background flights during the summer and a knowledge of soil moisture. Although our original plans included multiple test sites in the Syracuse area, these proved to be too costly and too time-consuming for this project; therefore our effort centered on the Scipio test site (see figure 6.2).

The Scipio test site is a flight line approximately 7.4 km long that lies 300 m east of NY Highway 34. It extends from 0.8 km north of Scipio Center to a point 1.6 km south of Fleming. The terrain is typical glaciated upland that is used for farming. A few scattered woodlots are included in the area.

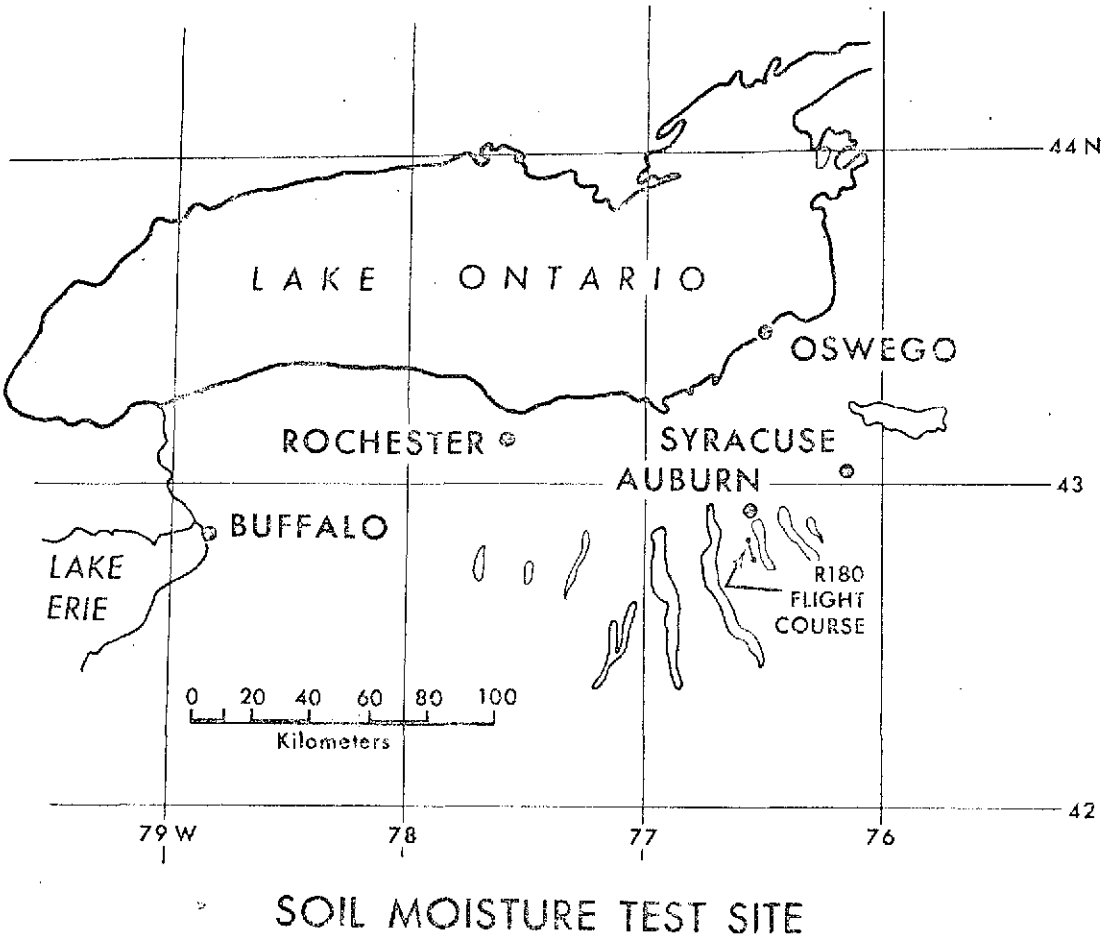

Figure 6.1. Index map showing location of Scipio test site.

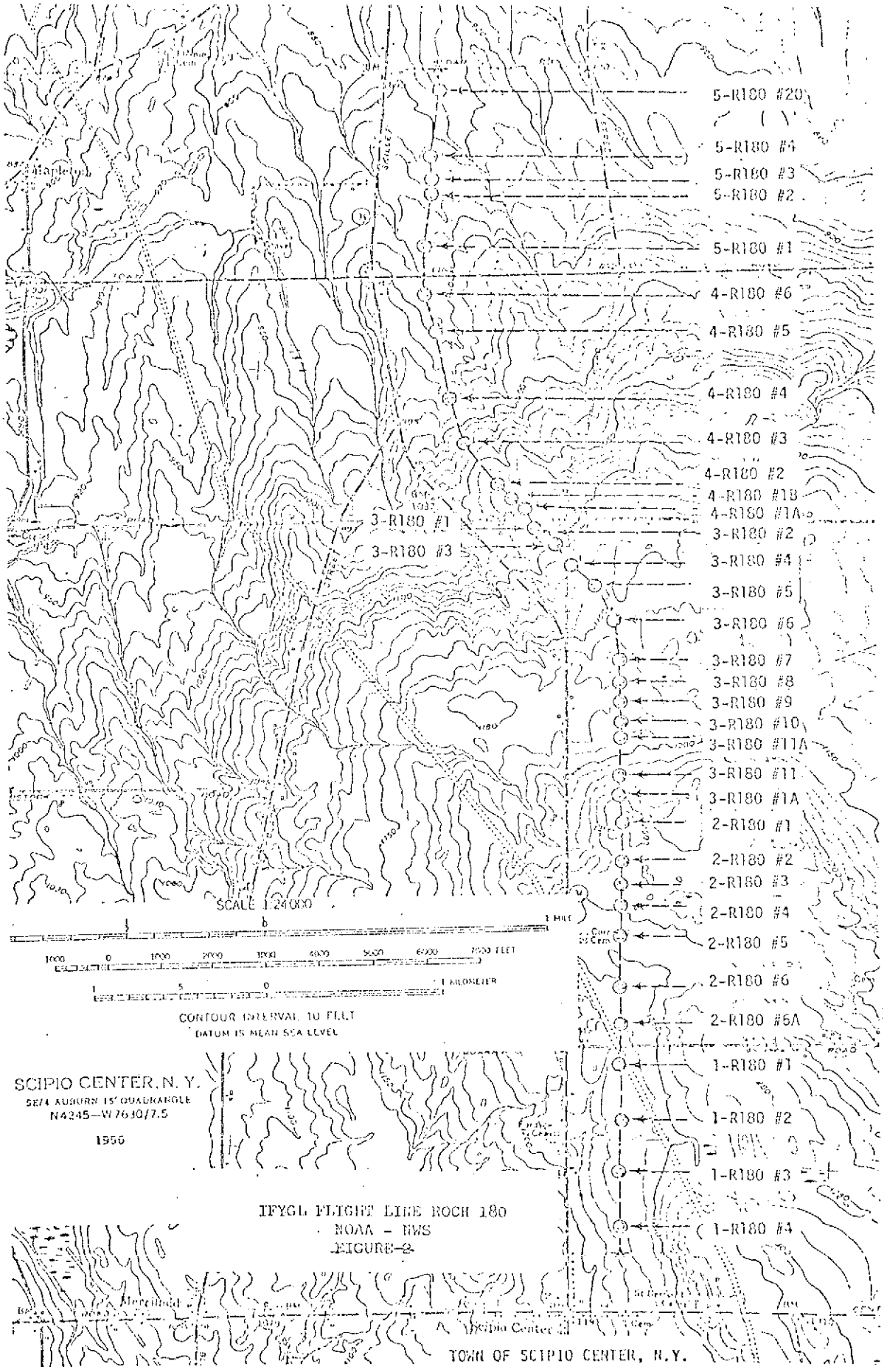

Figure 6.2 Topographic map of Scipio test site.

A number of aircraft overflights over the Scipio test site are listed in Table 6.1

Table 6.1
Aircraft overflights over Scipio test site

Date	Aircraft sensors
6/14/72	Passive microwave
6/15/72	Passive microwave
6/16/72	Gamma Ray; Passive microwave
10/11/72	Gamma Ray; Multispectral Photography, and Thermal IR

On October 11, 1972, ERTS-1 obtained cloudfree imagery of the test site. This data set provides unique coverage for soil moisture analysis. Ground truth consists of soil type, gravimetrically determined soil moisture, vegetation type and height, and a few telespectraradiometer readings. Aircraft data include gamma-ray data (90 and 150 agl* altitude); 4-band multispectral photography at 1700 m agl; and dual-band thermal scanner imagery, also at 1700 m agl.

Some of the above-mentioned data have been previously published. The passive microwave work under NOAA contract was published by Poe et al., 1973; the ground truth was published by Peck, et al., 1972, Peck and Larson, 1973; the thermal IR data is currently under analysis by L. LeSchack of DR&T Corp; and the gamma-ray results are available (Fritsche, 1972). The multispectral photography was taken using a four-lens camera mounted in the NOAA-NOS "Buffalo" survey aircraft.

Multispectral Camera Aircraft Survey

Eastman Kodak 2424 (black and white IR) film was used. The filters used in the camera were for .505-.557μm, .585-.680μm, .712-.745μm, and .808-.930μm, labeled A through D, respectively. These bands approximate the ERTS-1 MSS bands. Figure 6.3 is a combination of bands B, C and D, shown in false colors on a color-additive viewer. Note that:

1. Band B is portrayed in red at 100% intensity.

2. Band C is portrayed in green at 100% intensity.

3. Band D is a negative portrayed in blue at 60% intensity.

In the course of the study, 72 different filter-band combinations were evaluated before the above combination was chosen.

From the many aircraft photos taken at low (760 m agl) altitude, one, IR x 1-077, was selected because of a large fallow field without any

*Agl, above ground level.

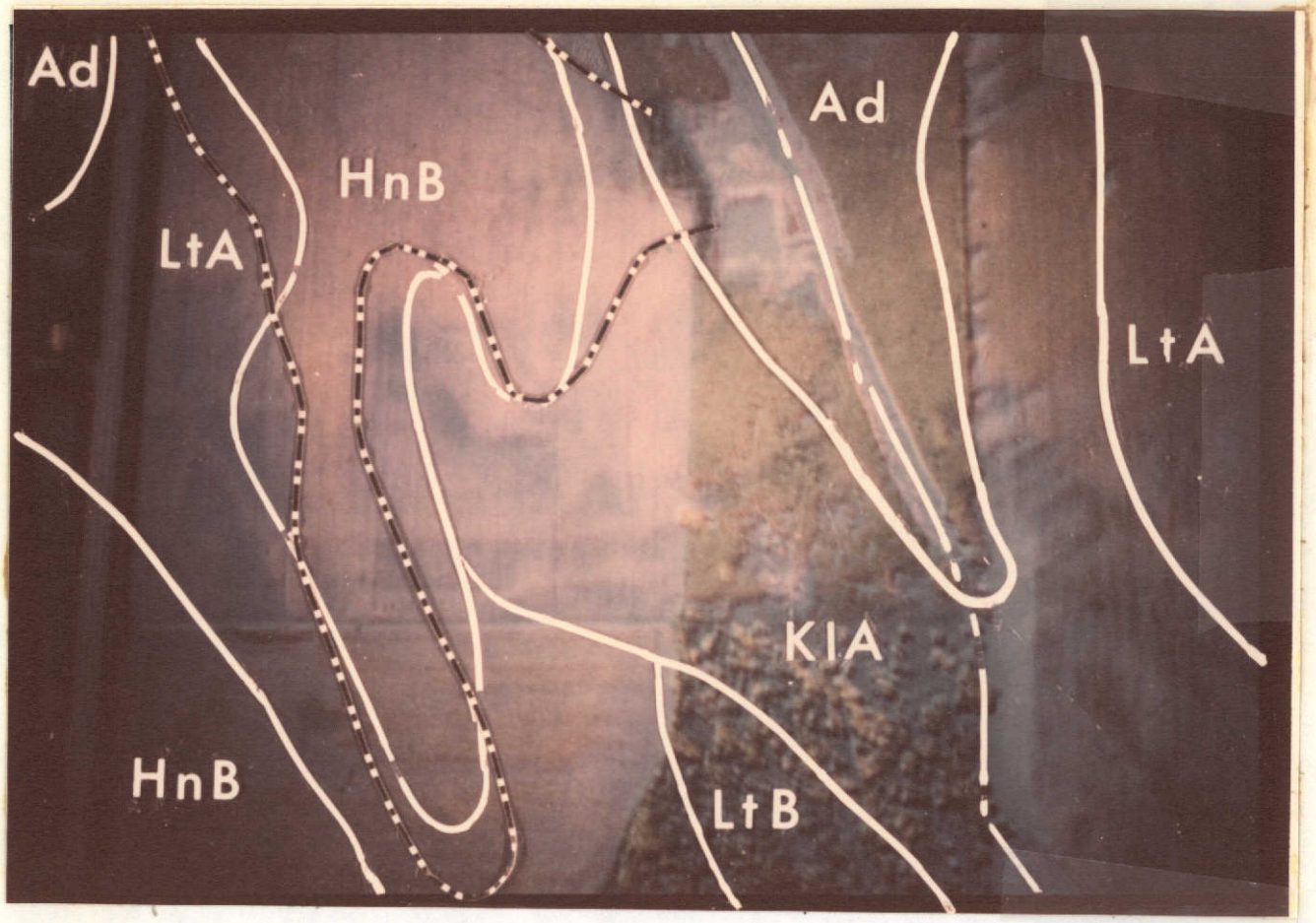

Figure 6.3 Aircraft multispectral image from CAV with soil boundaries shown.

vegetation affecting the spectral reflectance. A soil Conservation Service map of the region (SCS, 1970, Cayuga County, N.Y., No. 53) at 1:24,000 scale was used to determine the soil types. A densitometric analysis of the field was performed using a grid overlay and all four bands of imagery. Digitized densities (referred to a standard optical stepwedge datum) were read from the densitometer.

Analysis of Aircraft MS Images

A graph of density as a function of wavelength was prepared for points falling within each of the three soil types (figure 6.4). Three points were located within the grid coordinate sampled in soil KIA; five points were selected within soil LtA; nine were sampled within soil HnB. These reconstructed spectral reflectance curves, although crude and not normalized, demonstrate that multispectral imagery can be used to generate spectral information on soil types and on the range of spectral densities, which can be converted to spectral reflectances. It should be possible to build up a statistical base of reflectance curves under varying soil moisture conditions.

Once defined, these moisture dependent spectral reflectance curves could be used to evaluate soil moisture conditions over the test areas and provide at least semiquantitative soil moisture conditions (saturated, moderate, or dry) by aerial techniques in those areas where vegetation is not a problem. Unfortunately there are severe limitations on the technique. First, the spectral reflection of vegetation is overpowering in the near IR; and secondly, particle size and packing of the soil affects reflectance, as does sun angle and atmospheric attenuation due to haze, dust, fog, colloids, aerosols, etc. Nevertheless, the early spring floods characteristic of the Midwestern States and the widespread similar soil types in the area make the area well suited for this technique.

The cleared fallow field in figure 6.3 was selected because the reflection from vegetation could be avoided. It was immediately apparent that the HnB soil between LtA and KIA could be distinguished. In attempting to transfer the soil boundaries from the soil map we found that the contacts were slightly off (on the order of 30-60 m). Figure 6.3 shows the mechanically transferred boundaries. Note the misalignment of the HnB/KIA contact in the center of the image. We have assumed that the low level multispectral photography (1:5,000) is undoubtedly more accurate than the 1:15,840-scale soil map. If this be so, then examination of figure 6.4 suggests that details of the soil contacts in this bare field could be improved if multispectral imagery were utilized. The soils here are all similar silt loams yet the changes in reflectance in band D (ERTS-1 band 7) (figure 6.5) are interpreted as changes in the soil moisture near or at the surface. In both the color Additive viewer (figure 6.3) and the color analyzer (figure 6.6) the "thumb" of KIA appears to be a very wet area. In the upper right-hand corner of figure 6.6 a square pond containing water (in black) provides a convenient calibration. Also a drainage ditch extends from the pit area south as shown on the soil map.

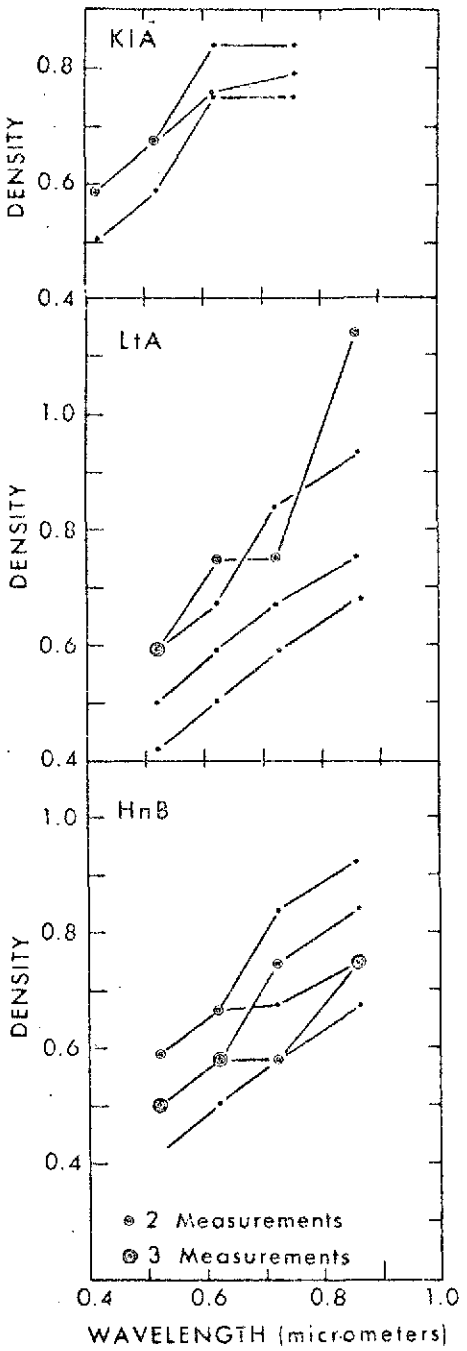

Figure 6.4 Film density curves as a function of wavelength for (A) three samples of KIA soil; (B) five samples of LtA soil; and (C) nine samples of HnB soil prepared from multispectral aircraft images, Figure 6.3.

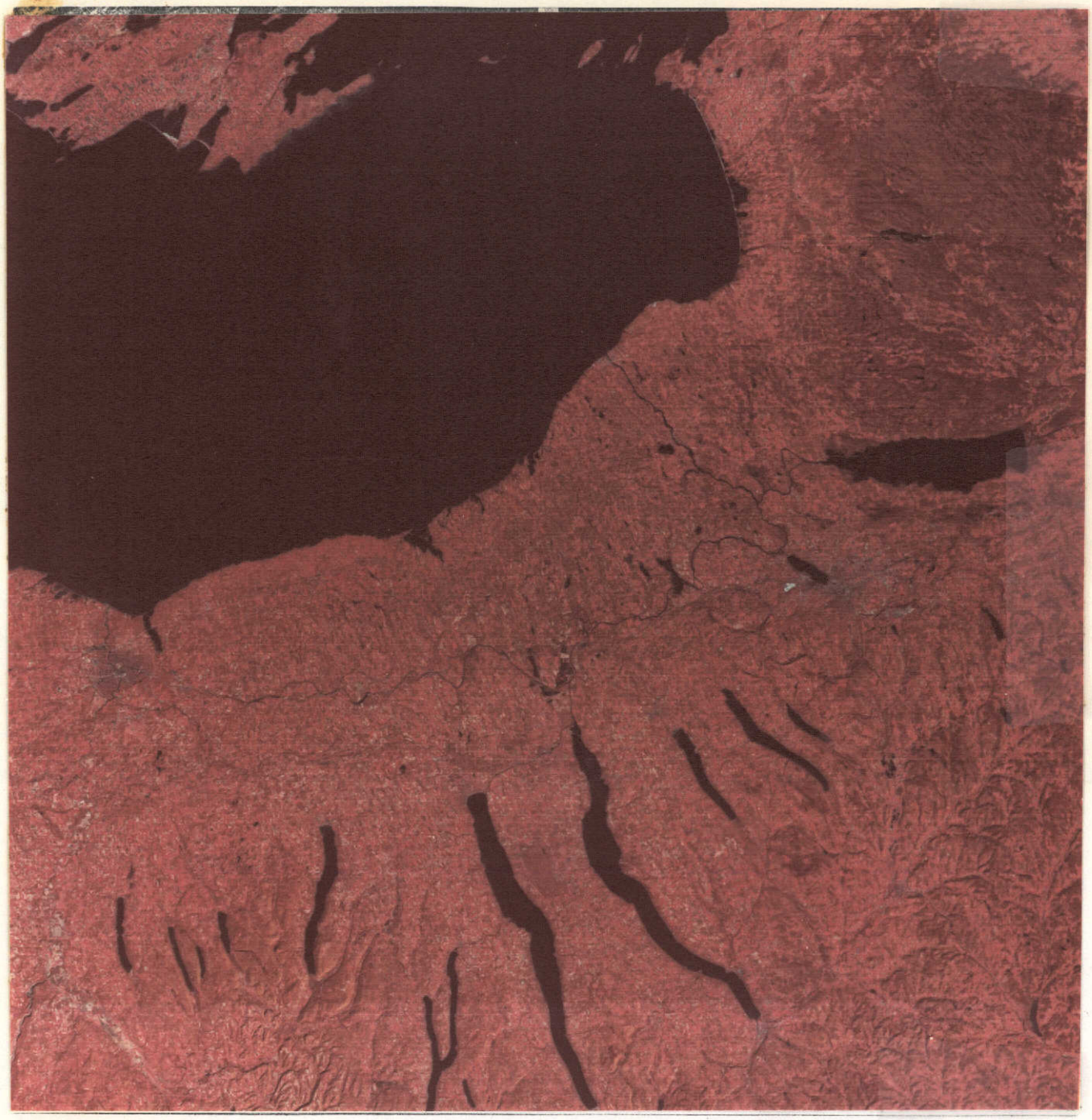

Figure 6.5. ERTS-1 image of the Scipio test site area, October 25, 1973.

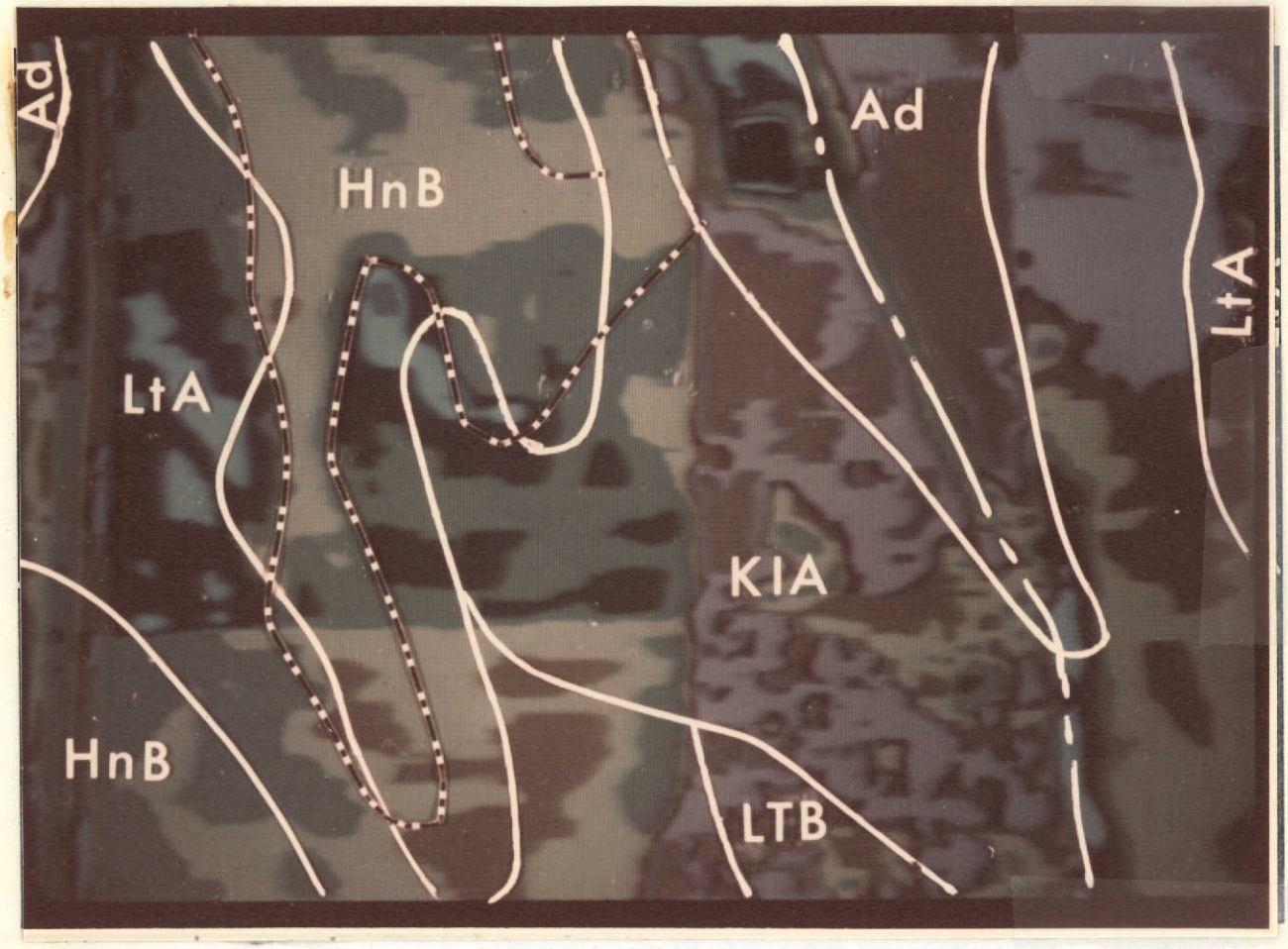

Figure 6.6 Aircraft multispectral image (0.8-0.95μm) viewed through Antech Color Analyzer showing variations in reflectance.

Concluding Remarks

When considering the use of satellite reflectance data one must take into account resolution. The problems of distinguishing details of soil moisture with a resolution of 80 m are quite different from those of low level aircraft surveys where details as small as a meter can be resolved. We attempted to relate spectral reflectance from the CCT printout to generalized soil moisture but more unsuccessful. Relatively homogeneous test sites, such as areas in the Midwest, would be more appropriate. No other meaningful conclusions are warranted from our study of the ERTS-1 digital data at this test site. Soil moisture was not directly detectable using ERTS data over the heavily vegetated Scipio test site.

The results of thermal dual-channel aircraft surveys over this test site will be reported separately because this effort, though related to the current ERTS-1 study, was financed totally by NOAA/NESS funds.

Chapter 7 FLOOD MAPPING

One of the many useful hydrological applications of satellite data as noted earlier in a study by the National Academy of Sciences (1969) is the monitoring and forecasting of floods. Work by Rango and Salomonson (1974) and Deutsch et al. (1974) has shown several useful applications to flood assessment using ERTS-1 data. Accuracy of approximately five percent in mapping flood extent at a scale of 1:250,000 is attainable using imagery from the near-IR MSS band 7 (0.8-1.1μm). Excessive soil moisture and vegetation stress results in reduced reflectance in the near-IR for 10-12 days after the flood peak, thereby permitting post-flood mapping (figure 7.1) (Rango and Salomonson, 1974).

The 50-year return period flood inundation boundaries have been easily determined on the Appomatox and Nottaway Rivers in Virginia (Rango and Salomonson, 1974) and the Gila River in Arizona (Morrison and Cooley, 1973). Hallberg, et al. (1973), found the effects of the 100-year flood clearly evident along the East and West Nishnabotna Rivers in Iowa.

Satellite flood mapping is fast and inexpensive but a quick-look capability is necessary if ERTS-1 imagery is really to be utilized by government officials directly concerned with flood assessment and relief programs. Satellite flood mapping is certainly energy conserving when compared with conventional aerial surveys.

ERTS-1 imagery applications include evaluating levee systems during floods and aiding flood plain zoning efforts by determining the limits of floods for specific return periods.

The 18-day repeat cycle of ERTS-1 prohibits operational flood forecasting and monitoring. The NOAA-2, NOAA-3, and NOAA-4 satellites provide daily coverage of flooded areas. However, at a resolution of 900 m, the VHRR onboard NOAA-4 is restricted to flood evaluation of large (valley widths >3 km) rivers. Wiesnet, et al. (1974) demonstrated the capability of flood inundation mapping along the Mississippi River near St. Louis, comparing a NOAA-2 digitally-displayed scene in late March with an ERTS-1 image taken four days later (figure 7.2). By measuring both satellite flood areas, they found that the NOAA-2 measurement exceeded the ERTS-1 value by 13%. This result is surprisingly good considering the coarse resolution of NOAA-2 VHRR: 900 meters versus 80 meters in the ERTS-1 MSS. Several limitations due to the 900-m resolution of the NOAA-2 and -4 data should be noted. The VHRR cannot be used for flash floods; it cannot be used for flood mapping on small streams (i.e. valley widths < 3 km); and it does not permit precise delineation and mensuration of flooded areas. Nevertheless, the 12-hour day/night flood watch capability of the NOAA VHRR and its near realtime availability make it a highly useful environmental monitoring tool to furnish rapid synoptic information on developing floods for hydrologic evaluation.

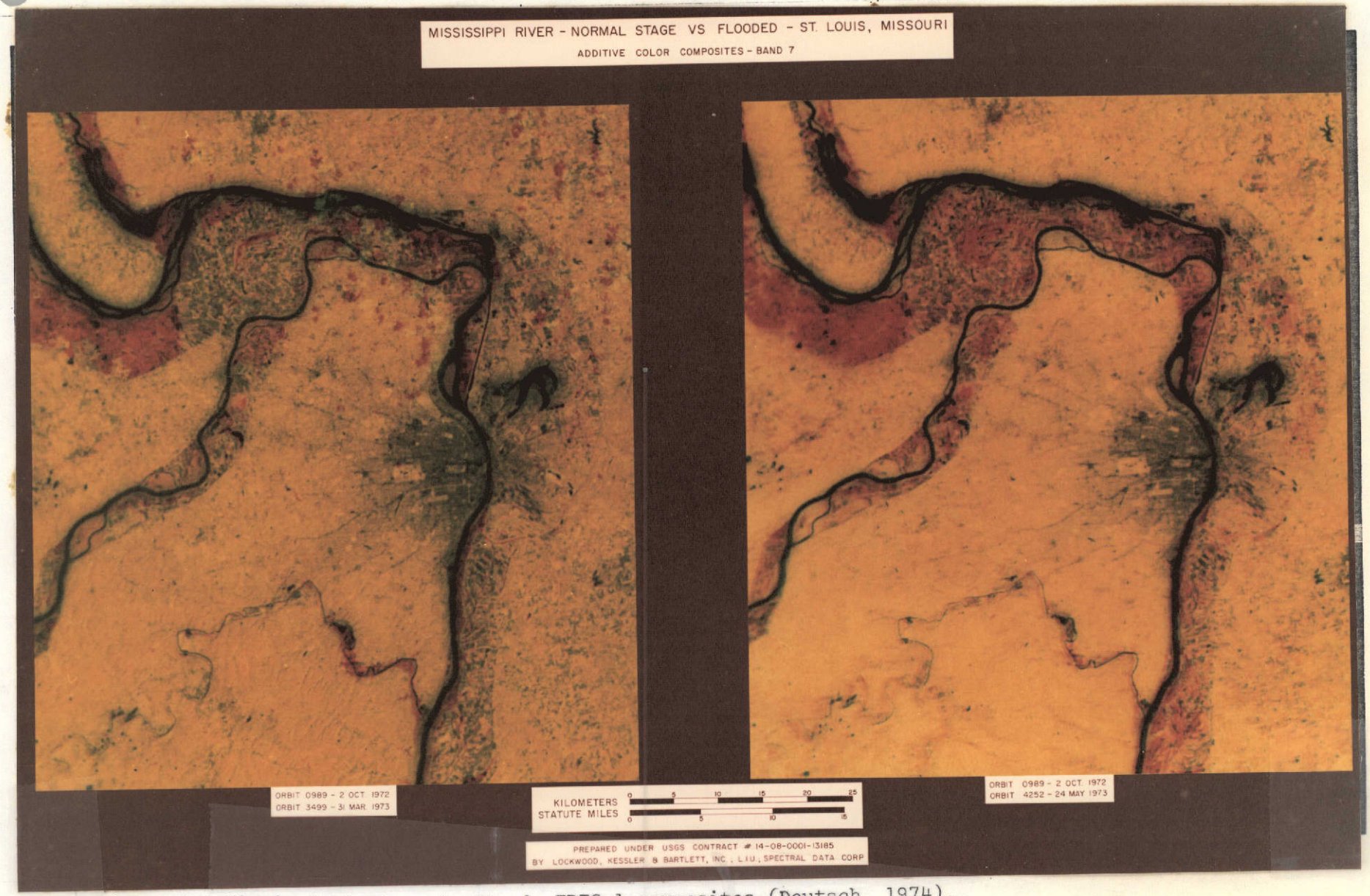

Figure 7.1 Mississippi River in flood, ERTS-1 composites (Deutsch, 1974).

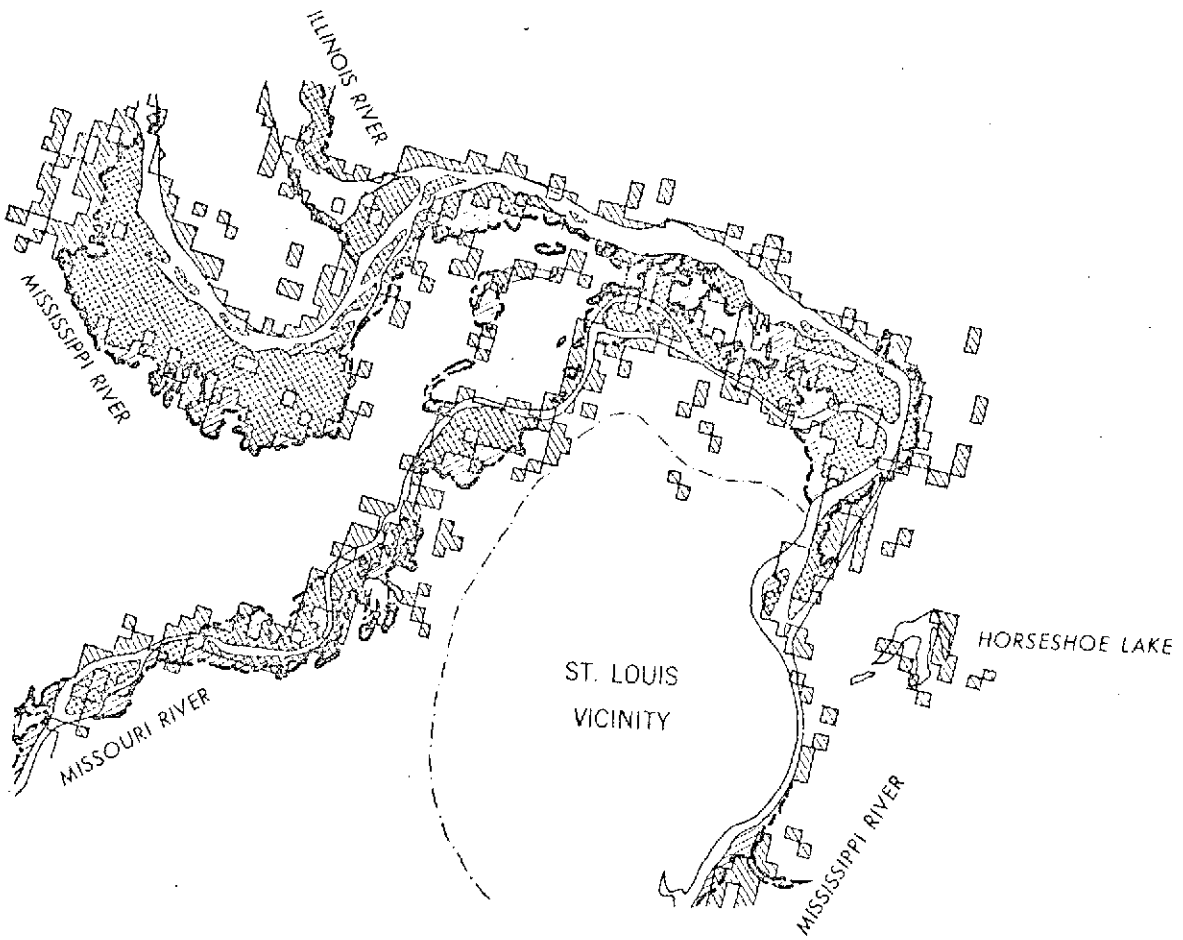

Figure 7.2. Map of the St. Louis area showing flood boundaries for March 31, 1973, from the ERTS-1 MSS image as a heavy dashed line. The flood boundaries for March 27, 1973, from the NOAA-2 VHRR-IR image are shown by a solid line and appear rectangular. Cross hatched pattern indicates flooded areas detected in the images from both satellites.

Chapter 8 MISCELLANEOUS HYDROLOGIC APPLICATIONS

ERTS-1 data has a plethora of potential and actual hydrological applications that deserve mention despite the fact that these uses are beyond the scope of the original proposal. For additional references and for a summary of satellite hydrology's state of the art, Rango, et al. (1974) is a good reference.

Geomorphology

Quantitative geomorphology deals in part with river basins. In certain poorly mapped regions, or in developing nations, excellent drainage basin maps can be prepared from ERTS images, thus affording information on such important parameters as:

1. basin shape
2. basin size
3. up-to-date vegetation patterns and types
4. up-to-date land use patterns

Monitoring of basins from image to image can provide data relevant to:

1. surface area changes of lakes and reservoirs
2. channel changes
3. development and erosion of point bars
4. meander geometry
5. flood plain formation, growth, and erosion
6. landslides, rockfalls, and mudflows

Water Quality

Many ERTS investigators have reported on the turbidity detection capability of ERTS-1 (Strong, 1973; Smith and Rogers, 1974). Others have attempted to correlate turbidity with suspended solids and with MSS data (Stortz and Sydor, 1974).

The basic problem in this approach continues to be the ground identification of the substance causing the turbidity. Strong (1973) has shown that certain algal blooms can be identified by ERTS-1 MSS data alone, but it is not always possible to determine whether the turbidity is inorganic suspended sediment, organic matter or algae.

Great Slave Lake, during the short summer season of the Northwest Territories, is relatively unspoiled and unpolluted, but naturally occurring

silt and other suspended sediment do surge into the lake from the nearby rivers. The unfrozen season is short in this Arctic area so that the run-off is concentrated in the summer months during the snowmelt season. In the ERTS-1 image (figure 8.1), sediment-laden Slave River is shown discharging turbid water into Great Slave Lake.

The delta of the mouth of the river is evident, and the distributaries are also clearly seen. Note that the highest concentration of suspended sediment (lightest tone) is emanating from Old Steamboat Channel, the southernmost channel visible. Note the deep blue of the Gaudet Bay and other smaller bays northeast of the delta and compare it with the lake waters adjacent to the bays. Note the small oxbow lake east of the delta and the intermediate blue color at that point.

Winds at 10 knots from the southwest (5.1/cm/sec) were prevalent over the lake as ERTS-1 passed over. These winds distributed the sediment in a pattern extending northeast along the shoreline, thus reflecting a northeast longshore current. The sharp westerly prong of sediment just off the northernmost channel, Resdelta Channel, occurs at a point where a sandbar is charted. The effects of a moderate southwesterly wind on the water clarity of the lake are clearly demonstrated by this image. The west half of the lake is extremely clear and free of turbidity.

Oil slicks and acid waste dumping have been detected by other ERTS-1 investigators, demonstrating the satellite's pollution monitoring capability. (See Stumpf and Strong, 1974 and Wezernak and Thomson, 1973.)

Phreatophyte Measurements

Phreatophyte monitoring is a seldom mentioned but very possible application of ERTS-1. Phreatophytes are water-using plants that consume ground water in arid and semiarid regions thus reducing the amount available for aquifer recharge. The amounts of water thereby transpired are great, and may materially affect subsurface water yield. For the past 50 years, these plants (chiefly Salt Cedar) have been extending their range throughout the semiarid regions of the West despite large scale attempts at eradication.

Glaciers

Glaciers are one hydrologic feature that can be adequately monitored using an 18-day revisit cycle. Glaciers do not move quickly and the 80-meter resolution of ERTS is extremely important for effective glacier work. It is vastly superior to the NOAA series of satellites in this respect. The inclusion of a better than 300 m resolution thermal channel on an ERTS satellite would be extremely beneficial for glaciologists.

Ground Water

Ground water can be detected by ERTS only indirectly by seeps and springs, or by vegetation in arid lands. ERTS-1 can, however, be used to distinguish geologic formations that are known aquifers and so provide

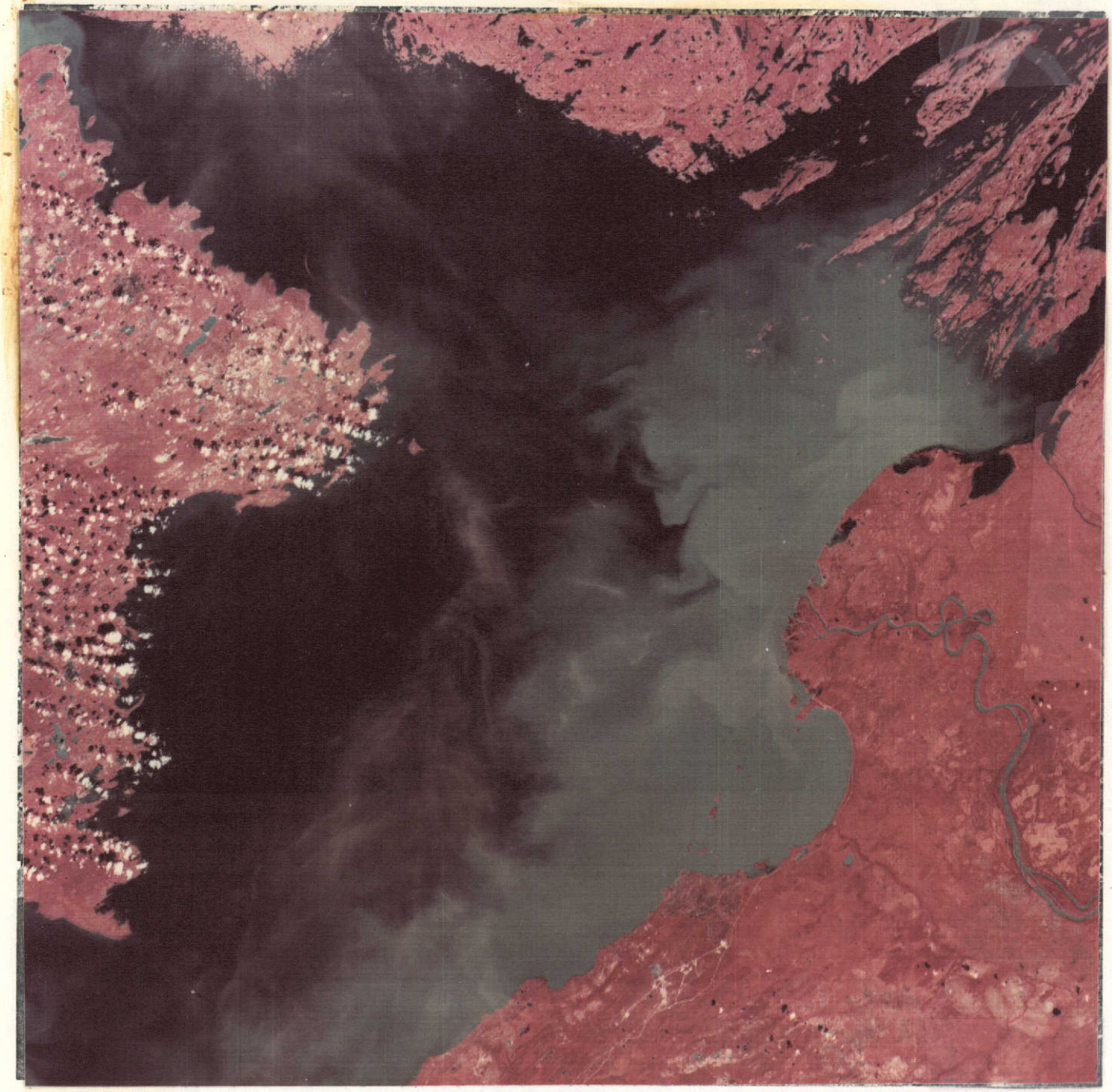

Figure 8.1. ERTS-1 image of the center of Great Slave Lake, District of MacKenzie, Canada, August 16, 1972, showing lake turbidity.

valuable data on the areal extent of the aquifer for further development by drilling. In developing nations in remote areas this approach saves considerable time for the ground-water hydrologist. It should be employed in drought-stricken lands of developing nations where aerial photography is sparse or nonexistent.

REFERENCES

Angstrom, A., 1925, "The Albedo of Various Surfaces of Ground," Geografiska Ann., Vol. 7, p. 323.

Barnes, B.S., 1942, "Discussion of Method of Predicting Runoff from Rainfall by R.K. Linsley, Jr. and W.C. Ackerman," Trans. Am. Soc. Civil Engrs., Vol. 107, pp. 836-841.

Barnes, J.C. and C.J. Bowley, 1970, "The use of Environmental Satellite Data for Mapping Annual Snow-Extent Decrease in the Western United States," Final Report (Contract NOAA/NESS No. E-252-69(N), Allied Research Assoc., Concord, Mass., 105 pp.

Barnes, J.C. and C.J. Bowley, 1973, "Use of ERTS Data for Mapping Snow Cover in the Western United States," Symposium on Significant Results obtained from the Earth Resources Technology Satellite-1, Vol. 1, pp. 855-862.

Barnes, J.C. and C.J. Bowley, 1974, "Use of ERTS Data for Mapping Snow Cover in the Western United States," Final Report to NASA, GSFC.

Boyce, D.E., 1973, "The 1972-73 Great Lakes Ice Season," Mariners Weather Log, Vol. 17, No. 5, pp. 285-288.

Chow, V.T., 1964, Handbook of Applied Hydrology, McGraw-Hill Book Co., pp. 10-35 to 10-38.

Condit, H.R., 1970, "The Spectral Reflectance of American Soils," Photogrammetric Engineering, Vol. 36, No. 9, pp. 955-966.

Corps of Engineers, 1960, Runoff from Snowmelt, Engineering and Design Manual EM 1110-2-1406, pp. 5-6.

Crowder, W.K., H.L. McKim, S.F. Ackley, W.D. Hibler, 3d and D.M. Anderson, 1974, "Mesoscale Deformation of Sea Ice from Satellite Imagery," Proc. Symp. on Advanced Concepts and Techniques in the Study of Snow and Ice Resources, Monterey, Calif., National Acad. of Sciences, Washington, D.C., pp. 563-573.

Curtis, L.F., 1973, "The Application of Photography to Soil Mapping from the Air," in Photographic Techniques in Scientific Research, Cruise, J., and A. Newman, Academic Press, London and New York, 1973, pp. 57-110.

Deutsch, M. and F. Ruggles, 1974, "Optical Data Processing and Project Applications of the ERTS-1 Imagery Covering the 1973 Mississippi River Valley Floods, Water Resources Bulletin, Vol. 10, No. 5, pp. 1023-1039.

Ferguson, H.L. and B.E. Goodison, 1974, Mean Snowpack Water Equivalent Maps and Snow Course Data Problems over Southern Ontario, Proc. Eastern Snow Conf., Ottawa, Feb. 1974, pp. 91-111.

Fritsche, A., 1972, IFYGL (Scipio Center) Data Analysis, Informal Rept., 16 Nov. 1972, EG&G, Las Vegas, Nev., 5 pp.

Garstka, W.D., L.D. Love, B.C. Goodell and F.A. Bertle, 1958, Factors Affecting Snowmelt and Streamflow, U.S. Bureau of Reclamation and U.S. Forest Service.

General Electric Corp., 1972, Data Users Handbook, NASA-Goddard Space Flight Center, Document No. 71SD4249.

Goddard Space Flight Center, NASA, 1969, Nimbus III User's Guide, National Aeronautics and Space Administration, Greenbelt, Md., 238 pp.

Hallberg, G.R., B.E. Hoyer and A. Rango, 1973, "Application of ERTS-1 Imagery to Flood Inundation Mapping," Symposium on Significant Results obtained from the Earth Resources Technology Satellite-1," Vol. 1, pp. 745-754.

McGinnis, D.F., 1972, "Detecting Melting Snow and Ice by Visible and Near-infrared Measurements from Satellites," Intern. Symp. on Role of Snow and Ice in Hydrology, Vol. 2, pp. 751-761.

Meier, M.F., 1973, "Evaluation of ERTS Imagery for Mapping and Detection of Changes of Snowcover on Land and on Glaciers," Symposium on Significant Results obtained from the Earth Resources Technology Satellite-1, Vol. 1, pp. 863-875.

Morrison, R.B. and M.E. Cooley, 1973, "Assessment of Flood Damage in Arizona by means of ERTS-1," Symposium on Significant Results obtained from the Earth Resources Technology Satellite-1, Vol. 1, pp. 755-760.

National Academy of Sciences, 1969, Useful Applications of Earth-oriented Satellites-Hydrology, Washington, D.C., pp. 25-42.

NOAA, 1973, Climatological Data, California, National Oceanic and Atmospheric Administration, Vol. 77, No. 4-6.

O'Brien, H.W. and R.H. Munis (in press), "Red and Near-infrared Spectral Reflectance of Snow," U.S. Army Cold Regions Research and Engineering Laboratory Report.

Peck, E.L., V.C. Bissell, E.B. Jones, and D.L. Burge, 1971, Evaluation of Snow Water Equivalent by Airborne Measurement of Passive Terrestrial Gamma Radiation, Jour. Water Resources Research, Vol. 7, No. 5, pp. 1151-1159.

Peck, E.L., V.C. Bissell, and R.K. Farnsworth, 1972, Airborne Snow Reconnaissance, Interim Rept. No. 1, Internat. Field Year for the Great Lakes, Nat. Weather Service, NOAA, 33 pp.

Peck, E.L. and L.W. Larson, 1973, Airborne Snow Reconnaissance, Interim Rept. No. 3, Internat. Field Year for the Great Lakes, Nat. Weather Service, NOAA, 16 pp.

Phillips, D.W. and J.A.W. McCulloch, 1972, The Climate of the Great Lakes Basin, Atmos. Environ. Service, Climatologic Studies No. 20, 40 pp.

Planet, W.G., 1970, "Some Comments on Reflectance Measurements of Wet Soils," Remote Sensing of Environment, Vol. 1, pp. 127-129.

Poe, G., D. Meeks and A.T. Edgerton, 1973, "Airborne Passive Microwave Measurements of NOAA Hydrology Sites," Report No. 1752FR-1, DOC Contract No. 2-37116.

Rango, A., D.F. McGinnis, V.V. Salomonson and D.R. Wiesnet, 1974, "New Dimensions in Satellite Hydrology," Trans. Am. Geo. Union, Vol. 55, No. 7, pp. 703-711.

Rango, A. and V.V. Salomonson, 1974, Regional Flood Mapping from Space, Water Resources Research, Vol. 10, No. 3, pp. 473-484.

Rantz, S.E., 1972, Runoff Characteristics of Calif. Streams, Geological Survey Water-supply paper 2009-A, p. A14.

Rondy, D.R., 1969, Great Lakes Ice Atlas, U.S. Lake Survey Research Report 5-6,

Smith, V.E. and R.H. Rogers, 1974, "Automatic Classification of Eutrophication of Inland Lakes from Spacecraft Data (abs.)," Proc. 9th Int'l. Symposium on Remote Sensing of Environment, Ann Arbor, Mich., pp. 105-106.

Snider, C.R., 1971, A System for Predicting Freezeup and Thaw Dates for the Great Lakes, NOAA Tech. Memo. NWS CR-48, 106 pp.

Storz, K. and M. Sydor, 1974, Remote Sensing of Lake Superior (abs.), Proc. 9th Int'l. Symposium of Remote Sensing of Environment, Ann Arbor, Mich., p. 100.

Strong, A.E., E.P. McClain and D.F. McGinnis, 1971, "Detection of Thawing Snow and Ice Packs through the Combined use of Visible and Near-infrared Measurements from Earth Satellites," Monthly Weather Review, Vol. 99, No. 11, pp. 828-830.

Strong, A.E., 1973, "New Sensor on NOAA-2 Satellite Monitors the 1972-73 Great Lakes Ice Season," Remote Sensing and Water Resources Management, Amer. Water Res. Assoc., Urbana, Illinois, pp. 171-178.

Strong, A.E., 1974, "Remote Sensing of Algal Blooms by Aircraft and Satellite in Lake Erie and Utah Lake," Remote Sensing of Environment, Vol. 3, pp. 99-107.

Strong, A.E. and H.G. Stumpf, in press, An Evaluation of ERTS Data for Oceanography Uses thru Treat Lake Studies, Final Report, NASA, GSFC, Contract No. S70246-AG.

Stumpf, H.G. and A.E. Strong, 1974, "ERTS-1 View an Oil Slick?" Remote Sensing of Environment, Vol. 3, No. 1, pp. 87-90.

USGS, 1969, Index to Surface Water Stations, 1968 Edition, USGS, Washington, D.C., 641 pp.

Webb, M.S., 1974, "Surface Temperatures of Lake Erie," Water Resources Research, Vol. 10, No. 2, pp. 199-210.

Wezernak, C.T. and F.J. Thomson, 1973, Barge Dumping of Wastes in the New York Bight, Proc. Symposium ERTS-1, Sept. 29, 1972, NASA-Goddard Space Flight Center, Greenbelt, Md., pp. 142-145.

Wiesnet, D.R., 1973, "Detection of Snow Conditions in Mountainous Terrain," Earth Resources Technology Satellite-1 Symposium Proceedings, pp. 131-132.

Wiesnet, D.R. and D.F. McGinnis, 1974, "Snow Extent Mapping and Lake Ice Studies using ERTS-1 MSS together with NOAA-2 VHRR," Third ERTS-1 Symposium, Vol. 1, pp. 995-1009.

Wiesnet, D.R., D.F. McGinnis and J.A. Pritchard, 1974, "Mapping of the 1973 Mississippi River Floods by the NOAA-2 Satellite," Water Resources Bulletin, Vol. 10, No. 5, 1040-1049.